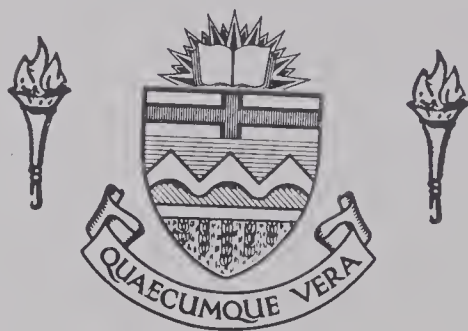


For Reference

NOT TO BE TAKEN FROM THIS ROOM

Ex libris
UNIVERSITATIS
ALBERTAENSIS



THE UNIVERSITY OF ALBERTA

RELEASE FORM

NAME OF AUTHOR: PATRICK F. DALEY

TITLE OF THESIS: TOPICS IN SH WAVE PROPAGATION

DEGREE FOR WHICH THESIS WAS PRESENTED: Ph.D.

YEAR THIS DEGREE GRANTED: 1981

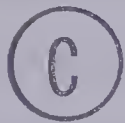
Permission is hereby granted to THE UNIVERSITY OF ALBERTA LIBRARY to reproduce single copies of this thesis and to lend or sell such copies for private, scholarly or scientific research purposes only.

The author reserves other publication rights, and neither the thesis nor extensive extracts from it may be printed or otherwise reproduced without the author's written permission.

THE UNIVERSITY OF ALBERTA

TOPICS IN SH-WAVE PROPAGATION

by



PATRICK F. DALEY

A THESIS

SUBMITTED TO THE FACULTY OF GRADUATE STUDIES AND RESEARCH
IN PARTIAL FULFILMENT OF THE REQUIREMENTS FOR THE DEGREE
OF DOCTOR OF PHILOSOPHY

IN

GEOPHYSICS

DEPARTMENT OF PHYSICS

EDMONTON, ALBERTA

SPRING, 1981

THE UNIVERSITY OF ALBERTA
FACULTY OF GRADUATE STUDIES AND RESEARCH

The undersigned certify that they have read, and recommend to the Faculty of Graduate Studies and Research, for acceptance, a thesis entitled TOPICS IN SH-WAVE PROPAGATION submitted by PATRICK F. DALEY in partial fulfilment of the requirements for the degree of DOCTOR OF PHILOSOPHY in GEOPHYSICS.

ABSTRACT

This thesis is a collection of three papers (Chapters 1-3) and a research note (Chapter 4) which as of November 16, 1979 have the following dispositions. Chapter one has been published in its entirety, appearing in the June, 1979 issue of the Bulletin of the Seismological Society of America; chapter two is forthcoming in a slightly abridged form in a fall issue of the Canadian Journal of Earth Sciences; chapter three has been submitted for publication to Geophysics; and chapter four is as yet unsubmitted. Each of the chapters is self-contained and does not require the presence of the others.

No apology is made for the treating of the seemingly trivial case of SH waves when dealing with the problems discussed, as it is the author's intent to present in the simplest possible form certain topics in elastic wave propagation. All results derived here can and in some cases have been applied by the authors to more sophisticated topics in elastic wave propagation. A large part of this thesis may appear tutorial in nature, but this is necessary to prepare a basis from which to explore obvious extensions.

There are many reports in the literature of anomalies in travel time data when an isotropic homogeneous earth model is used to interpret field data. In several instances, the introduction of a layered trans-

versely isotropic model has successfully explained these kinematic irregularities. However, it is useful, in fact essential, to confirm the kinematic fit with a dynamic (amplitude) comparison.

An asymptotic expansion of the displacement vector in terms of inverse powers of frequency is employed in chapter one to investigate the dynamic properties of SH waves propagating in plane layered transversely isotropic media. Both reflected and head waves are considered in terms of the asymptotic expansion, and their ranges of validity are discussed.

Although solutions to the most general case of wave propagation in anisotropic media can be found in the literature it is instructive to consider this simple case in which many quantities inherent to wave propagation in anisotropic media can be more readily understood and can be solved analytically rather than reverting to numerical methods.

In chapter two the problem of SH waves propagating in a transversely isotropic plane layered medium is discussed through the use of integral transforms and evaluation by steepest descents. This procedure yields not only the asymptotic solution which is also attainable using an asymptotic ray series approach, but also allows for the investigation of the interference of the reflected and head waves in the vicinity of the critical point

(point of critical refraction). It is in this region that asymptotic ray theory breaks down or in the least introduces considerable error in the displacement amplitudes.

The theory for the simple case of SH rays propagating in plane layered media consisting of thick layers separated by thin layered transition zones is examined in chapter three. The SH case was chosen, as the basic idea of the method is conveyed without an excess of mathematics that is necessitated by the introduction of potentials in the P-SV case.

A stationary phase approximation is employed when evaluating the integral which yields the displacement due to an arbitrary ray propagating in the above mentioned medium, and the validity of this approximation is discussed.

The comparison of ray, numerical integration and ray-reflectivity synthetic sections indicates that the transition zone method gives quite acceptable results for small source receiver offsets. This method is suitable for application in the oil industry as individual arrivals associated with ray paths in the thick layers are identified in the synthetic trace. Furthermore, compared to other methods, this technique is quite cost efficient.

In several papers in seismological literature it

has been shown mathematically that a periodic isotropic two layered medium behaves as a homogeneous transversely isotropic medium. This assumption has been shown to be valid as far as the propagation of elastic waves is concerned provided that the seismic wavelengths used are large when compared to the thicknesses of the individual isotropic layers. Chapter four contains seismograms computed using two different methods which compare the kinematic and dynamic properties of the periodic structure with its equivalent isotropic homogeneous structure for SH waves. Although this comparison seems quite trivial, none has appeared in the literature which is probably due to the prohibitive computing costs involved.

TABLE OF CONTENTS

CHAPTER		PAGE
1.	SH WAVES IN LAYERED TRANSVERSELY ISOTROPIC MEDIA - AN ASYMPTOTIC EXPANSION APPROACH	1
1.1	Introduction	1
1.2	Mathematical Preliminaries	1
1.3	Rays and Snell's Law	5
1.4	Calculation of Ray Amplitudes	8
1.5	Reflection and Transmission Coefficients	13
1.6	Geometrical Spreading	18
1.7	The Head Wave	29
1.8	Numerical Results	35
1.9	Conclusion	43
2.	SH WAVES IN LAYERED TRANSVERSELY ISOTROPIC MEDIA - A WAVE APPROACH	44
2.1	Introduction	44
2.2	Mathematical Preliminaries	45
2.3	The Contour of Integration	49
2.4	The Reflected Wave	58
2.5	The Head Wave	66
2.6	Interference Reflected Head Wave	73
2.7	Numerical Results	81

CHAPTER	PAGE
3. RAY-REFLECTIVITY METHOD FOR SH WAVES IN STACKS OF THIN AND THICK LAYERS	83
3.1 Introduction	83
3.2 Theoretical Preliminaries	86
3.3 Reflectivity and Transmittivity	89
3.4 Stationary Phase Approximation	97
3.5 Numerical Results	101
3.6 Conclusion	105
4. A COMPARISON OF SYNTHETIC SEISMOGRAMS FOR A THINLY STRATIFIED MEDIUM AND A TRANSVERSELY ISOTROPIC MEDIUM	106
4.1 Introduction	106
4.2 Notation and the Two Methods	107
4.3 Numerical Discussion	113
APPENDIX A. GAUSS' INTEGRAL THEOREM	118
APPENDIX B. REFLECTION AND TRANSMISSION COEFFICIENTS	121
BIBLIOGRAPHY	124

LIST OF TABLES

Table	Page
CHAPTER 1	
1.1 Velocity depth structure I	39
1.2 Velocity depth structure II	39
CHAPTER 2	
2.1 Specification of media used in Figures 2.7 and 2.8	78
CHAPTER 4	
4.1 Specification of the media	117

LIST OF FIGURES

	Page
CHAPTER 1	
1.1 Geometry of wavefronts and rays	9
1.2 SH wavefront incidence at the boundary between two elastic media	14
1.3 Definition of interface coordinates and ray segments	21
1.4 Ray tube geometry	24
1.5 Discontinuity of a ray tube at an interface	26
1.6 Head wave geometry	31
1.7 H1H1 and H2H1 coefficients	36
1.8 H1H2 and H2H2 coefficients	37
1.9 Effect on amplitudes by varying the anisotropy	40
1.10 Amplitude distance curve for ray $(S1)^4 (S1)_1^4$	41
1.11 Amplitude distance curve for ray $(S1)^4 (S1)_2^4$	42
CHAPTER 2	
2.1 Geometry of incidence and notation for a point source of SH waves	46
2.2 A ray diagram showing the labelling of the layers and interfaces	52
2.3 Contour of integration	56
2.4 Modulus and argument of μ_1 and g_1 vs. p_0	65
2.5 Modulus and argument of μ_2 and g_2 vs. p	71

CHAPTER 2 (cont'd)

2.6	Real and imaginary parts of the Weber function	76
2.7	Amplitude distance curves for a ray with multiplicity one	79
2.8	Amplitude distance curves for a ray with multiplicity three	80

CHAPTER 3

3.1	Geometry of media for plane interfaces and quasi-interfaces	87
3.2	Description of layers and layer parameters	91
3.3	Definition of notation of reflectivities and transmittivities	96
3.4	Velocity depth structure of the model	102
3.5	Comparison of three methods of computing synthetic seismograms	104

CHAPTER 4

4.1	Geometry of the media and definition of parameters	109
4.2	Comparison of the two methods of computing synthetic seismograms	115

CHAPTER 1

SH WAVES IN LAYERED TRANSVERSELY ISOTROPIC MEDIA -
AN ASYMPTOTIC EXPANSION APPROACH

1.1 Introduction

An asymptotic expansion of the displacement vector in terms of inverse powers of frequency is employed to investigate the dynamic (amplitude) properties of SH waves propagating in plane layered transversely isotropic media. Both reflected and head waves are considered in terms of the asymptotic expansion, and their ranges of validity and accuracy are discussed.

Although the solution of the most general case of wave propagation in an anisotropic medium has been presented in the literature (Cerveny (1972)), it is instructive to consider this simple case in which many quantities inherent to wave propagation in anisotropic media can be more readily understood and can be solved for analytically rather than reverting to numerical methods.

1.2 Mathematical Preliminaries

In a transversely isotropic inhomogeneous elastic medium, neglecting body forces, the equation of motion for the propagation of an SH wave can be written as

$$(1.1) \quad \frac{\partial^2 \vec{u}}{\partial t^2} = \frac{1}{\rho} \left[\frac{\partial}{\partial x_1} \left(c_{44} \frac{\partial \vec{u}}{\partial x_1} \right) + \frac{\partial}{\partial x_2} \left(c_{44} \frac{\partial \vec{u}}{\partial x_2} \right) + \frac{\partial}{\partial x_3} \left(c_{66} \frac{\partial \vec{u}}{\partial x_3} \right) \right]$$

where (x_1, x_2, x_3) are the rectangular Cartesian coordinates and C_{44} , C_{66} and ρ are the elastic parameters and density required to specify the medium for SH wave propagation (Potsma (1955), and Sato and Lapwood (1968)). These quantities may be arbitrary continuous functions of position.

As the SH displacement vector is normal to the plane of incidence in a transversely isotropic medium, the displacement vector \vec{u} can be chosen without loss of generality as

$$(1.2) \quad \vec{u} = (0, u, 0).$$

Although the problem as specified by equations (1.1) and (1.2) can be treated in two dimensions (the (x_1, x_3) plane), it is mathematically convenient for what follows to retain the derivative with respect to x_2 .

Analogous to methods used in geometrical optics (Luneberg (1944), Kline (1951)) the solution of the equation of motion will be assumed to have the form of an asymptotic series in inverse powers of frequency (Babich and Aleksiev (1958), Karal and Keller (1959), Cervený (1972), Hron and Kanasewich (1971)) so that

$$(1.3) \quad \vec{u}(x_1, x_2, x_3, t) = \sum_{n=0}^{\infty} \frac{\vec{U}_n(x_1, x_2, x_3) \exp i\omega[t - \tau(x_1, x_2, x_3)]}{(i\omega)^n}$$

$$\vec{U}_n(x_1, x_2, x_3) = U_n(x_1, x_2, x_3) \vec{n}_{SH}$$

where

- ω - frequency
- \vec{n}_{SH} - a unit vector in the x_2 direction
- $\tau(x_1, x_2, x_3)$ - a phase function which describes the wavefront propagation
- $U_n(x_1, x_2, x_3)$ - complex amplitude which is only coordinate dependent.

The substitution of the assumed asymptotic series solution (1.3) into the equation of motion (1.1), yields with the added conditions that U_{-1} and U_{-2} be identically equal to zero, the following relation

$$(1.4) \quad N(U_n) - M(U_{n-1}) + L(U_{n-2}) = 0$$

where

$$(1.5) \quad \left\{ \begin{array}{l} N(U_n) = (A_{44}p_1^2 + A_{44}p_2^2 + A_{66}p_3^2 - 1)U_n \\ M(U_n) = A_{44}p_1 \frac{\partial U_n}{\partial x_1} + A_{44}p_2 \frac{\partial U_n}{\partial x_2} + A_{66}p_3 \frac{\partial U_n}{\partial x_3} \\ \quad + \frac{1}{\rho} \left[\frac{\partial}{\partial x_1} \left(\rho A_{44} p_1 U_n \right) + \frac{\partial}{\partial x_2} \left(\rho A_{44} p_2 U_n \right) + \frac{\partial}{\partial x_3} \left(\rho A_{66} p_3 U_n \right) \right] \\ L(U_n) = \frac{1}{\rho} \left[\frac{\partial}{\partial x_1} \left(\rho A_{44} \frac{\partial U_n}{\partial x_1} \right) + \frac{\partial}{\partial x_2} \left(\rho A_{44} \frac{\partial U_n}{\partial x_2} \right) + \frac{\partial}{\partial x_3} \left(\rho A_{66} \frac{\partial U_n}{\partial x_3} \right) \right] \end{array} \right.$$

with $A_{44} = \frac{C_{44}}{\rho}$, $A_{66} = \frac{C_{66}}{\rho}$ and $p_i = \frac{\partial \tau}{\partial x_i}$ being the

i -th component of the slowness vector. Discussions of the slowness vector and slowness surfaces can be found

in Musgrave (1970) and Kraut (1963).

Equation (1.4) must be equal to zero for all values of n ($n = 0, \infty$). Thus for $n = 0$, remembering that U_{-1} and U_{-2} are assumed equal to zero, the following condition must hold

$$(1.6) \quad (A_{44}p_1^2 + A_{44}p_2^2 + A_{44}p_3^2 - 1)U_0 = 0.$$

Assuming that U_0 is not identically zero then

$$(1.7) \quad G(x_i, p_i) = A_{44}p_1^2 + A_{44}p_2^2 + A_{66}p_3^2 = 1. \quad i = 1, 2, 3.$$

The quantities p_i are the slowness vector components and are related to the wavefront normal velocity (phase velocity) through the relation (Cerveny (1972), Cerveny and Psencik (1972))

$$(1.8) \quad p_i = \frac{N_i}{V} \quad i = 1, 2, 3$$

where N_i are the directional cosines of the wavefront normal; in case,

$$N_1 = \sin\theta\cos\phi$$

$$(1.1) \quad N_2 = \sin\theta\sin\phi$$

$$N_3 = \cos\theta.$$

The angle θ is the angle the wavefront normal makes

with the x_3 axis and ϕ is the angle of azimuth of the wavefront normal measured from the x_1 axis. Thus utilizing equations (1.7), (1.8) and (1.9) the wavefront normal velocity can be written as

$$(1.10) \quad v^2 = A_{44} \sin^2 \theta + A_{66} \cos^2 \theta$$

from which it is obvious that the wavefront is rotationally invariant about the x_3 axis.

1.3 Rays and Snell's Law

The quantity $G(x_i, p_i)$ defined in the preceding section is a homogeneous function of order 2 in p_i . From Eulers theorem on homogeneous functions, the relations

$$(1.11) \quad \sum_{i=1}^3 p_i \frac{\partial G}{\partial p_i} = 2G \quad \text{can be obtained.}$$

The equation $G(x_i, p_i) = 1$ is a nonlinear partial differential equation for $\tau(x_i)$ (which describes the propagation of the wavefront) and may be solved using the method of characteristics (Courant and Hilbert (1962)). The equations of the characteristics corresponding to the partial differential equation $G(x_i, p_i) = 1$ can be written with the help of relation (1.11) as

$$(1.12) \quad \left\{ \begin{array}{l} \frac{dx_1}{d\tau} = \frac{1}{2} \frac{\partial G}{\partial p_1} = A_{44} p_1 = \frac{A_{44} \sin \theta \cos \phi}{V} \\ \frac{dx_2}{d\tau} = \frac{1}{2} \frac{\partial G}{\partial p_2} = A_{44} p_2 = \frac{A_{44} \sin \theta \cos \phi}{V} \\ \frac{dx_3}{d\tau} = \frac{1}{2} \frac{\partial G}{\partial p_3} = A_{66} p_3 = \frac{A_{66} \cos \theta}{V} \end{array} \right.$$

The terms $\frac{dx_i}{d\tau}$ are interpreted physically as the components of the ray velocity; that is, the velocity of energy propagation. In general, in an anisotropic medium, the direction of energy propagation does not coincide with the wavefront normal direction (Musgrave (1970)). If α is denoted as the angle the ray makes with the x_3 axis (which will henceforth be assumed to be the vertical axis) and β the angle the ray makes with the x_1 axis, the relations between the ray angles and wavefront normal angles can be found by taking the ratios of the components of the ray velocity (equations (1.12)) so that

$$(1.13) \quad \tan \alpha = \frac{A_{44}}{A_{66}} \tan \theta$$

$$\tan \beta = \tan \phi$$

The magnitude of the ray velocity, a , is obtained from the inner product of $\frac{d\vec{x}}{d\tau} = \left(\frac{dx_1}{d\tau}, \frac{dx_2}{d\tau}, \frac{dx_3}{d\tau} \right)$ with itself, viz.,

$$(1.14) \quad a = \left(\frac{d\vec{x}}{d\tau} \cdot \frac{d\vec{x}}{d\tau} \right)^{\frac{1}{2}} = \left(\frac{A_{44}^2 \sin^2 \theta}{V^2} + \frac{A_{66}^2 \cos^2 \theta}{V^2} \right)^{\frac{1}{2}}$$

or using equation (1.13)

$$(1.15) \quad \frac{1}{a^2} = \frac{\sin^2 \alpha}{A_{44}} + \frac{\cos^2 \alpha}{A_{66}}.$$

Equation (1.15) is that of an ellipse, signifying that the SH wavefront is an ellipsoid. The absence of the azimuthal angle β from (1.15) implies that the SH wavefront is an ellipsoid of revolution, the x_3 axis being the axis of symmetry. It should be noted that at $\theta = \alpha = 0$, $V = a = \sqrt{A_{66}}$ and at $\theta = \alpha = \frac{\pi}{2}$, $V = a = \sqrt{A_{44}}$. Two new variables a_z and a_x corresponding respectively to $\sqrt{A_{66}}$ and $\sqrt{A_{44}}$, the velocities along the minor and major axis of the ellipsoid, will be introduced so that

$$(1.16) \quad V^2 = a_x^2 \sin^2 \theta + a_z^2 \cos^2 \theta$$

$$(1.17) \quad \frac{1}{a^2} = \frac{\sin^2 \alpha}{a_x^2} + \frac{\cos^2 \alpha}{a_z^2}.$$

The designation of the vertical axis of the ellipsoid as the minor and the horizontal axis as the major is done as in most seismological applications $a_x > a_z$; that is, the degree of anisotropy of the medium $\frac{a_x}{a_z}$ is usually greater than one.

The geometry of a part of an SH wavefront in an inhomogeneous transversely isotropic medium is shown in Figure 1. It can be seen that the projection of the ray velocity onto the wavefront normal yields the magnitude of the normal velocity, so that

$$(1.18) \quad \vec{V} \cdot \vec{a} = v^2.$$

This same result can be obtained using

$$\vec{V} = \left(\frac{N_1^2}{p_1}, \frac{N_2^2}{p_2}, \frac{N_3^2}{p_3} \right) \quad \text{and}$$

$$\vec{a} = (a_x^2 p_1, a_x^2 p_2, a_z^2 p_3)$$

together with equations (1.8) and (1.9). By definition of the inner product, $\vec{V} \cdot \vec{a} = Va \cos(\theta - \alpha)$ so that

$$(1.19) \quad a \cos(\theta - \alpha) = v.$$

1.4 Calculation of Ray Amplitudes

The solution for the complex amplitude components $U_n(x_1, x_2, x_3)$ of the ray series expansion (1.3) is an iterative one; that is, if the solution for U_n is to be found all U_k , $k < n$ must be known. In equation (1.4) it can then be assumed that $L(U_{n-1})$ is known. Call this quantity q_n . From (1.4) with $(A_{44}p_1^2 + A_{44}p_2^2 + A_{66}p_3^2 - 1) = 0$ the following expression results:


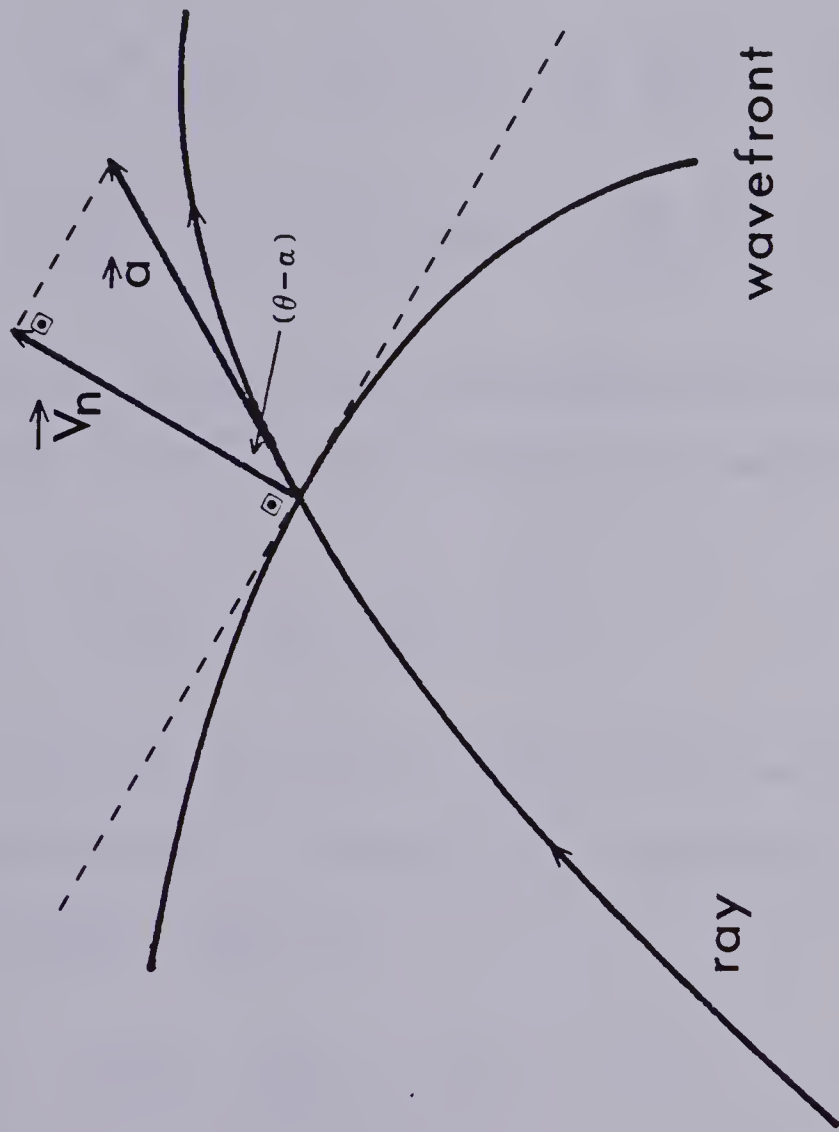


Figure 1.1 Geometry of the wave front and ray and the relation between the wave front normal velocity V_N and the ray velocity a .



$$\begin{aligned}
& 2A_{44}p_1 \frac{\partial U_n}{\partial x_1} + 2A_{44}p_2 \frac{\partial U_n}{\partial x_2} + 2A_{66}p_3 \frac{\partial U_n}{\partial x_3} + \frac{U_n}{\rho} \\
(1.20) \quad & \times \left[\frac{\partial}{\partial x_1} (\rho A_{44}p_1) + \frac{\partial}{\partial x_2} (\rho A_{44}p_2) + \frac{\partial}{\partial x_3} (\rho A_{66}p_3) \right] = q_n.
\end{aligned}$$

With the aid of equations (1.12) this can be written

$$\begin{aligned}
& 2 \left[\frac{\partial U_n}{\partial x_1} \frac{dx_1}{d\tau} + \frac{\partial U_n}{\partial x_2} \frac{dx_2}{d\tau} + \frac{\partial U_n}{\partial x_3} \frac{dx_3}{d\tau} \right] + \frac{U_n}{\rho} \\
(1.21) \quad & \left[\frac{\partial}{\partial x_1} (\rho a_1) + \frac{\partial}{\partial x_2} (\rho a_2) + \frac{\partial}{\partial x_3} (\rho a_3) \right] = q_n
\end{aligned}$$

where $a_i, i = 1, 2, 3$ are the components of the ray velocity.

Equation (1.21) can be written more compactly as

$$(1.22) \quad \frac{dU_n}{d\tau} + \frac{U_n}{2\rho} \nabla \cdot (\rho \vec{a}) = \frac{q_n}{2}.$$

Employing a vector integral theorem due to Gauss as demonstrated in Appendix A1 equation (1.22) becomes the transport equation

$$(1.23) \quad \frac{dU_n}{d\tau} + \frac{U_n}{2\rho VJ} \frac{d}{d\tau} (\rho VJ) = \frac{q_n}{2}$$

the quantity J being defined in the appendix. The solution of (1.22) is given by

$$(1.24) \quad U_n(t) = U_n(t_0) \left[\frac{(\rho VJ)_{t_0}}{(\rho VJ)_t} \right]^{\frac{1}{2}} + \frac{1}{2(\rho VJ)_t^{\frac{1}{2}}} \int_{t_0}^t (\rho VJ)_\tau^{\frac{1}{2}} q_n(\tau) d\tau$$

where t_0 defines a reference wave surface, at which the value of $U_n(t_0)$ is an initial condition which is assumed known. The integration is taken to be along the ray path from the reference wave surface to an arbitrary wave surface denoted by t .

Consequently from formula (1.24), $U_n(t)$ can be determined at an arbitrary point along the ray if its value at a previous point along the ray is known. In seismological applications the zero order or leading term in the ray expansion is usually considered to be a sufficiently good approximation. As $q_0 = 0$, equation (1.24) becomes for $n = 0$

$$(1.25) \quad U_0(t) = U_0(t_0) \left[\frac{(\rho V J)_{t_0}}{(\rho V J)_t} \right]^{\frac{1}{2}}.$$

In the problem under consideration ρ , V and J are all easily computed along the ray.

Inspection of equation (1.25) reveals that an infinite value of the ray amplitude is predicted at caustics, where the function J , which is related to the Jacobian of the transformation from Cartesian coordinates (x_1, x_2, x_3) to ray coordinates (α, β, τ) , vanishes.

Although some increase in amplitude in the vicinity of a caustic may be physically justified by claiming that energy flux becomes highly concentrated when a ray tube collapses to a condition of zero cross sectional

area, the inapplicability of equation (1.25) in the region of a caustic stems from purely mathematical considerations.

It is well known, for example, Babich and Buldirev (1972) or Cervený et. al. (1977), that the ray series expansion in equation (1.3) can be used only in such regions where the ray field is regular, implying a non-zero value of the Jacobian $D(x_1, x_2, x_3)/D(\alpha, \beta, \tau)$. As this necessary condition for the application of the ray series expansion technique is clearly violated at a caustic, no attempt should be made to discredit asymptotic ray theory by extending its results into this region.

Fortunately, alternative high frequency techniques have been developed for the evaluation of ray amplitudes in the vicinity of a caustic. Numerous papers on these techniques appear in the literature and are well documented, for example, in the monographs of Stravroudis (1972), Babich and Buldirev (1972), Babich and Kirpichnikova (1974) and Cervený et. al. (1977).

As the results produced by these alternative methods link smoothly with the asymptotic ray theory solution in the regions where the latter is justified (Choi (1978)), equation (1.25) can be used at any point of the regular ray field, provided that the effect of each caustic which the ray passes through, is included. In the high frequency limit this effect amounts to a change in phase of $\pm \frac{\pi}{2}$ for each caustic passed through.

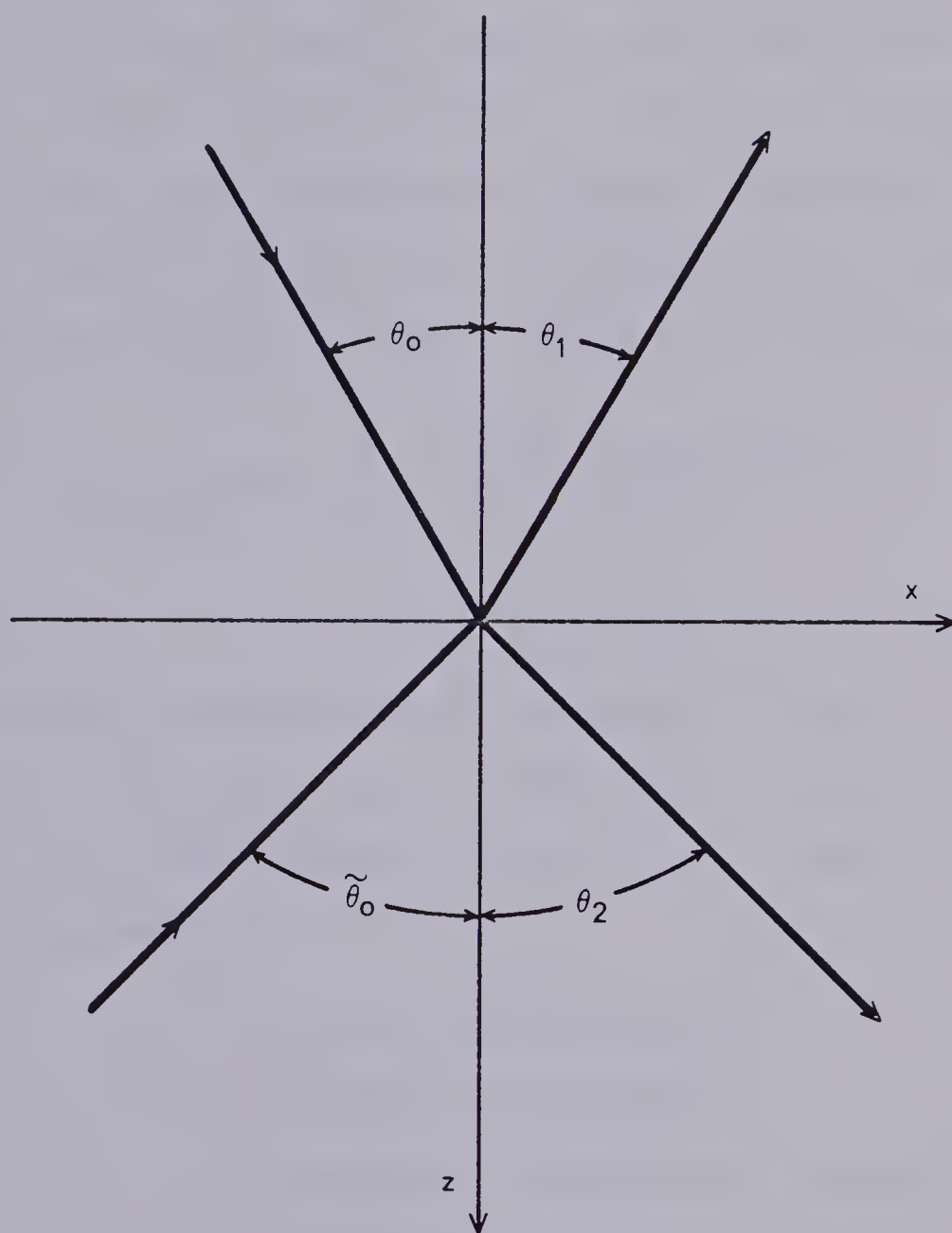
1.5 Reflection and Transmission Coefficients

At an interface between two transversely isotropic media an SH wavefront impinging on the interface from either medium gives rise to a reflected and transmitted wavefront. Let θ_0 (upper medium) and $\theta_{\tilde{0}}$ (lower medium) be the acute angles the incident SH wavefront normals make with the vertical axis and θ_v , $v = 1, 2$ be the acute angles the reflected and transmitted wavefronts make with the vertical axis. The reflected or transmitted wavefront in the upper medium will be specified by $v = 1$ while $v = 2$ will typify the same quantities in the lower medium, as shown in Figure 2. To simplify notation in what follows, the horizontal axis will be denoted as the x-axis and the vertical axis as the z-axis with the positive direction chosen to be downwards. Further, it will be assumed that the interface is planar and that the axes of rotational invariance of the wavefronts are aligned perpendicular to the interface. Thus Snell's Law for this case can be written

$$(1.26) \quad \frac{\sin \theta_0}{V_1} = \frac{\sin \theta_v}{V_v}$$

where it is to be remembered that V_0 and V_v are functions of θ_0 and θ_v . Employing the equations (1.13), (1.14) and (1.15) a modified Snell's Law can be obtained in terms of the ray velocities and angles in the form

Figure 1.2 The wave front normals of incidence (θ_0 and $\bar{\theta}_0$) and reflection and refraction (θ_1 and θ_2) of SH wave fronts at an interface between two transversely isotropic media.



$$(1.27) \quad \frac{a_0 \sin \alpha_0}{a_{x_0}} = \frac{a_v \sin \alpha_v}{a_{x_v}} .$$

If the two media described above are in welded contact, the two boundary conditions which must be satisfied at their common interface are the continuity of shear stress and displacement. The plane of incidence can be chosen without any loss of generality as the (x,z) plane. Under the last assumption, an arbitrary displacement vector in either medium can be written as

$$(1.28) \quad \vec{u}_v(x,z,t) = \sum_{n=0}^{\infty} \frac{\vec{U}_{nv}(x,z) \exp[i\omega(t-\tau_v)]}{(i\omega)^n}$$

where $\vec{U}_{nv}(x,z) = U_{nv}(x,z) \vec{n}_{SH}$, \vec{n}_{SH} being a unit vector perpendicular to the plane of incidence (in the y direction). The subscript v identifies the type and medium of the displacement vector while τ_v does the same for the wavefront.

$v = 0$ - incident from medium 1

$v = \tilde{0}$ - incident from medium 2

$v = 1$ - reflected/transmitted in medium 1

$v = 2$ - reflected/transmitted in medium 2

Continuity of displacement has

$$(1.29) \quad U_{n1} - U_{n2} = \begin{cases} -U_{n0} \\ U_{n\tilde{0}} \end{cases}$$

It should be recalled that

$$(1.30) \quad \frac{\partial \tau_v}{\partial x} = \frac{\sin \theta_v}{V_v}$$

and that

$$(1.31) \quad \frac{\partial \tau_v}{\partial x} = (-1)^{v+\delta_{v0}} \frac{\cos \theta_v}{V_v} .$$

The choice of sign in (1.31) is determined by the physical requirement that the solution for the disturbance approach zero as the wavefront moves away from the interface to infinity.

The continuity of shear stress requires

$$(1.32) \quad \sum_{v=1}^2 (-1)^v \sigma_{yz}(\vec{u}_v) = \begin{cases} \sigma_{yz}(\vec{u}_0) \\ -\sigma_{yz}(\vec{u}_{\tilde{0}}) \end{cases}$$

where

$$\sigma_{yz}(\vec{u}_v) = C_{44}^{(v)} \left[\frac{\partial (u_y)_v}{\partial z} + \frac{\sigma (u_z)_v}{\partial y} \right] .$$

This yields

$$(1.33) \quad \sum_{v=1}^2 \frac{C_{44}^{(v)} \cos \theta_v U_{nv}}{V_v} = F + \sum_{v=1}^2 (-1)^v C_{44}^{(v)} \frac{\partial U_{(n-1)v}}{\partial z}$$

where for incidence from above

$$F = \frac{C_{44}^{(0)} \cos \theta_0}{V_0} U_0 - C_{44}^{(0)} \frac{\partial U_{(n-1)0}}{\partial z}$$

and for incidence from below

$$F = \frac{C_{44}^{(\tilde{0})} \cos \theta_{\tilde{0}}}{V_{\tilde{0}}} U_{n\tilde{0}} + C_{44}^{(\tilde{0})} \frac{\partial U_{(n-1)\tilde{0}}}{\partial z}.$$

In the zero order approximation ($n=0$) equations (1.29) and (1.33) yield two sets of linear equations in two unknowns; the unknowns being the ratios of the reflected and transmitted amplitudes to the incident amplitude. At this point it should be recalled that in an earlier section $U_{(-1)\nu}$ was set equal to zero.

As the axis of rotational invariance was chosen perpendicular to the interface, it follows that $\theta_0 = \theta_1$, and $\theta_{\tilde{0}} = \theta_2$ and consequently $V_{\tilde{0}} = V_1$ and $V_{\tilde{0}} = V_2$.

At the interface $C_{44}^{(0)} = C_{44}^{(1)} = B_1$ and $C_{44}^{(0)} = C_{44}^{(2)} = B_2$.

Thus

$$(1.34a) \quad \begin{bmatrix} 1 & -1 \\ \frac{B_1 \cos \theta_1}{V_1} & \frac{B_2 \cos \theta_2}{V_2} \end{bmatrix} \begin{bmatrix} U_{01} \\ U_{02} \end{bmatrix} = \begin{bmatrix} -1 \\ \frac{B_1 \cos \theta_1}{V_1} \end{bmatrix} U_{00}$$

for a wavefront incident from above (medium 1) and

$$(1.34b) \quad \begin{bmatrix} 1 & -1 \\ \frac{B_1 \cos \theta_1}{V_1} & \frac{B_2 \cos \theta_2}{V_2} \end{bmatrix} \begin{bmatrix} U_{01} \\ U_{02} \end{bmatrix} = \begin{bmatrix} 1 \\ \frac{B_2 \cos \theta_2}{V_2} \end{bmatrix} U_{00}^{\sim}$$

for incidence from below (medium 2). The solutions of (1.34a) and (1.34b) are given as $R_{\mu\nu}$ where μ typifies the incident and ν the resultant wavefront moving away from the interface.

$$(1.35) \quad \left\{ \begin{aligned} R_{11} &= \left(\frac{B_1 \cos \theta_1}{V_1} - \frac{B_2 \cos \theta_2}{V_2} \right) / D \\ R_{12} &= \frac{2B_1 \cos \theta_1}{V_1} / D \\ R_{21} &= \frac{2B_2 \cos \theta_2}{V_2} / D \\ R_{22} &= \left(\frac{B_2 \cos \theta_2}{V_2} - \frac{B_1 \cos \theta_1}{V_1} \right) / D \\ D &= \frac{B_1 \cos \theta_1}{V_1} + \frac{B_2 \cos \theta_2}{V_2} \end{aligned} \right.$$

1.6 Geometrical Spreading

The quantity J mentioned in equations (1.23), (1.24) and (1.25) can be physically interpreted as the measure of incremental cross sectional area of a ray tube (as shown in the appendix) and consequently it is conceptually convenient to write equation (1.25) in the form

$$(1.36) \quad U(M) = U(M_O) \left[\frac{V(M_O) \rho(M_O)}{V(M) \rho(M)} \right]^{\frac{1}{2}} \left[\frac{d\sigma(M_O)}{d\sigma(M)} \right]^{\frac{1}{2}}$$

where M_O is a point on the reference surface and M is an arbitrary point along the ray.

If the ray traverses through a medium from a reference point M_O and encounters an interface at the point O and is either reflected back into the medium of incidence or transmitted into the second medium, the amplitude measured by a receiver at point M is generally different than that given by equation (1.36) as the discontinuity of the elastic parameters at the interface introduces effects which must be taken into account. The ray now essentially consists of two segments and the amplitude at M can be written as

$$(1.37) \quad U(M) = U(M_O) \left[\frac{V(M_O) \rho(M_O)}{V(M) \rho(M)} \right]^{\frac{1}{2}} \left[\frac{d\rho(M_O)}{d\rho(M)} \right]^{\frac{1}{2}}$$

$$\left[\frac{V' \rho'}{V \rho} \right]_O^{\frac{1}{2}} \left[\frac{d\sigma'}{d\sigma} \right]_O^{\frac{1}{2}} R$$

where V and ρ denote the velocity and density at the point O on the side of the incident ray, V' and ρ' denote the same parameters at the beginning of the second segment of the ray and R is the appropriate reflection or transmission coefficient.

Assuming that a total ray is composed of $k+1$

segments, where a ray segment will be defined as the part of the total ray between one reflection or refraction and the next (Figure 3), equation (1.37) can be generalized to read

$$(1.38) \quad U(M) = \frac{U(M_o)}{L} \left[\frac{V(M_o) \rho(M_o)}{V(M) \rho(M)} \right]^{\frac{1}{2}} \prod_{j=1}^k \left[\frac{V'_j \rho'_j}{V_j \rho_j} \right]^{\frac{1}{2}}_{O_j} R_j$$

where the primed quantities are as previously defined, R_j is the reflection or transmission coefficient at the point O_j and L is given by

$$(1.39) \quad L = \left[\frac{d\sigma(M)}{d\sigma(M_o)} \right]^{\frac{1}{2}} \prod_{j=1}^k \left[\frac{d\sigma}{d\sigma'} \right]^{\frac{1}{2}}_{O_j}$$

and serves as a measure of the geometrical spreading of the ray tube.

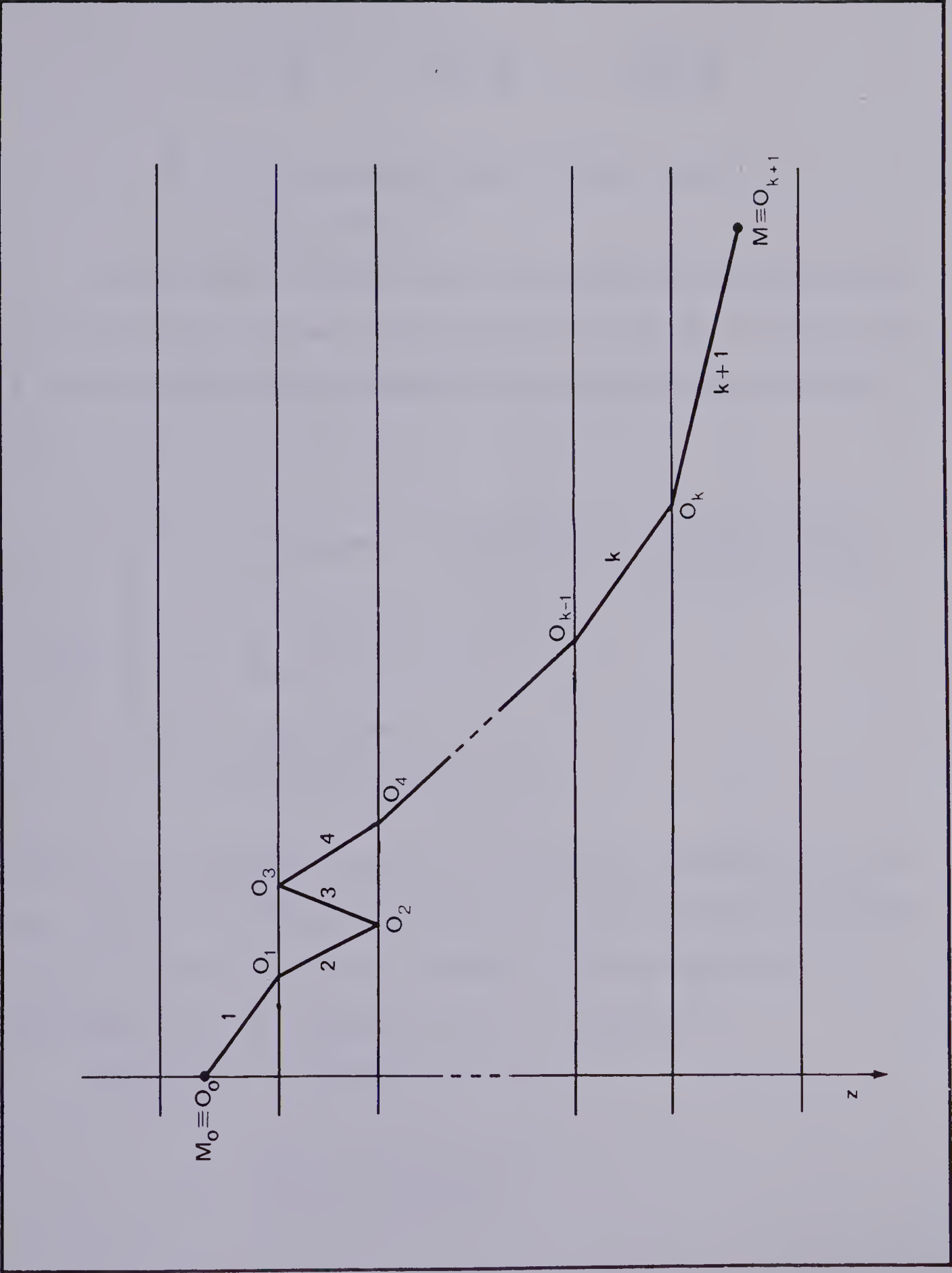
The remainder of this section will be devoted to obtaining an expression for the geometrical spreading L , for the simple case of plane parallel homogeneous layers, in which the axes of rotational invariance of the wave-fronts are perpendicular to the interfaces.

If α and β are parameters which describe the ray, $d\sigma$ can be expressed using the standard formula from the differential geometry of surfaces as

$$(1.40) \quad d\sigma = J d\alpha d\beta$$

where

Figure 1.3 Definition of interface coordinates and ray segments.



$$J = (EH - G^2)^{\frac{1}{2}}$$

$$E = \frac{\partial \vec{R}}{\partial \alpha} \cdot \frac{\partial \vec{R}}{\partial \alpha} \quad G = \frac{\partial \vec{R}}{\partial \alpha} \cdot \frac{\partial \vec{R}}{\partial \beta} \quad H = \frac{\partial \vec{R}}{\partial \beta} \cdot \frac{\partial \vec{R}}{\partial \beta}$$

\vec{R} = the position vector of the ray of
magnitude R.

As the SH wavefront is an ellipsoid of revolution in a homogeneous medium, the components (x,y,z) of the vector R can be expressed in standard polar coordinate notation as

$$(1.41) \quad \begin{cases} x = R \sin \alpha \cos \beta = a_x t \sin \alpha \cos \beta = \frac{a_x t \sin \alpha \cos \beta}{\{F + (1-F) \sin^2 \alpha\}^{\frac{1}{2}}} \\ y = \frac{a_x t \sin \alpha \sin \beta}{\{F + (1-F) \sin^2 \alpha\}^{\frac{1}{2}}} \\ z = \frac{a_x t \cos \alpha}{\{F + (1-F) \sin^2 \alpha\}^{\frac{1}{2}}} \end{cases}$$

where $a = a_x / \{F + (1-F) \sin^2 \alpha\}^{\frac{1}{2}}$ is the ray velocity, a_x is the velocity of the wavefront in the horizontal direction ((x,y) plane), a_z is the velocity of the wavefront in the vertical (z) direction and $F = (a_x / a_z)^2$.

Implementing equations (1.40)

$$E = \frac{a_x^2 t^2 (\sin^2 \alpha + F^2 \cos^2 \alpha)}{(F + (1-F) \sin^2 \alpha)^3}$$

$$G = 0$$

$$H = \frac{a_x^2 t^2 \sin^2 \alpha}{(F + (1-F) \sin^2 \alpha)}$$

and thus

$$(1.42) \quad d\sigma = \frac{R^2 \sin \alpha d\alpha d\beta}{\cos(\theta - \alpha)},$$

θ being the angle which the wavefront normal makes with the vertical axis.

The reference surface will be chosen such that the component of the position vector defining a point on the wave surface has unit length in the vertical direction. This being so, with $R = at$, t must have a magnitude of

$$\frac{1}{|a_z|}. \quad \text{Thus, } R_o = \frac{a}{|a_z|}, \text{ where } a_z \text{ has units of } t^{-1}.$$

This yields

$$(1.43) \quad d\sigma(M_o) = \frac{a^2 \sin \alpha_o d\alpha_o d\beta_o}{|a_z|^2 \cos(\theta_o - \alpha_o)}.$$

An alternate expression for $d\sigma(M)$ can be obtained from simple geometrical considerations (Figure 4).

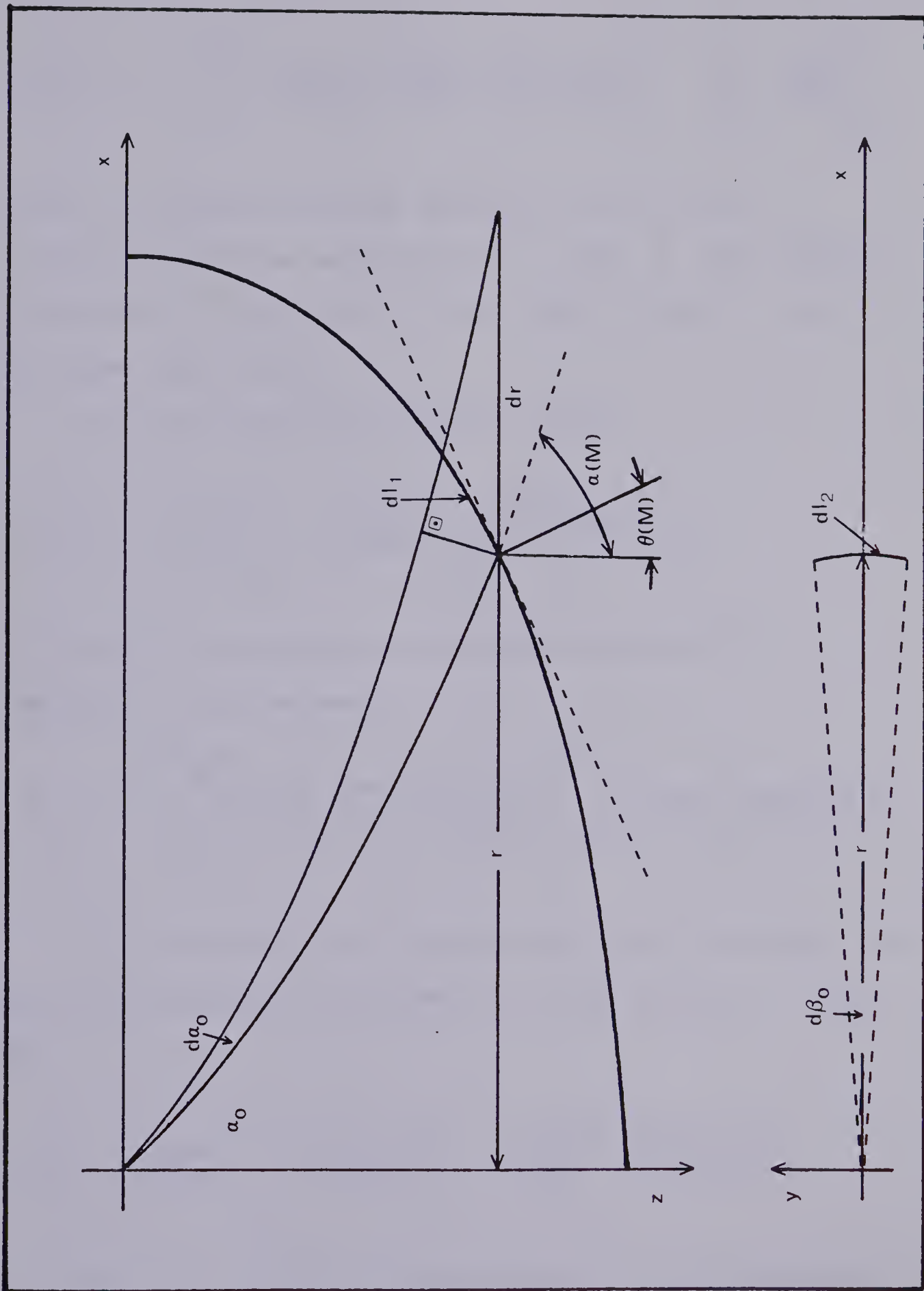
$$(1.44) \quad d\sigma(M) = d\ell_1 d\ell_2$$

where it can be seen from Figure 4

$$(1.45) \quad \begin{cases} d\ell_1 = \left| \frac{\partial r}{\partial \alpha_o} \right| \frac{\cos \alpha_M d\alpha_o}{\cos(\theta_M - \alpha_M)} \\ d\ell_2 = r d\beta_o \end{cases}$$



Figure 1.4 The geometry of a ray tube and definition of quantities used to calculate an alternate expression for $d\sigma(M)$ [Equation (1.45)].



which yields

$$(1.46) \quad L = \left[\frac{a_z^2}{a_1^2} r \left| \frac{\partial r}{\partial \alpha_O} \right| \frac{\cos \alpha_M}{\sin \alpha_O} \frac{\cos(\theta_O - \alpha_O)}{\cos(\theta_M - \alpha_M)} \right]^{\frac{1}{2}} \prod_{j=1}^k \left[\frac{d\sigma}{d\sigma'} \right]^{\frac{1}{2}}_{O_j}$$

where it has been assumed that M_O lies in layer 1 accounting for the subscripts on a_z and a and further, that $d\sigma(M)$ is valid even if the point M does not lie in the same layer as M_O .

It can be seen from Figure 5 that

$$(1.47) \quad \left[\frac{d\sigma}{d\sigma'} \right]^{\frac{1}{2}}_{O_j} = \left[\frac{\cos \alpha}{\cos \alpha'} \right]^{\frac{1}{2}}_{O_j} \left[\frac{\cos(\theta' - \alpha')}{\cos(\theta - \alpha)} \right]^{\frac{1}{2}}_{O_j}$$

and after introducing this interface correction, equation (1.46) becomes

$$(1.48) \quad L = \left[\frac{a_z^2}{a_1^2} r \left| \frac{\partial r}{\partial \alpha_O} \right| \frac{\cos \alpha_M}{\sin \alpha_O} \frac{\cos(\theta_O - \alpha_O)}{\cos(\theta_M - \alpha_M)} \right]^{\frac{1}{2}} \prod_{j=1}^k \left[\frac{\cos \alpha}{\cos \alpha'} \right]^{\frac{1}{2}}_{O_j} \left[\frac{\cos(\theta' - \alpha')}{\cos(\theta - \alpha)} \right]^{\frac{1}{2}}_{O_j}.$$

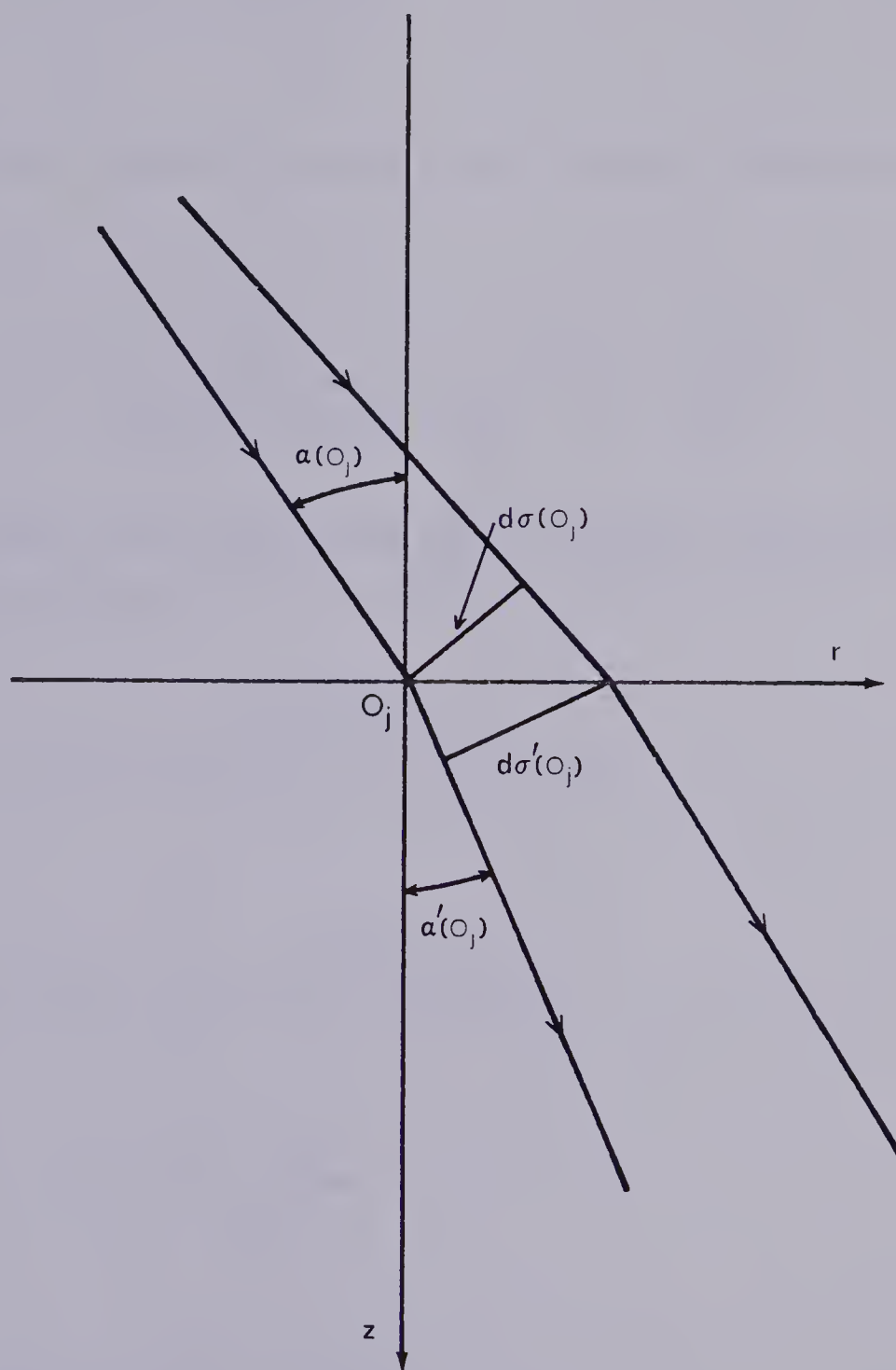
In the case under consideration, the interfaces are plane and the media homogeneous so that $\alpha'(O_{j-1}) = \alpha(O_j)$ and

$$(1.49) \quad \prod_{j=1}^k \left[\frac{\cos \alpha}{\cos \alpha'} \right]^{\frac{1}{2}}_{O_j} \left[\frac{\cos(\theta' - \alpha')}{\cos(\theta - \alpha)} \right]^{\frac{1}{2}} = \left[\frac{\cos \alpha_O}{\cos \alpha_M} \right]^{\frac{1}{2}} \left[\frac{\cos(\theta_M - \alpha_M)}{\cos(\theta_O - \alpha_O)} \right]^{\frac{1}{2}}.$$

To aid in numerical computations it is convenient to parameterize all angles in terms of one angle, say



Figure 1.5 The discontinuity of a ray tube at an interface indicating the interface correction which must be introduced into the expression for geometrical spreading. It can be seen that at the interface $d\sigma/d\sigma' = d\ell/d\ell'$, as the spreading in the azimuthal direction is the same on both sides of the interface.



$\alpha_0 = \alpha_1$. If the acute angle the j -th ray segment makes with the vertical is denoted as α_j then from equation (1.27)

$$(1.27)' \quad \frac{\frac{a_1 \sin \alpha_1}{2}}{a_{x_1}} = \frac{\frac{a_j \sin \alpha_j}{2}}{a_{x_j}}$$

where the ray velocity along the j -th ray segment is given by

$$(1.50) \quad a_j = \frac{a_{x_j}}{(F_j + (1-F_j) \sin^2 \alpha_j)}, \quad F_j = \left(\frac{a_{x_j}}{a_{z_j}} \right)^2.$$

From the above two equations the following quantities can be obtained

$$(1.51) \quad \left\{ \begin{aligned} \sin \alpha_j &= \frac{\sqrt{k_j F_j} \sin \alpha_1}{[1 + (F_j - 1) k_j \sin^2 \alpha_1]^{\frac{1}{2}}} \\ \cos \alpha_j &= \left[\frac{1 - k_j \sin^2 \alpha_1}{1 + (F_j - 1) k_j \sin^2 \alpha_1} \right]^{\frac{1}{2}} \\ k_j &= \frac{a_1^2 a_{x_j}^2}{a_{x_1}^4} \end{aligned} \right.$$

For plane homogeneous layers

$$(1.52) \quad r = \sum_{j=1}^{k+1} r_j = \sum_{j=1}^{k+1} h_j \tan \alpha_j = \sum_{j=1}^{k+1} \frac{h_j \sqrt{k_j F_j} \sin \alpha_1}{(1 - k_j \sin^2 \alpha_1)^{\frac{1}{2}}}$$

where h_j is the thickness of the layer in which the j -th ray segment is propagating and r_j is the horizontal distance the j -th ray segment travels.

As an analytic expression for r_j in terms of α_1 exists the calculation of $\frac{\partial r}{\partial \alpha_0} = \frac{\partial r}{\partial \alpha_1}$ presents no problems so that

$$(1.53) \quad \frac{\partial r}{\partial \alpha_1} = \sum_{j=1}^{k+1} \frac{h_j a_{xj}^2 a_1^2}{a_{zj} a_{z1}^2 a_{x1}^2} \frac{\cos \alpha_1}{(1 - k_j \sin^2 \alpha_1)^{3/2}}.$$

Substituting the expressions (1.49), (1.52) and (1.53) into equation (1.48), the resultant expression measuring the geometrical spreading, equation (1.54) becomes

$$(1.54) \quad L = \frac{a_1}{a_{x1}^2} \cos \alpha_1 \left[\sum_{j=1}^{k+1} \frac{h_j a_{xj}^2}{a_{zj} (1 - k_j \sin^2 \alpha_1)^{1/2}} \sum_{j=1}^{k+1} \frac{h_j a_{xj}^2}{a_{zj} (1 - k_j \sin^2 \alpha_1)^{3/2}} \right]^{1/2}.$$

For homogeneous media, the density and normal velocity is constant along each ray segment. This results in equation (1.38), the expression for the complex amplitude, reducing to

$$(1.55) \quad U(M) = \frac{U(M_0)}{L} \prod_{j=1}^{k+1} R_j$$

where L is given by (1.54).

1.7 The Head Wave

In this section the head wave corresponding to critically refracted ray will be examined. This problem for the isotropic case, including SH waves as well as coupled P-SV waves has been treated extensively in the literature, notably the book by Cervený and Ravindra (1971) in which numerous references are cited. The approach used will employ asymptotic ray theory which as the name suggests asymptotically approaches the solution attainable by exact (integral transform) methods. This asymptotic solution is reasonably accurate at distances removed from the critical point, however it tends to break down in the vicinity of this point. Other methods of solution must be used here, due not only to the inapplicability of asymptotic ray theory but also the effects introduced due to the interference of the reflected and head wave near the critical point (Cervený, (1965), Cervený (1967)).

Considered will be two half spaces in welded contact, the parameters of the upper and lower media being denoted 1 and 2, respectively. The velocity structure will be assumed such that for some real angle of incidence $\alpha_1^*, \alpha_2^* = \frac{\pi}{2}$ so that from equation (1.27)

$$a_1 \frac{\sin \alpha_1^*}{a_{x_1}} = \frac{1}{a_{x_2}} \quad \text{which is equivalent to saying that for}$$

some θ_1^* (wavefront normal angle) $\theta_2^* = \frac{\pi}{2}$ so that

$$\frac{\sin \theta_1^*}{V_1} = \frac{1}{a_{x_2}} .$$

A reference point M_O will be chosen a distance h above the interface at $t=0$ and a two segment ray, the geometry of which is shown in Figure 6 will be considered. Then

$$(1.56) \quad \left\{ \begin{array}{l} r = h \tan \alpha_1 + H \tan \alpha_2, \\ \bar{l} = \frac{H}{\cos \alpha_2} = (r - h \tan \alpha_1) / \sin \alpha_2. \end{array} \right.$$

and

$$(1.57) \quad \frac{\partial r}{\partial \alpha_1} = \frac{1}{\cos^2 \alpha_2} \frac{a_{x_2}^2 a_{z_2}^2 a_1^3 \cos \alpha_1}{a_{x_1}^2 a_{z_1}^2 a_2^3} \left[\bar{l} + \frac{h a_{x_1}^2 a_{z_1}^2 a_2^3 \cos^2 \alpha_2}{a_{x_2}^2 a_{z_2}^2 a_1^3 \cos^3 \alpha_1} \right]$$

$$= \frac{1}{\cos^2 \alpha_2} \frac{\partial \tilde{r}}{\partial \alpha_1}$$

so that the measure of the geometrical spreading from equation (1.48) is

$$(1.58) \quad L = \frac{1}{\cos \alpha_2} \left[\frac{a_{z_1}^2}{a_1^2} r \left| \frac{\partial \tilde{r}}{\partial \alpha_1} \right| \cot \alpha_1 \right]^{1/2} = \frac{\tilde{L}}{\cos \alpha_2} .$$

The expression for the zero order term approximation


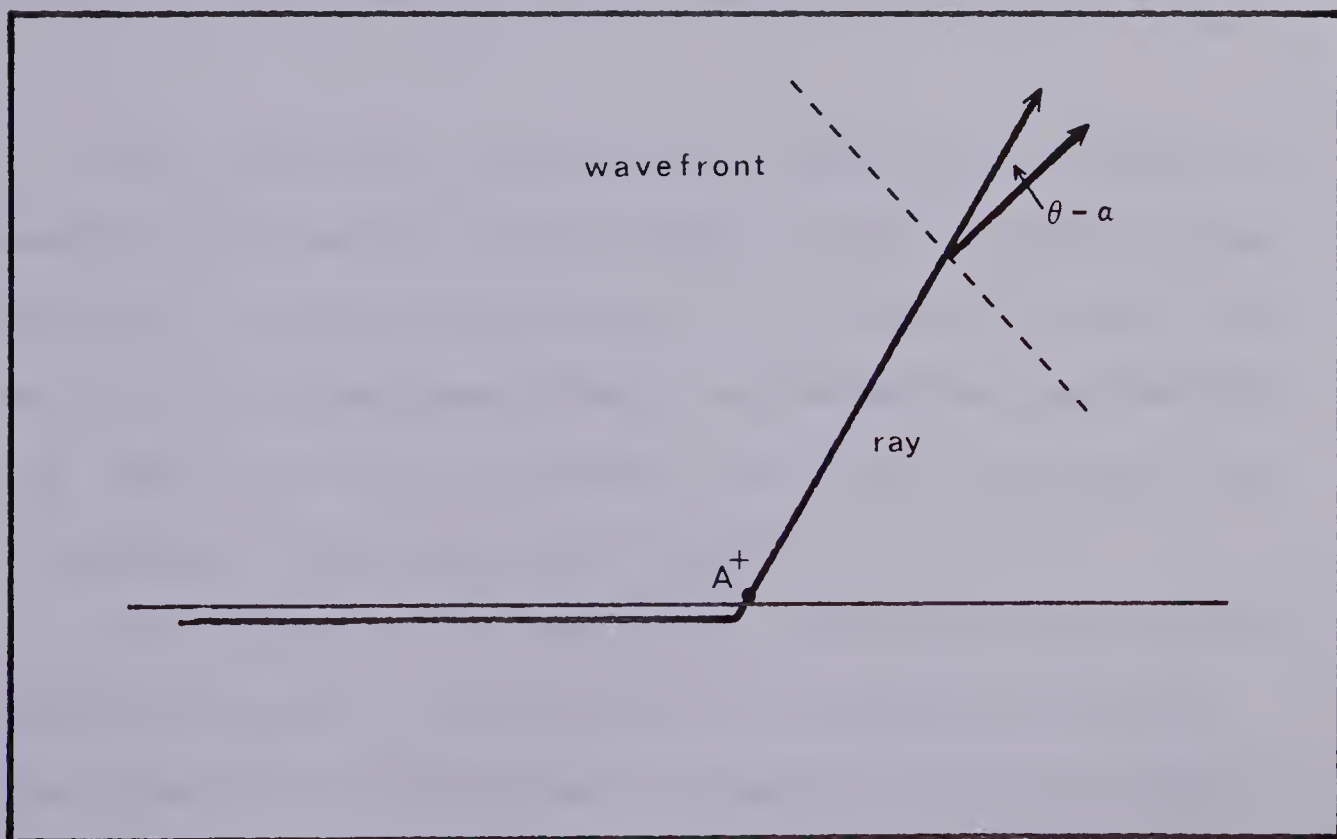
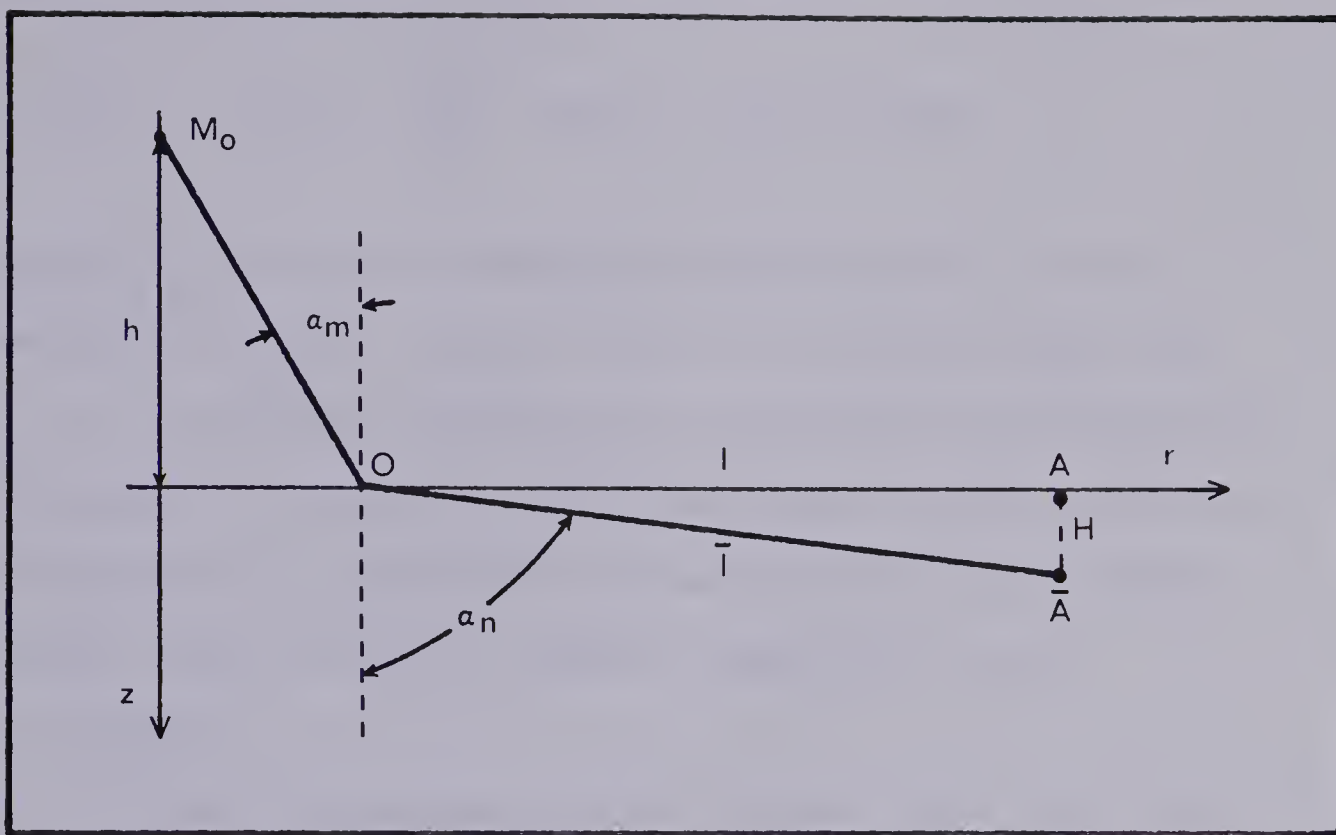


Figure 1.6 The geometry and notation used in deriving an expression for the head wave amplitude. The points A^+ and A^- lie, respectively, above and below the interface. To obtain the amplitude at A^- in terms of the amplitude at A^+ , the transmission effects across the interface must be taken into account.



of the complex amplitude at the point A is

$$(1.59) \quad U_0(A) = \frac{R_{12}}{\tilde{L}} \cos \alpha_2 = \tilde{U}_0(A) \cos \alpha_2$$

where R_{12} is the transmission coefficient given by equation (1.35). From (1.59) it is obvious that for $\alpha_2 = \frac{\pi}{2}$ (critical refraction), the complex amplitude at the point A_+ just below the interface is zero, and as a consequence to determine the amplitude at A_+ , higher order terms in the ray series expansion must be considered.

It will be shown in what follows, that the first non vanishing term or leading term in the series is

$$(1.60) \quad \vec{u}(A_+) = \frac{1}{(i\omega)} U_1(A_+) \exp i\omega\{[t-\tau_{12}(A_+)]\} \vec{n}_{SH}.$$

The critically refracted ray can be considered as a special case of the ray incident at the interface from medium 2. Before proceeding, it is useful to take into account the interface effects and obtain an expression for this critically refracted ray at A_- just above the interface in the upper half-space.

To determine the amplitude just above the interface at A_- in medium 1 the effects of transmission across the interface from medium 2 to medium 1 must be determined. For $\theta_2 = \alpha_2 = \frac{\pi}{2}$ the continuity of displacement

and shear stress at the interface for incidence from medium 2 using equations (1.29) and (1.33) yields

$$(1.61) \quad \begin{bmatrix} 1 & -1 \\ \frac{B_1 \cos \theta_1}{V_1} & \frac{B_2 \cos \theta_1}{V_2} \end{bmatrix} \begin{bmatrix} U_1(A_+) \\ U_1(A_-) \end{bmatrix} = \begin{bmatrix} 0 \\ \frac{B_2 \partial U_0(A_+)}{\partial z} \end{bmatrix}$$

$\theta_2^* = \frac{\pi}{2}$

where it is to be remembered that θ_j and V_j ($j=1,2$) refer to the wavefront and not the ray.

The solution of (1.61) for the complex amplitude of the first term in the ray series in the ray refracted back into medium 1 is

$$(1.62) \quad U_1(A_-) = \frac{B_2}{B_1 \cos \theta_1^* / V_1^*} \frac{\partial U_0(A_+)}{\partial z} = M_{21} \frac{\partial U_0(A_+)}{\partial z}.$$

Thus the expression for the displacement vector at a point A_- just above the interface is

$$(1.63) \quad \vec{u}^*(A_-) = \frac{M_{21}}{(i\omega)} \frac{\partial U_0(A_+)}{\partial z} \exp\{i\omega[t - \tau_{121}(A_-)]\} \vec{n}_{SH}.$$

But from equations (1.57), (1.58) and (1.59)

$$(1.64) \quad \begin{aligned} \frac{\partial U_0(A_+)}{\partial z} &= \lim_{H \rightarrow 0} \frac{\partial U_0(A_+)}{\partial H} = \frac{1}{\ell} \lim_{\alpha_2^* \rightarrow \frac{\pi}{2}} \frac{\partial U_0(A_+)}{\partial \alpha_2} \\ &= \frac{1}{\ell} \left[\tilde{U}_0(A_+) \right]_{\alpha_2^* = \frac{\pi}{2}} = \frac{R_{12}^* F_2^{\frac{1}{2}} \tan \alpha_1^*}{r^{\frac{1}{2}} \ell^{3/2}}. \end{aligned}$$

This ray which is critically refracted at the interface between the two halfspaces and transmitted back into the first halfspace is called a head wave (Cerveny and Ravindra (1971)). Introducing the head wave coefficient $\Gamma_{121} = R_{12}^* M_{21}$ the head wave amplitude at A_- can be written as

$$(1.65) \quad \vec{u}^*(A_-) = \frac{\Gamma_{121} F_2^{\frac{1}{2}} \tan \alpha_1^*}{\omega r(A_-) \ell^{3/2}} \exp\{[t - \tau_{121}(A_-)] - \frac{i\pi}{2}\} \vec{n}_{SH}.$$

To compute the displacement of the head wave due to the leading term in the ray series at the point M in medium 1, the following relation can be used

$$(1.66) \quad U^*(M) = \left[\frac{d\sigma(A_-)}{d\sigma(M)} \right]^{\frac{1}{2}} U^*(A_-).$$

As the waves emanating from A_- are conical, geometrical spreading occurs only in the azimuthal (β) direction so that

$$(1.67) \quad \frac{d\sigma(A_-)}{d\sigma(M)} = \frac{r(A_-)}{r(M)}$$

and the head wave displacement vector at M is given by

$$(1.68) \quad \vec{u}^*(M) = \frac{\Gamma_{121} F_2^{\frac{1}{2}} \tan \alpha_1^*}{\omega r(M) \ell^{3/2}} \exp\{i\omega[t - \tau_{121}(M)] - \frac{i\pi}{2}\} \vec{n}_{SH}.$$

1.8 Numerical Results

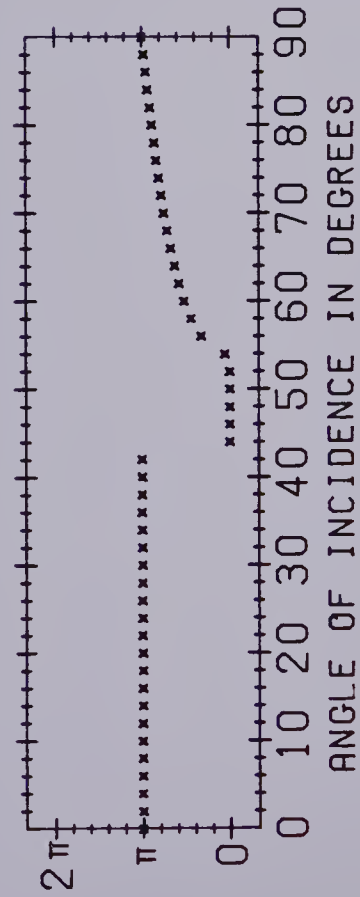
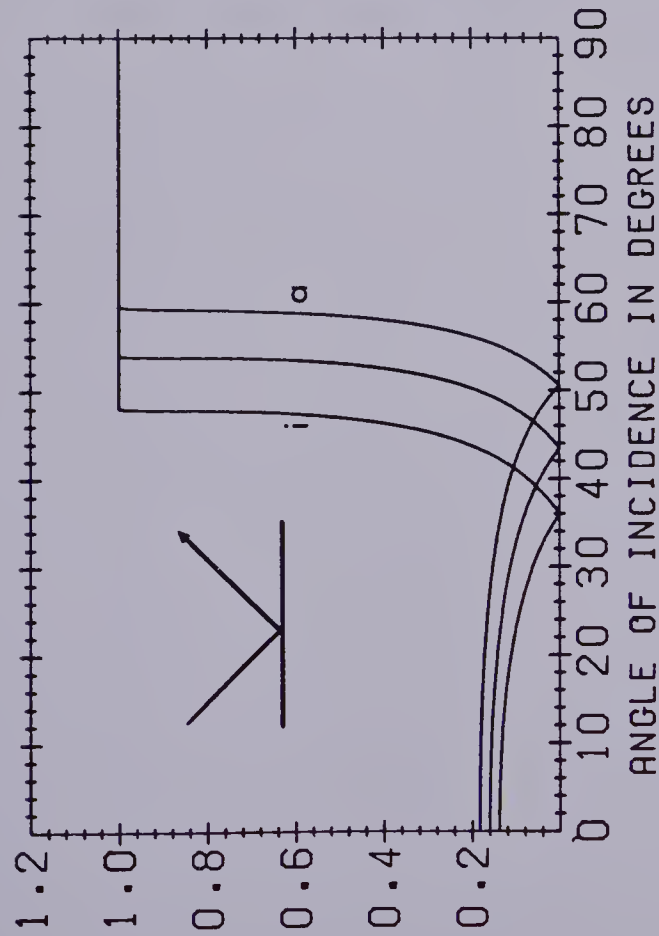
Figures 7 and 8 demonstrate the effects that varying anisotropy has on reflection and transmission coefficients. The parameters a_x and a_z are varied in the upper medium (medium 1) while the velocities in the second medium are held constant. The coefficients are plotted for 0%, 10% and 20% anisotropy in medium 1 and 10% anisotropy in medium 2. The degree of anisotropy in both media is defined to be $\frac{(a_x - a_z)}{a_z} \times 100\%$. The actual velocities used for each of the three curves are given in Table 1.

An attempt has been made to negate the effects of changing impedance at the interface by forcing $(a_{x1} + a_{z1})$ to be constant in each of the three cases considered. As the coefficients are complex quantities, two plots, one of ray angle of incidence vs. amplitude and one of ray angle of incidence vs. phase, are presented for each of the four coefficients. The phase is plotted only once (for 10% anisotropy) as it is obvious how it will behave in the other two cases.

A comparison of log. amplitude-distance curves for a once reflected ray and its corresponding head wave is given in Figure 9. The curves lettered (a) correspond to 0% anisotropy in layer 1 while those lettered (b) refer to 20% anisotropy in layer 1 and the velocities used are those given in Table 1. The loga-

Figure 1.7 The reflection coefficient H_{1H1} and the transmission coefficient H_{2H1} for 0(i), 10, and 20(a) percent anisotropy in layer 1, for the media specified in Table 1.

H1H1



H2H1

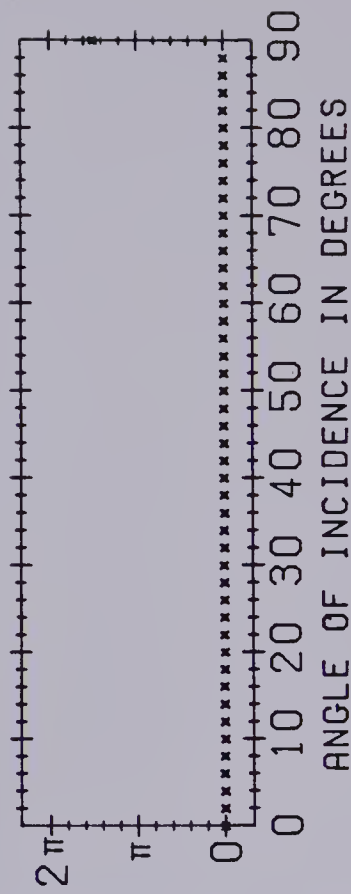
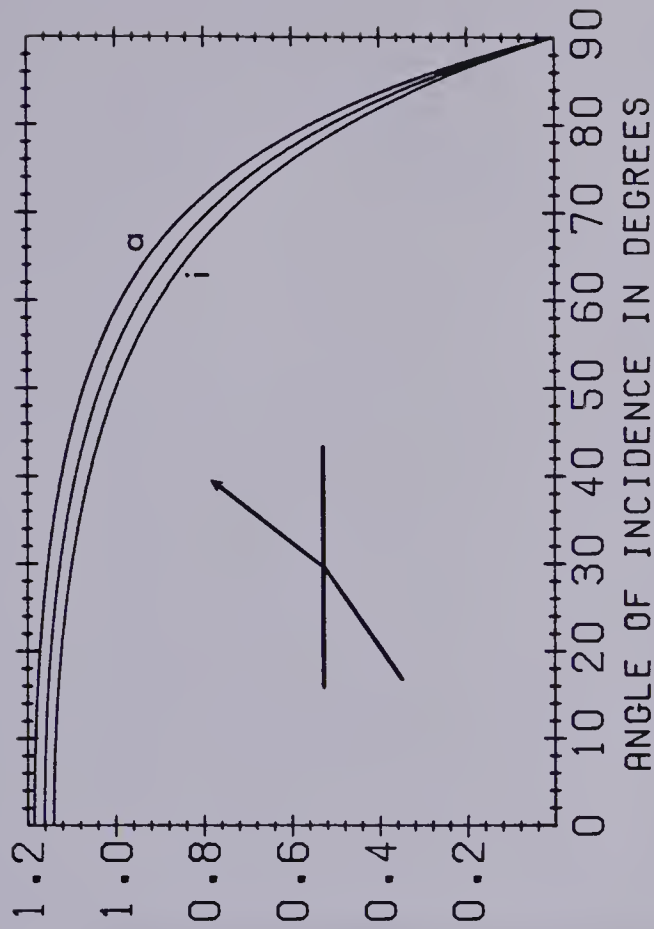
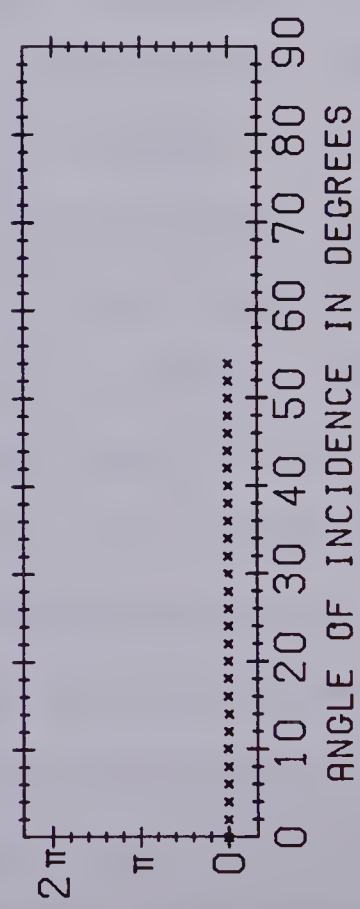
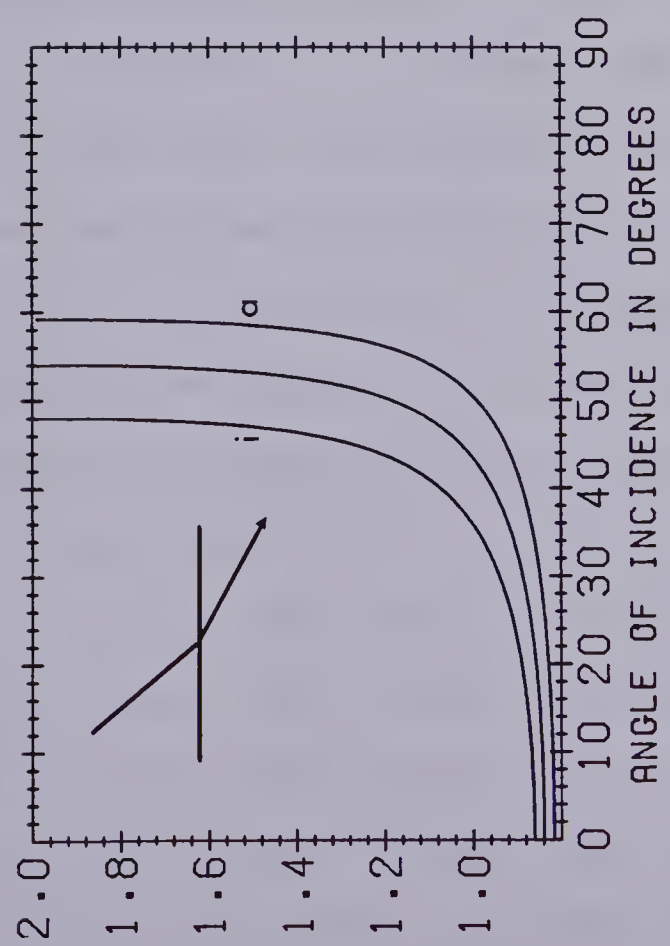
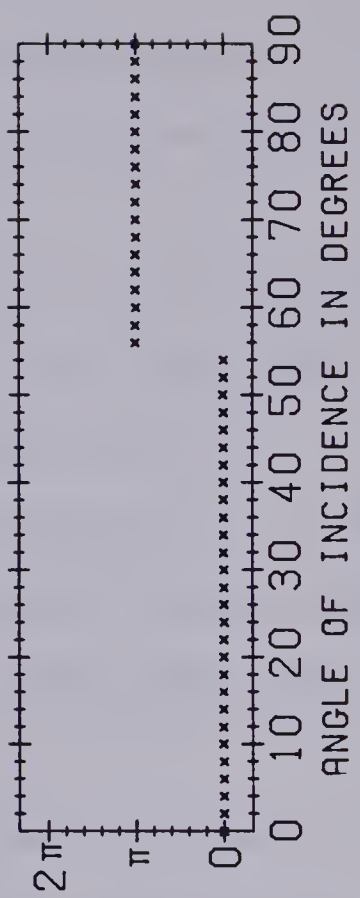
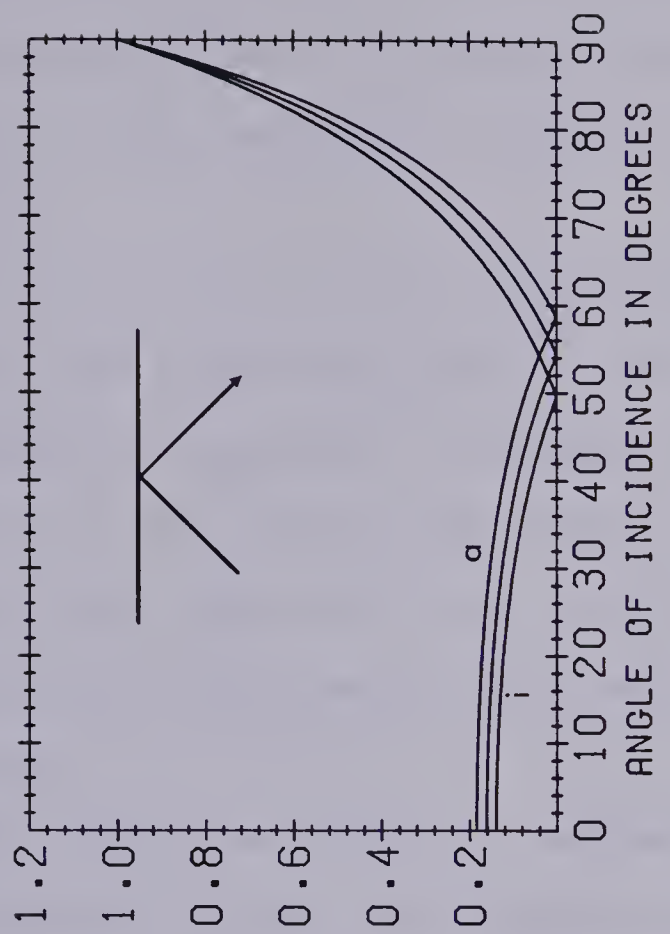


Figure 1.8 The transmission coefficient H_1H_2 and the reflection coefficient H_2H_2 for 0(i), 10, and 20(a) percent anisotropy in layer 1, for the media specified in Table 1.

H1H2



H2H2



rithmic singularities in the reflected amplitudes are due to a zero in the reflection coefficient H_1H_1 as shown in Figure 7a.

At the critical points (denoted by v 's in Figure 9) the head wave amplitude blows up due to the fact that the asymptotic expansion is proportional to $\ell^{-3/2}$ (Equation (1.68)) and at the critical points $\ell = 0$. As was previously mentioned other methods must be employed to accurately determine the head wave amplitude near this point.

When computing synthetic seismograms in plane layered media without lateral inhomogeneities it is convenient to use the concepts of kinematic and dynamic analogues (Hron (1972)). For the rays shown in the inserts of Figures 10 and 11, using the velocity-depth structure of Table 2, it follows that each of the three possible rays with four segments in both layers 1 and 2 have the same kinematic properties; that is, they all arrive at a given epicentral distance at the same time. Consequently the travel time need only be computed once, and as the geometrical spreading depends only on the number of ray segments, it too has only to be computed once for each of the three rays (a kinematic group).

Also, since two of the three rays encounter the same set of reflection and transmission coefficients, though not in the same order, they both have identical dynamic properties, that is, their complex amplitudes

Table 1.1

% anis.	a_{x_1}	a_{z_1}	ρ_1	h_1	a_{x_2}	a_{z_2}	ρ_2
0	1.15	1.15	2.02	2.0	1.55	1.41	2.18
10	1.21	1.10	2.02	2.0	1.55	1.41	2.18
20	1.26	1.05	2.02	2.0	1.55	1.41	2.18

Velocities (a_{x_1} , a_{z_1} , a_{x_2} , a_{z_2}) are in km/sec, densities (ρ_1, ρ_2) are in g/cm³, and the thicknesses (h_1, h_2) are in km. The degree of anisotropy is defined as $\frac{a_x - a_z}{a_z} \times 100\%$.

Table 1.2

Layer	a_x km/sec	a_z km/sec	ρ gm/cc	h km
1	1.32	1.05	2.02	2.0
2	1.76	1.41	2.18	2.0
HSPACE	2.20	1.76	2.30	--

Figure 1.9 The effect on the amplitude of the reflected wave (r) and the head wave (h) of varying the anisotropy in layer 1 and 0 percent (a) to 20 percent (b). The elastic parameters of the two-layered model are given in Table 1.

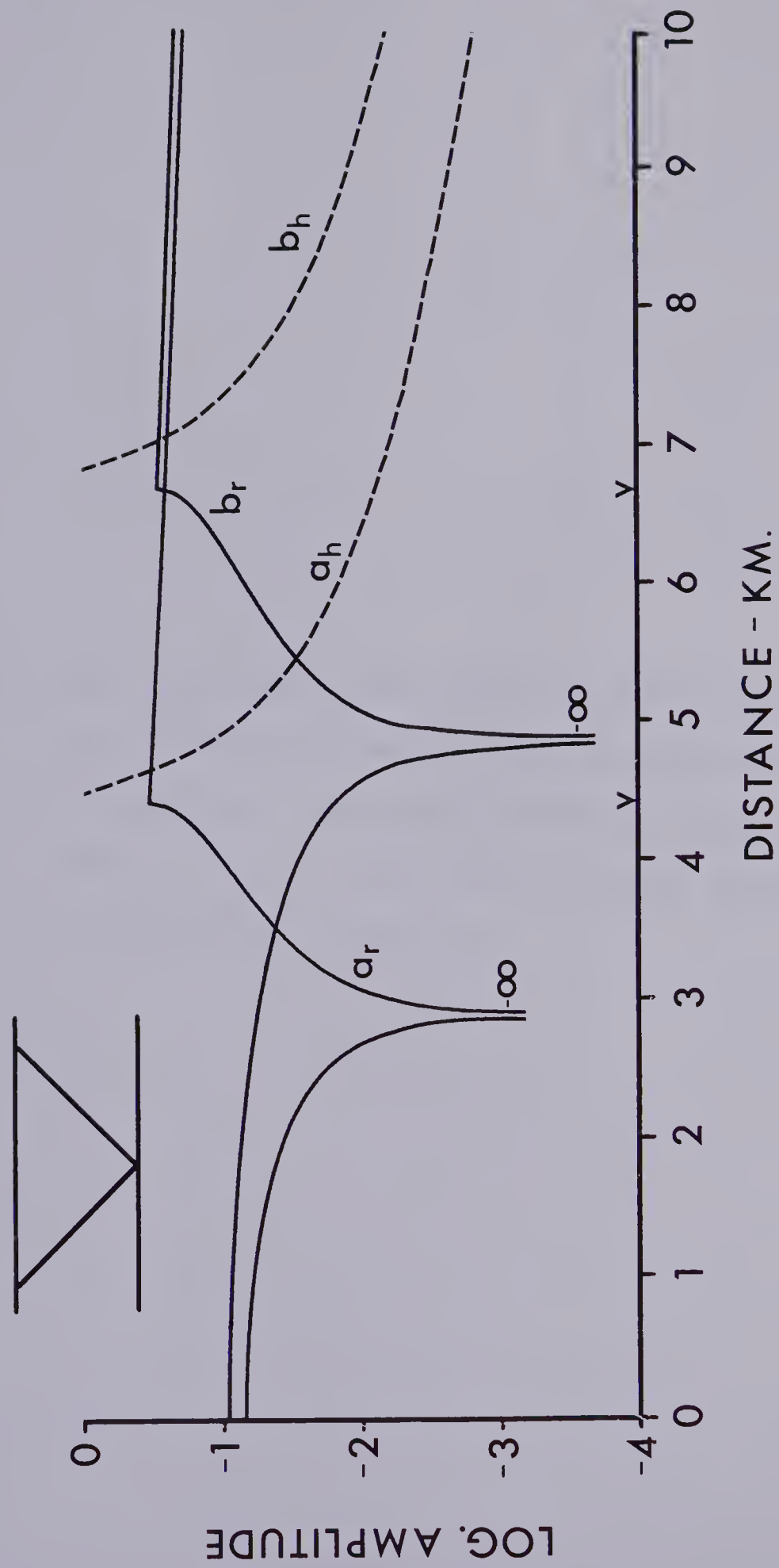
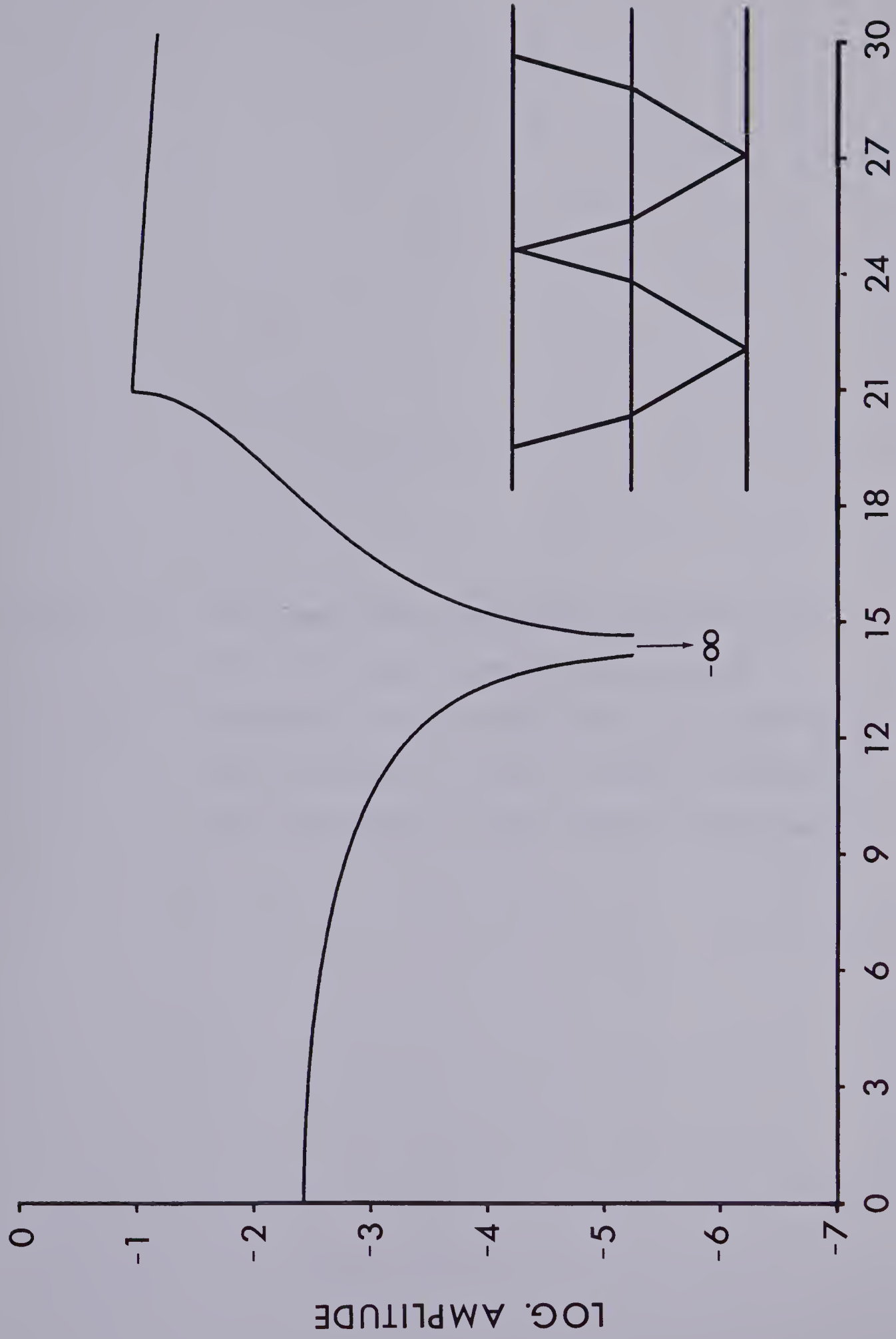


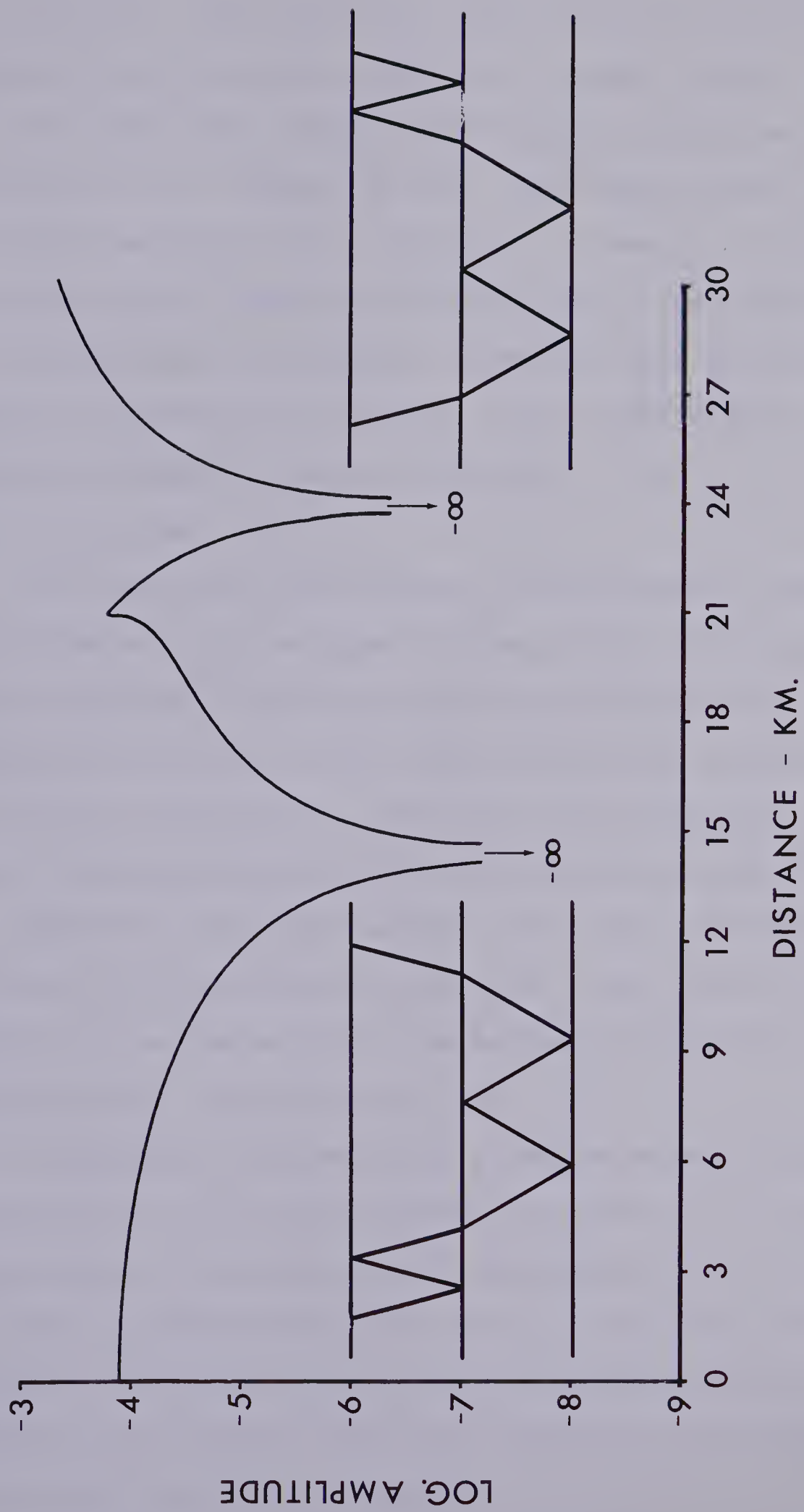
Figure 1.10 The logarithmic amplitude distance curve for the first dynamic group in the kinematic group having four ray segments in each of layers 1 and 2. The three-layered model is specified by Table 2.



DISTANCE - KM.



Figure 1.11 The logarithmic amplitude distance curve for the second dynamic group in the kinematic group having four ray segments in each of layers 1 and 2. Table 2 contains the parameters of this three-layered model.



are the same. This being the case amplitude calculations need only be carried out once for a dynamic group.

Thus the three rays in the kinematic group can be divided into two dynamic groups, the second dynamic group in this case having only one entry. However, as the ray parameter is the same for all three rays, the reflection and transmission coefficients common to both groups of dynamic analogues are the same, and a considerable saving in computer time is realized.

1.9 Conclusion

The theoretical development of the dynamic properties for SH waves in plane layered transversely isotropic media using asymptotic ray theory has been presented with an emphasis put on having the final formulae in a form that are readily programable. Besides reflected waves, head waves are investigated within the limited framework that the asymptotic expansion allows. The head wave amplitude requires the evaluation of the first order term in the asymptotic expansion while the reflected amplitude requires only the zero order term.

A numerical discussion of a simple velocity depth structure was given which showed the effects of varying anisotropy on reflection and transmission coefficients and hence amplitude distance curves. The merits of employing kinematic and dynamic analogues to reduce computing costs when calculating synthetic seismograms were cited along with an example.

CHAPTER 2

SH WAVES IN LAYERED TRANSVERSELY ISOTROPIC
MEDIA - A WAVE APPROACH

2.1 Introduction

The problem of SH waves propagating in transversely isotropic homogeneous plane layered media is discussed through the use of integral transforms. This procedure yields not only the asymptotic solution which is also attainable using asymptotic ray series of geometrical optics (Karal and Keller (1959), Cerveny (1972), Cerveny and Psencik (1972)) but also allows for the investigation of the interference of the reflected and head waves in the vicinity of the critical point (point of critical refraction). It is in this region that asymptotic ray theory breaks down or in the least introduces considerable error in the displacement amplitudes.

Although exact solutions can be obtained using integral transforms, they become unsuitable for numerical calculations, and consequently the exact solutions are approximated using the method of steepest descents. Direct waves will not be considered in the following work.

The dynamic properties of reflected and head waves at and around the critical point have been solved for homogeneous isotropic media in the case of the coupled P-SV problem (Cerveny (1962), Cerveny (1965), Cerveny

(1967), Cervený and Ravindra (1971)). The notation in this paper will be similar to the above mentioned works as will be the contour of integration used.

2.2 Mathematical Preliminaries

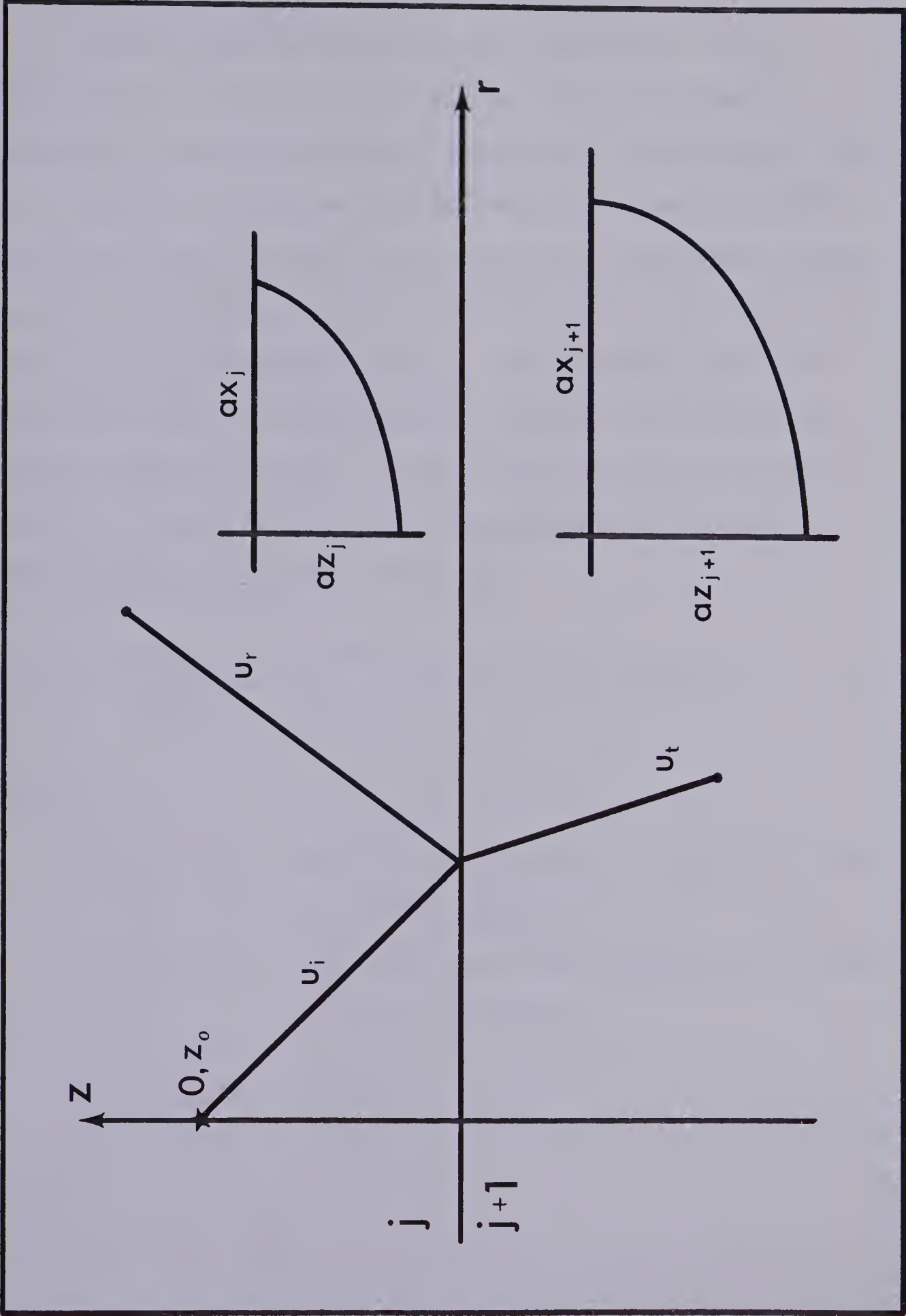
Consider two perfectly elastic transversely isotropic homogeneous media, j and $j+1$, in welded contact, with a point source of SH waves situated at a point z_0 above the interface between the two media. The interface will be defined as the $z = 0$ plane. As SH wavefronts in transversely isotropic media are ellipsoids of revolution, it will be further assumed that the axes of anisotropy are aligned perpendicular to the $z = 0$ plane (Figure 2.1). Introducing cylindrical coordinates (r, ϕ, z) , the equation of motion in the j -th (upper) medium can be written

$$(2.1) \quad A_j \frac{1}{r} \frac{\partial}{\partial r} \left(\frac{r \partial \vec{u}_j}{\partial r} \right) + B_j \frac{\partial^2 \vec{u}_j}{\partial z^2} - \frac{\partial^2 \vec{u}_j}{\partial t^2} = \frac{A_j L(t) \delta(r) \delta(z - z_0)}{r}$$

where $L(t)$ is the time dependence of the source, and in usual notation $A_j = A_{44}^{(j)}$ and $B_j = A_{66}^{(j)}$ (Cervený and Psensik (1972), Daley and Hron (1977)). Both quantities A_j and B_j have dimensions of velocity squared and in most seismological applications the condition $A_j > B_j$ holds. The plane of incidence can be chosen without loss of generality as the $\phi = 0$ plane and thus the displacement vector can be expressed as $\vec{u}_j = u_j \hat{i}_\phi$ where \hat{i}_ϕ is a unit vector in the ϕ direction or in the case of



Figure 2.1 Geometry of incidence and notation used in the case of a point source of SH waves at $r=0, z=z_0$. At the interface at $z=0$ the media j and $j+1$ are in welded contact.



$\phi = 0$, the y direction.

Snell's Law is valid at the interface, but if expressed in terms of ray angles and velocities as opposed to wavefront normal angles and velocities, takes on a slightly different form (Sato and Lapwood (1968), Daley and Hron (1978)). In general the wavefront normal angles and velocities are different from ray angles and velocities (Musgrave (1970)). The problem under consideration here can be treated totally using only ray angles and velocities; these being the most practical, for it is along the ray that the energy is propagated. The statement of Snell's Law is

$$(2.2) \quad \frac{a_j \sin \alpha_j}{a_{xj}^2} = \frac{a_{j+1} \sin \alpha_{j+1}}{a_{xj+1}^2}, \quad a_{xj} \rightarrow a_{xj} \quad a_{zj} \rightarrow a_{zj}$$

where

$a_{xj} = (A_j)^{\frac{1}{2}}$ - the velocity along the major (r) axis of the ellipsoid.

$a_{zj} = (B_j)^{\frac{1}{2}}$ - the velocity along the minor (z) axis of the ellipsoid.

$\frac{1}{a_j^2} = \frac{\sin^2 \alpha_j}{a_{xj}^2} + \frac{\cos^2 \alpha_j}{a_{zj}^2}$ - defines the ray velocity a_j .

$$F_j = \frac{A_j}{B_j} = \frac{a_{xj}^2}{a_{zj}^2}$$

α_j - the angle the ray makes with the z axis.

A time dependence of $e^{-i\omega t}$ will be assumed so that $u = \bar{u} e^{-i\omega t}$ and equation (2.1) becomes

$$(2.3) \quad A_j \frac{1}{r} \frac{\partial}{\partial r} \left(\frac{r \partial^2 \bar{u}_j}{\partial r} \right) + B_j \frac{\partial^2 \bar{u}_j}{\partial z^2} + \omega^2 \bar{u}_j = -A_j \frac{\delta(r) \delta(z-z_0)}{r}$$

with vector notation being dropped as the result of a previous discussion.

Using the Fourier-Bessel transform as

$$(2.4) \quad \tilde{u}_j(k, h, \omega) = \int_0^\infty r J_0(kr) dr \int_{-\infty}^\infty \bar{u}_j(r, z, \omega) e^{-ihz} dz$$

and its inverse as

$$(2.5) \quad \bar{u}_j(r, z, \omega) = \frac{1}{2\pi} \int_0^\infty k J_0(kr) dk \int_{-\infty}^\infty \tilde{u}_j(k, h, \omega) e^{ihz} dh$$

the solution of equation (2.3) can be written

$$(2.6) \quad \bar{u}_j = \frac{F_j}{2\pi} \int_0^\infty J_0(kr) k dk \int_{-\infty}^\infty \frac{\exp[ih(z-z_0)] dh}{(h^2 + \lambda_j^2)}$$

where $\lambda_j^2 = \left(F_j k^2 - \frac{\omega^2}{B_j} \right).$

Solving the integral over h by the method of residues yields

$$(2.7) \quad u_j = -F_j e^{-i\omega t} \int_0^\infty \frac{J_0(kr) \exp[-\lambda_j |z-z_0|] k dk}{\lambda_j}$$

which is the displacement for the direct wave at any point (r, z) in the j -th medium.

The expressions for the displacement of the reflected wave in the j -th medium and the transmitted wave in the $j+1$ medium at an arbitrary point (r, z) are respectively

$$(2.8) \quad u_r = -F_j e^{-i\omega t} \int_0^{\infty} \frac{R_j(k) J_0(kr) \exp[-\lambda_j(z-z_0)] k dk}{\lambda_j}$$

and

$$(2.9) \quad u_t = -F_j e^{-i\omega t} \int_0^{\infty} \frac{T_j(k) J_0(kr) \exp[\lambda_{j+1}z - \lambda_j z_0] k dk}{\lambda_j}$$

where

$$\lambda_{j+1} = \left(F_{j+1} k^2 - \frac{\omega^2}{B_{j+1}} \right)^{\frac{1}{2}}.$$

$R_j(k)$ and $T_j(k)$ are the reflection and transmission coefficients and can be determined from the interface conditions of continuity of displacement and shear stress. For completeness these coefficients are discussed in Appendix A.

2.3 The Contour of Integration

It is convenient to express the Bessel function $J_0(kr)$ in the equation for the reflected displacement in terms of Hankel functions of the first and second kind as (Watson (1944))

$$(2.10) \quad J_0(kr) = \frac{1}{2} \left[H_0^{(1)}(kr) + H_0^{(2)}(kr) \right].$$

With the added facts that $H_0^{(2)}(e^{-i\pi}kr) = -H_0^{(1)}(kr)$ and $R_j(k) = R_j(-k)$ as shown in Appendix B, it is possible to write the equation (2.8) as

$$(2.11) \quad u_r = -\frac{F_j}{2} e^{-i\omega t} \int_{-\infty}^{\infty} \frac{R_j(k) H_0^{(1)}(kr) \exp[-\lambda_j(z+z_0)] k dk}{\lambda_j}.$$

With the change of variable $k = \frac{\omega}{\sqrt{B_j}} = k_j q$ (2.11) can be written

$$(2.12) \quad u_r = -\frac{k_j F_j}{2} e^{-i\omega t + \frac{i\pi}{2}} \int_{-\infty}^{\infty} \frac{R_j(q) H_0^{(1)}(k_j q r) \exp[ik_j (1-F_j q^2)^{\frac{1}{2}}(z+z_0)] q dq}{(1-F_j q^2)^{\frac{1}{2}}}.$$

On the Riemann sheet where the contour of integration lies the radicals λ_j and λ_{j+1} must have the following choices of sign to ensure the vanishing of the exponential terms as $z \rightarrow \infty$

$$(2.13) \quad \lambda_j = -ik_j (1-F_j q^2)^{\frac{1}{2}} = -ik_j w_j$$

$$\lambda_{j+1} = -i \frac{\omega}{\sqrt{B_{j+1}}} \left(1 - \frac{A_{j+1}}{B_j} q^2 \right)^{\frac{1}{2}} = -ik_{j+1} w_{j+1}$$

and for $\frac{B_j}{A_{j+1}} < q^2$ the argument of $w_{j+1} = \frac{\pi}{2}$.

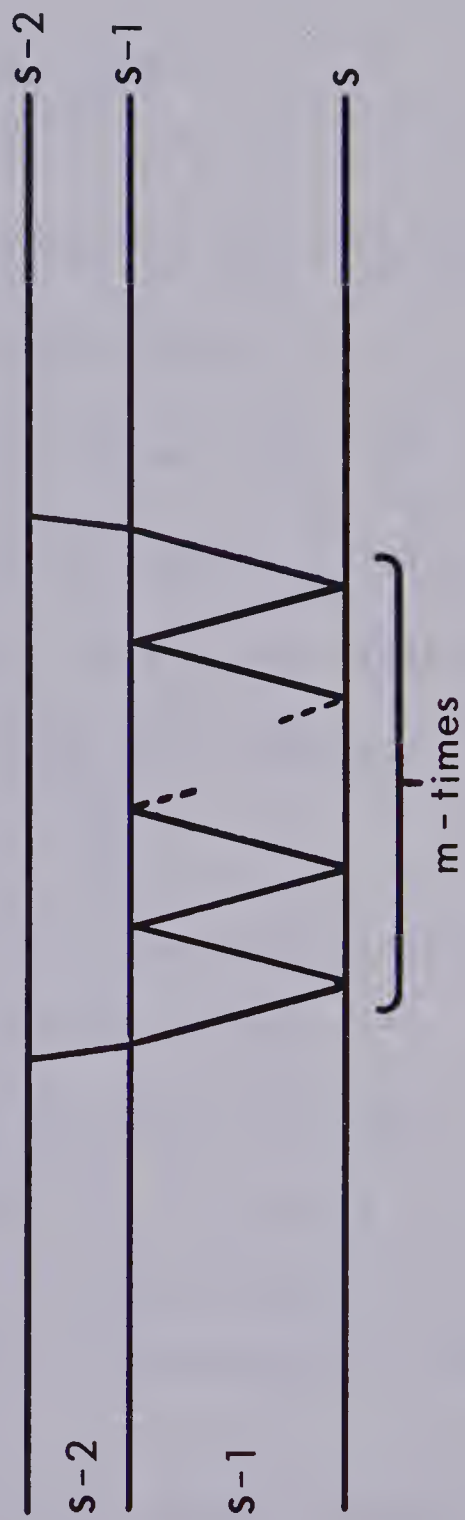
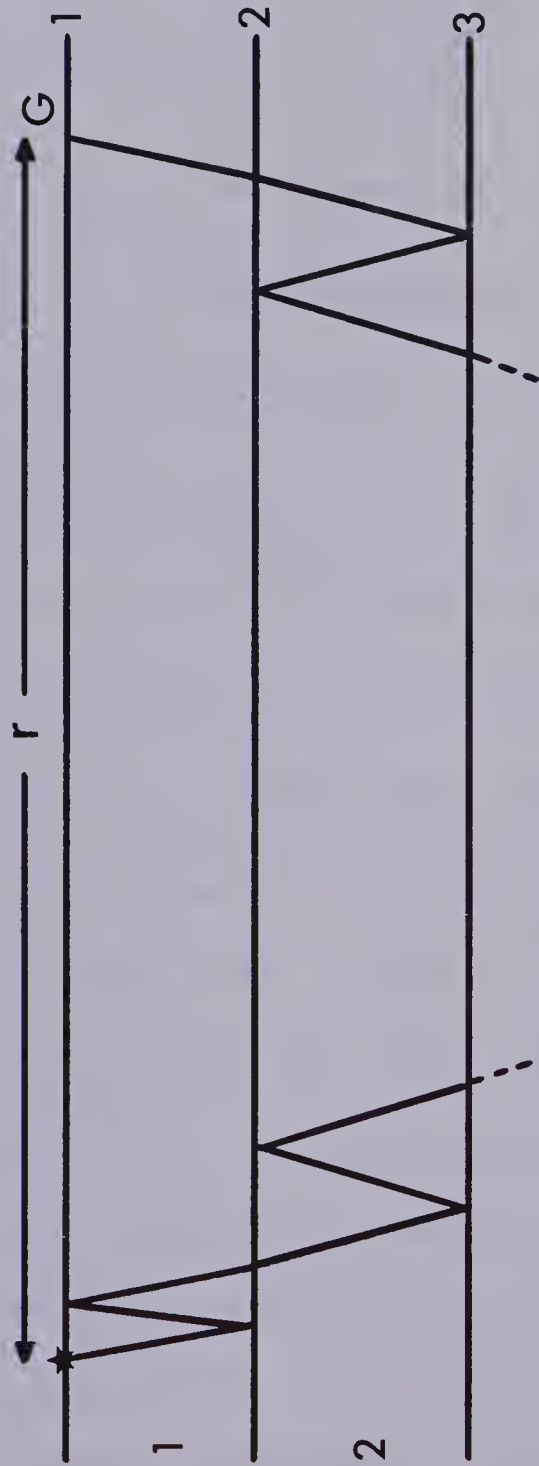
Before proceeding further it is useful to generalize the problem of the reflected wave to one of $s-1$ transversely isotropic layers overlying a halfspace (the s -th layer). The source and receiver will be assumed to be in medium 1 just below the first interface (the free interface) and the distance between the two is r . It will be assumed that there are $2m$ ray segments in the $(s-1)$ -th layer, implying that the ray will be reflected m times from the s -th interface. A ray segment will be defined as the part of the total ray between one reflection or refraction and the next (Figure 2.2). The modified expression for the reflected displacement can then be written as

$$(2.14) \quad u_r = - \frac{F_1 k_1}{2} e^{-i\omega t + \frac{i\pi}{2}} \int_{-\infty}^{\infty} \frac{Z(q) R_s^m(q) H_0^{(1)}(k_1 q r) \exp[ik_1 \tilde{F}(q)] q dq}{(1 - F_1 q^2)^{\frac{1}{2}}}$$

where

$$Z(q) = \begin{cases} 1 & \text{if } s = 2 \\ \text{the product of all reflection and transmission coefficients encountered by the ray} & \end{cases}$$

Figure 2.2 A ray diagram showing the labelling of the layers and interfaces.



except for those m reflection coefficients at the s -th interface ($s > 2$).

$R_s(q)$ - the reflection coefficient at the s -th interface

$$F(q) = \sum_{j=1}^{s-1} N_j h_j \left(\frac{B_1}{B_j} \right)^{\frac{1}{2}} \left(1 - \frac{A_j}{B_1} q^2 \right)^{\frac{1}{2}}$$

N_j - the number of ray segments in the j -th layer

h_j - the thickness of the j -th layer.

In writing (2.14) it has been assumed that $\frac{B_1}{A_1}$ is the maximum value in the sequences of values $\frac{B_1}{A_j}$ ($j=1, s$).

If this is not the case the radical in the denominator in (2.14) must be replaced by $\left(1 - \frac{A_\kappa}{B_1} q^2 \right)^{\frac{1}{2}}$ where κ refers to the layer that maximizes $\frac{B_1}{A_j}$.

The integrand of (2.14) has $2s$ branch points lying on the real axis of the q plane, at the points

$n_j = \pm \left(\frac{B_1}{A_j} \right)^{\frac{1}{2}}$ ($j=1, s$). The velocity structure will be assumed such that the minimum value of n_j ($j=1, s$) is n_s . This is necessary to ensure that the first head wave to appear will be the one from critical refraction at the s -th interface.

As the integration path in (2.14) passes through the point $q=0$ where the value of $H_O^{(1)}(k_1 q r)$ becomes infinite, it will be necessary to select a transformation that will take the contour from $-\infty$ to ∞ along the

real q axis into a new contour D which does not pass through the point $q=0$. A discussion of this contour will be made shortly.

If along this new contour D , $k_1 r |q_0| \gg 1$, where $|q_m|$ is the minimum value q attains along D , the asymptotic expansion for large argument of the Hankel function (Watson (1944)) is valid.

$$(2.15) \quad H_0^{(1)}(k_1 q r) \sim \left(\frac{2}{\pi k_1 r q} \right)^{\frac{1}{2}} \exp[ik_1 r q - \frac{i\pi}{4}].$$

With (2.15) equation (2.14) becomes

$$(2.16) \quad u_r = -F_1 e^{-i\omega t + \frac{i\pi}{4} \left(\frac{k_1}{2\pi r} \right)^{\frac{1}{2}}} \int_D \frac{Z(q) R_s^m(q) \exp[ik_1 F(q)] q^{\frac{1}{2}} dq}{(1 - F_1 q^2)^{\frac{1}{2}}}$$

where

$$F(q) = r q + \sum_{j=1}^{s=1} N_j h_j \left(\frac{B_1}{B_j} \right)^{\frac{1}{2}} \left(1 - \frac{A_j}{B_1} q^2 \right)^{\frac{1}{2}}.$$

The most common technique in approximating integrals of the type in (2.16) is by the method of steepest descents or saddle point method because of its simplicity and reasonable accuracy. The saddle point is given as the solution of

$$(2.17) \quad \left(\frac{d F(q)}{dq} \right)_{q=q_0} = 0$$

which after some algebra yields

$$(2.18) \quad q_0 = \frac{az_1 a_1 \sin \alpha_1}{ax_1^2} = \frac{az_1 a_j \sin \alpha_j}{az_j^2} \quad (j=1, s).$$

If the angle α_k is the acute angle between the ray and z axis in the layer having the second minimum value in the

sequence of values $\left(\frac{B_1}{A_j}, j=1, s \right)$, then the range of $\sin \alpha_k$ is $0 \leq \sin \alpha_k < 1$ and consequently the range of q_0 is $0 \leq q_0 \left(\frac{B_1}{A_k} \right)^{\frac{1}{2}} = \frac{az_1}{ax_k}$. Thus q_0 is always real and positive.

The path of steepest descents as it passes through the saddle point makes an angle of $\frac{3\pi}{4}$ with the positive imaginary q axis (Figure 2.3).

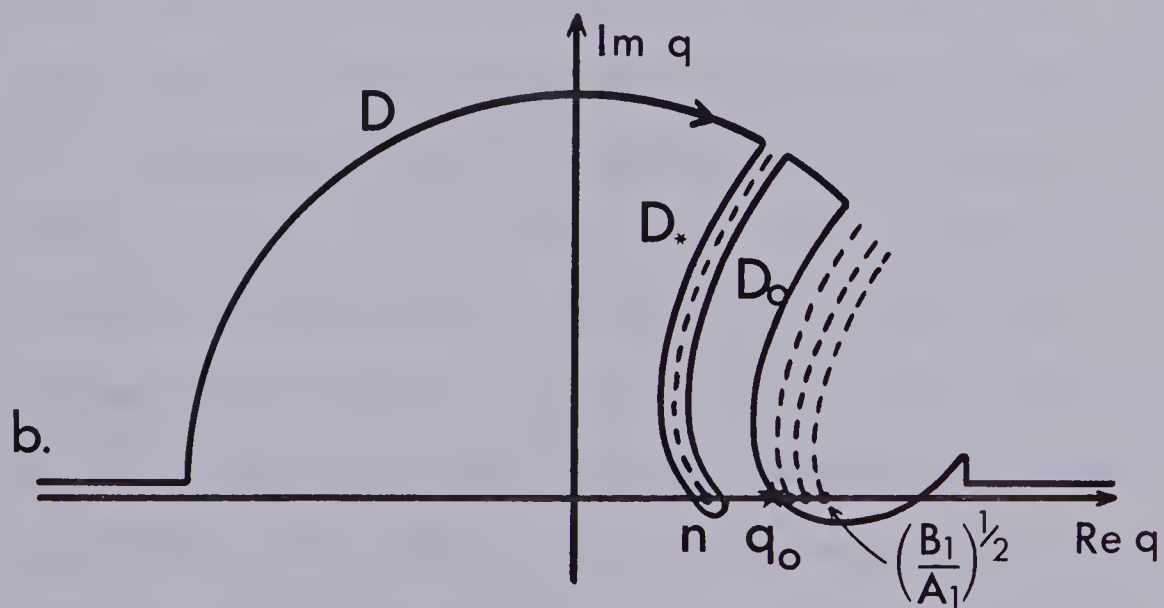
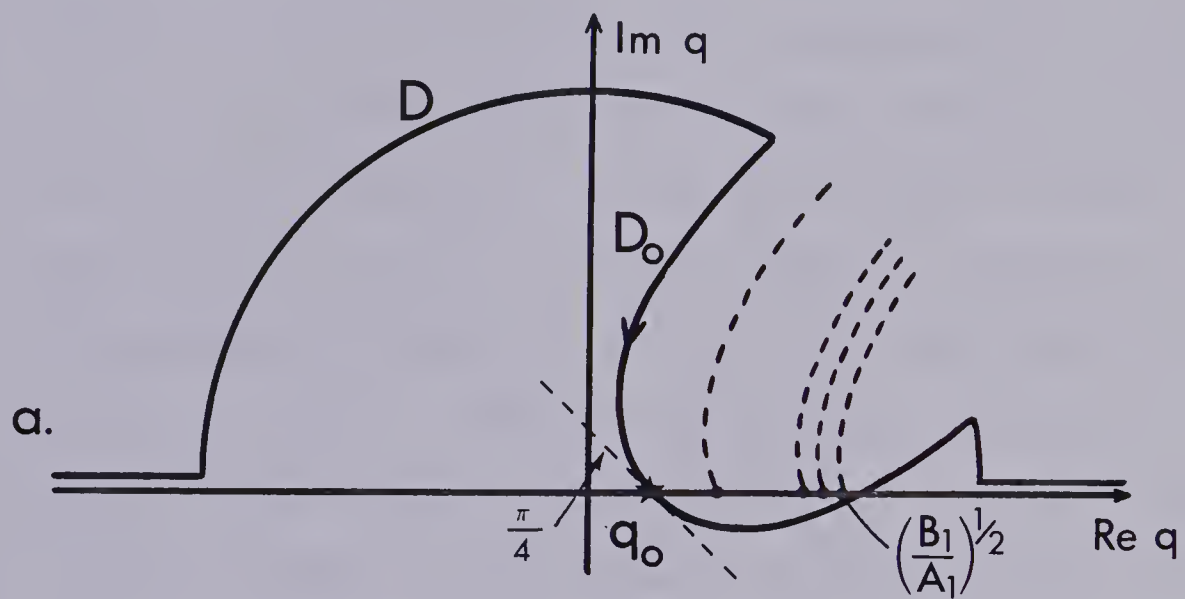
A basic assumption of the method of steepest descents is that the absolute value of the exponential terms in the integral decay rapidly on either side of the saddle point so that they can be approximated by the first term in a Taylor series about the saddle point, i.e. their value at the saddle point. This approach is not valid however, if the non-exponential terms vary rapidly near the saddle point. This occurs if the saddle point is near one of the branch points, say n_s , due to the radical w_s .

In the following sections, two regions of the value of the saddle point will be considered:

- (a) the saddle point q_0 lies between 0 and the first branch point n_s which from now on will be referred

Figure 2.3 The contours of integration for (a) the saddle point lying between 0 and the first branch point and (b) the saddle point lying between the first and second branch points. The choice of parameterization forces the contour in both cases to pass to the right of the branch point

$$\left(\frac{B_1}{A_1}\right)^{\frac{1}{2}}.$$



to as n . The integral is transformed to the new contour shown in Figure 2.3 by the change of variable

$$(2.19) \quad (1 - F_1 q^2)^{\frac{1}{2}} = (1 - F_1 q_0^2)^{\frac{1}{2}} + p \exp\left(-\frac{i\pi}{4}\right)$$

where p is real ($-\infty < p < \infty$). The integration of q from $-\infty$ to ∞ has been transformed to the integral around the partial semicircle D plus the integral around the loop D_0 through the saddle point q_0 defined by the parametric equation (2.19). As the radius of the semicircle is extended to infinity the contribution from D goes to zero and we are left with the integral along D_0 which yields the displacement of the reflected wave from the s -th interface.

- (b) the saddle point q_0 is greater than n but less than the value of the next branch point as in Figure 2.3. The integration path now consists of three parts; the integration along the semicircle D which goes to zero as the radius tends to infinity, the integration along D_0 which gives the contribution of the reflected wave, and the integration along D_* which yields the contribution due to the head wave from the s -th interface. Integration around the branch cut due to the branch point n is necessary to ensure that we remain on the same Riemann sheet. The branch cut is defined by the parametric equation

$$(2.20) \quad (1 - F_1 q^2)^{\frac{1}{2}} = (1 - F_1 n^2)^{\frac{1}{2}} + p \exp\left(-\frac{i\pi}{4}\right), p \text{ real}, (0 \leq p < \infty).$$

Analogous integration contours for this problem for isotropic media have been dealt with at great length in the literature (Cerveny (1965), Cerveny and Ravindra (1971), Ewing et al. (1957), Brekhovskikh (1960), Honda and Nakamura (1954)) and for this reason it would be redundant to repeat the discussion here.

2.4 The Reflected Wave

In this section an expression for the reflected displacement, the integral along contour D_0 , will be obtained employing the method of steepest descents. The exponential term can be expanded in a Taylor series in terms of the new integration variable p about $p = 0$ ($q = q_0$) as

$$(2.21) \quad ik_1 F(q) = ik_1 F(q_0) - \frac{k_1 \tilde{r} p^2}{2 F_1^2 q_0^3} + \dots$$

where

$$(2.22) \quad \tilde{r} = \sum_{j=1}^{s-1} H_j h_j \frac{B_1}{B_j} \tan \alpha_j, \quad \alpha_j \text{ being the acute angle}$$

the ray makes with the z axis in the j -th layer.

With the aid of equations (2.2) and (2.18) it can be shown that $ik_1 F(q_0) = i\omega \tau_r$ where τ_r is the travel time of the reflected wave.

Substituting equation (2.21) into (2.16) the

expression for the displacement u_o of the reflected wave is given by

$$(2.23) \quad u_o = e^{-i\omega(t-\tau_r)} \left(\frac{k_1}{2\pi r} \right)^{\frac{1}{2}} \int_{-\infty}^{\infty} Z(p) R_s^m(p) \exp[-H(q_o)p^2] \frac{dp}{q^{\frac{1}{2}}}$$

where

$$H(q_o) = \frac{k_1 \tilde{r}}{2F_1^2 q_o^3}.$$

Assuming $R_s(p)$ and $Z(p)$ vary only slightly about $p=0$ ($q=q_o$) i.e. q does not lie near a branch point, the non-exponential terms in (2.23) can be approximated by their value at $p = 0$ ($q=q_o$), because of the fact that the exponential term decays rapidly in a small region about $p = 0$. It should be remembered that as $H(q_o)$ is proportional to frequency $\left(k_1 = \frac{\omega}{\sqrt{B_1}} \right)$, the higher the frequency the more rapid is the decay about $p = 0$. Thus (2.23) becomes

$$(2.24) \quad u_o = e^{-i\omega(t-\tau_r)} \left(\frac{k_1}{2\pi r q_o} \right)^{\frac{1}{2}} Z(q_o) R_s^m(q_o) \int_{-\infty}^{\infty} \exp[-H(q_o)p^2] dp$$

$$= \frac{e^{-i\omega(t-\tau_r)} Z(q_o) R_s^m(q_o)}{L}$$

where

$$L = \frac{az_1}{a_1} \frac{(r\tilde{r})^{\frac{1}{2}}}{\sin\alpha_1} \quad \text{is called the geometrical spreading}$$

of the ray. Equation (2.24) is the high frequency or

asymptotic form of the reflected wave which is also attainable using asymptotic ray theory.

In the case where q_0 lies close to a branch point n , approximating $R_s(p)$ by $R_s(q_0)$ is not valid since $R_s(p)$ contains the radical $w_s = \left(1 - \frac{q^2}{n^2}\right)^{\frac{1}{2}}$. To accommodate for this the integral in (2.23) is divided into two parts by expressing $R_s(p)$ in the form

$$R_s(p) = C_1(p) - C_2(p)w_s.$$

Explicit expressions for $C_1(p)$ and $C_2(p)$ are given in Appendix B. It follows that

$$R_s^m = (C_1(p) - C_2(p)w_s)^m = C_1^m(p) \left(1 - \frac{C_2(p)}{C_1(p)w_s}\right)^m.$$

For q_0 close to n , w_s is approximately zero so that

$\frac{C_2(p)}{C_1(p)w_s} \ll 1$. If this condition is satisfied it can be

justified to approximate $R_s^m(p)$ by the first two terms in a binomial expansion, viz.

$$(2.25) \quad R_s^m(p) \approx C_1^m(p) - m C_1^{m-1}(p) C_2(p) w_s$$

so that equation (2.23) can be written in the form

$$(2.26) \quad u_0 = e^{i\omega(t-\tau_r)} \left(\frac{k_1}{2\pi r} \right)^{\frac{1}{2}} \left\{ \int_{-\infty}^{\infty} Z(p) C_1^m(p) \exp[-H(q_0)p^2] \frac{dp}{q^{\frac{1}{2}}} \right. \\ \left. - \int_{-\infty}^{\infty} Z(p) m C_1^{m-1}(p) C_2(p) w_s \exp[-H(q_0)p^2] \frac{dp}{q^{\frac{1}{2}}} \right\}.$$

As the functions $Z(p)$, $C_1(p)$ and $C_2(p)$ do not contain the radical w_s , they do not change rapidly in the neighborhood of $p = 0$ and as an initial approximation it is reasonable to assign to them their value at $p = 0$. Thus

$$(2.27) \quad u_0 = \frac{e^{-i\omega(t-\tau_r)}}{L} Z(q_0) \left\{ C_1^m(q_0) - m C_1^{m-1}(q_0) L \right. \\ \left. \left(\frac{k_1}{2\pi r q_0} \right)^{\frac{1}{2}} \times \int_{-\infty}^{\infty} w_s \exp[-H(q_0)p^2] dp \right\}.$$

The radical w_s can be alternately written using equation (2.19) in the form

$$(2.28) \quad w_s = \left(1 - \frac{A_s}{B_1} q^2 \right)^{\frac{1}{2}} = \left(1 - \frac{q^2}{n^2} \right)^{\frac{1}{2}} = \frac{i}{F_1^{\frac{1}{2}} n} \\ \left[(1-F_1 n^2)^{\frac{1}{2}} - (1-F_1 q^2)^{\frac{1}{2}} \right]^{\frac{1}{2}} \left[(1-F_1 n^2)^{\frac{1}{2}} + (1-F_1 q^2)^{\frac{1}{2}} \right]^{\frac{1}{2}} \\ = \frac{i}{F_1^{\frac{1}{2}} n} \left[(1-F_1 n^2)^{\frac{1}{2}} - (1-F_1 q_0^2)^{\frac{1}{2}} - p \exp\left(\frac{-i\pi}{4}\right) \right]^{\frac{1}{2}} \\ \times \left[(1-F_1 n^2)^{\frac{1}{2}} + (1-F_1 q_0^2)^{\frac{1}{2}} + p \exp\left(\frac{-i\pi}{4}\right) \right]^{\frac{1}{2}}.$$

Assuming that

$$(2.29) \quad H(q_o)^{\frac{1}{2}} \left[(1-F_1 n^2)^{\frac{1}{2}} + (1-F_1 q_o^2)^{\frac{1}{2}} \right] \gg 1$$

then w_s can be written approximately as

$$(2.30) \quad w_s = \frac{i}{F_1^{\frac{1}{2}} n} \left[(1-F_1 n^2)^{\frac{1}{2}} + (1-F_1 q_o^2)^{\frac{1}{2}} \right]^{\frac{1}{2}} \left[(1-F_1 n^2) - (1-F_1 q_o^2)^{\frac{1}{2}} - p \exp\left(\frac{-i\pi}{4}\right) \right]^{\frac{1}{2}}.$$

The argument of the first radical in the [] brackets is always zero while that for the second radical is, for $p=0$

$$(2.31) \quad \arg \left[(1-F_1 n^2)^{\frac{1}{2}} - (1-F_1 q_o^2)^{\frac{1}{2}} - p \exp\left(\frac{-i\pi}{4}\right) \right]^{\frac{1}{2}} = \begin{cases} -\frac{\pi}{2} & \text{for } q_o < n \\ 0 & \text{for } q_o > n \end{cases}.$$

The values of the argument are chosen to agree with equation (2.13) in Section 1.

With the change of variable $p \rightarrow H(q_o)^{\frac{1}{2}} p$ and the use of equation (2.30) the expression for the reflected displacement near the branch point n becomes

$$(2.32) \quad u_o = \frac{e^{-i\omega(t-\tau_r)}}{L} Z(q_o) \left\{ C_1^m(q_o) - \frac{im}{F_1^{\frac{1}{2}} n} C_1^{m-1}(q_o) \right. \\ \left. C_2(q_o) L \left(\frac{k_1}{2rq_o} \right)^{\frac{1}{2}} H(q_o)^{-3/4} \times \left[(1-F_1 n^2)^{\frac{1}{2}} + (1-F_1 q_o^2)^{\frac{1}{2}} \right]^{\frac{1}{2}} \right. \\ \left. g_1(p_o) \right\}$$

where

$$(2.33) \quad g_1(p_o) = \pi^{-\frac{1}{2}} \int_{-\infty}^{\infty} \left[p_o - p \exp\left(\frac{-i\pi}{4}\right) \right]^{\frac{1}{2}} \exp(-p^2) dp$$

$$p_o = H(q_o)^{\frac{1}{2}} \left[(1 - F_1 n^2)^{\frac{1}{2}} - (1 - F_1 q_o^2)^{\frac{1}{2}} \right]$$

and from equation (2.31) the argument of the radical under the integral in (2.33) is

$$(2.34) \quad \arg \left[p_o - p \exp\left(\frac{-i\pi}{4}\right) \right]^{\frac{1}{2}} = \begin{cases} -\frac{\pi}{2} & \text{for } p_o < 0 \quad (q_o < n) \\ 0 & \text{for } p_o > 0 \quad (q_o > n) \end{cases}.$$

The frequency dependent quantity $|p_o|$ can be thought of as a measure of the distance from the critical point; the critical point being defined as the receiver location at the first interface where the ray under consideration arrives for $q_o = n$. At the critical point $p_o = 0$.

Multiplying and dividing the second term of equation (2.32) by $p_o^{\frac{1}{2}}$ and employing the previously defined relations for L and w_s we are left with

$$(2.35) \quad u_o = \frac{e^{-i\omega(t-\tau_r)}}{L} Z(q_o) \left\{ C_1^m(q_o) - m C_1^{m-1}(q_o) C_2(q_o) \right. \\ \left. \left(1 - \frac{q_o^2}{n^2} \right)^{\frac{1}{2}} \mu_1(p_o) \right\}$$

where

$$(2.36) \quad \mu_1(p_o) = \pi^{-\frac{1}{2}} \int_{-\infty}^{\infty} \left[1 - p \exp\left(\frac{-i\pi}{4}\right) / p_o \right]^{\frac{1}{2}} \exp(-p^2) dp.$$

Graphs of the functions (modulus and phase) of $g_1(p_o)$ and $\mu_1(p_o)$ are shown in Figure 2.4.

Equation (2.35) can be further simplified if it is recalled that for $q_o \approx n$

$$(2.25)' R_s^m(q_o) = C_1^m(q_o) - m C_1^{m-1}(q_o) C_2(q_o) \left(1 - \frac{q_o^2}{n^2}\right)^{\frac{1}{2}}$$

and as a result

$$(2.37) u_o = \frac{e^{-i\omega(t-\tau_r)}}{L} Z(q_o) \left\{ R_s^m(q_o) + N \right\}$$

$$(2.38) N = -m C_1^{m-1}(q_o) C_2(q_o) \left(1 - \frac{q_o^2}{n^2}\right)^{\frac{1}{2}} (\mu_1(p_o) - 1).$$

Finally by setting $q_o = n$ and multiplying and dividing the expression for N by p_o with the added facts that

$$C_1(n) = 1$$

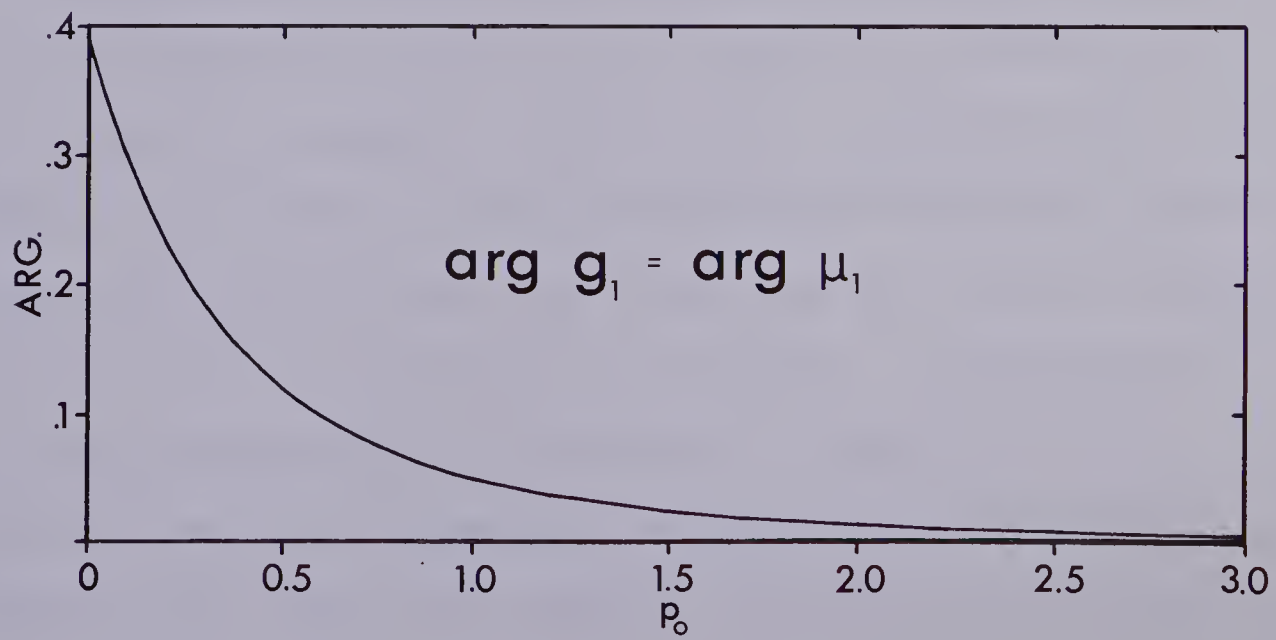
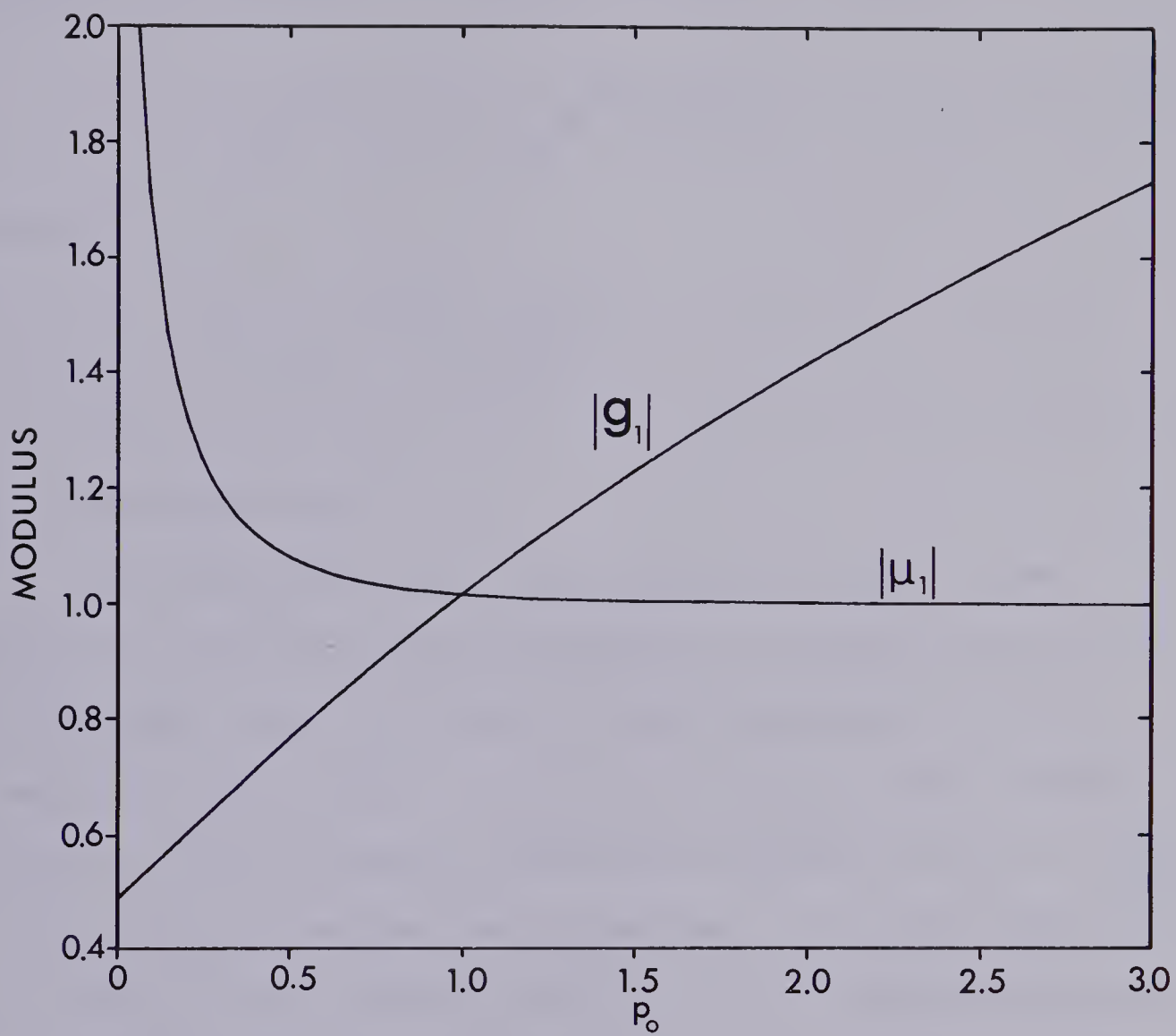
$$C_2(n) = \frac{\Gamma}{az_s} = \tilde{\Gamma} \quad \text{which will be called the modified head wave coefficient,}$$

N can be written

$$(2.39) \quad N = -im \left(\frac{2}{k_1 n \tilde{r}} \right)^{\frac{1}{2}} \tilde{\Gamma} 2^{\frac{1}{2}} (1 - F_1 n^2)^{\frac{1}{4}} \left[g_1(p_o) - p_o^{\frac{1}{2}} \right] \\ = -g^*(n) \left[i 2^{3/4} g_1(p_o) - i 2^{3/4} p_o^{\frac{1}{2}} \right]$$

with the result that near the critical point the

Figure 2.4 The modulus and argument (in radians) of
 μ_1 and g_1 vs. p_0 .



expression for the reflected wave has the form

$$(2.40) \quad u_o = \frac{e^{-i\omega(t-\tau_r)}}{L} Z(q_o) \left\{ R_\ell^m(q_o) - g^*(n) \left[i2^{3/4} g_1(p_o) - i2^{3/4} p_o^{1/2} \right] \right\}$$

where

$$g^*(n) = \frac{m\tilde{r}(1-F_1 n^2)^{1/4}}{(k_1 n\tilde{r})^{1/4}}.$$

2.5 The Head Wave

For the region of q referred to in case (b) in Section 2 there are two displacement contributions to be considered; the reflected one corresponding to the integral along D_o and the head wave displacement corresponding to the integral around the branch cut D_* . As the first part was solved for in Section 3 only the contribution due to the integral over D_* will be considered here.

Head waves can only arise at an interface if the incident wavefront has a finite radius of curvature in the plane of incidence. (Plane wave incidence cannot produce head waves). The resulting head wave is a three dimensional conical wave and hence has an infinite radius of curvature in the plane of incidence. Consequently, any other occurrences of incidence by the ray on the interface which produced the original head wave cannot produce other head wave segments (Cerveny and Ravindra

(1971)).

The expression for the displacement due to the head wave is given by

$$(2.41) \quad u_* = -F_1 e^{-i\omega t + \frac{i\pi}{4}} \left(\frac{k_1}{2\pi r} \right)^{\frac{1}{2}} \int_{D_*} \frac{Z(q) R_s^m(q) \exp[ik_1 F(q)] q^{\frac{1}{2}} dq}{(1-F_1 q^2)^{\frac{1}{2}}}$$

where all the quantities in (2.41) have been previously defined, the contour of integration is shown in Figure 3 and the asymptotic expansion of the Hankel function was assumed valid.

The integration contour D_* which circumvents the branch cut due to the radical $w_s = \left(1 - \frac{q^2}{n^2}\right)^{\frac{1}{2}}$ is given by the parametric equation

$$(2.20)' \quad (1-F_1 q^2)^{\frac{1}{2}} = (1-F_1 n^2)^{\frac{1}{2}} + p \exp\left(\frac{-i\pi}{4}\right) \quad 0 \leq p < \infty.$$

In terms of this new variable, the radical w_s , which has a different sign on each side of the cut, can be written

$$(2.42) \quad w_s = \frac{p^{\frac{1}{2}}}{F_1^{\frac{1}{2}} n} \left[p + 2(1-F_1 n^2)^{\frac{1}{2}} \exp\left(\frac{i\pi}{4}\right) \right]^{\frac{1}{2}} \exp\left(\frac{-i\pi}{4}\right)$$

where

$$\arg p^{\frac{1}{2}} = \begin{cases} 0 & \text{on the left hand side of the cut} \\ \pi & \text{on the right hand side of the cut} \end{cases}$$

and

$$\arg \left[p + 2(1-F_1 n^2)^{\frac{1}{2}} \exp\left(\frac{i\pi}{4}\right) \right]^{\frac{1}{2}} = \frac{\pi}{8} \quad \text{for } p = 0.$$

We will proceed with the solution of equation (2.41) under the assumption that the maximum value of the integral occurs near $p = 0$, and expand the function in the exponent in a Taylor series about $p = 0$ ($q=n$) so that

$$(2.43) \quad ik_1 F(q) = i\omega(t-\tau_h) - \frac{k_1 \ell}{F_1 n} (1-F_1 n^2) p \exp\left(\frac{i\pi}{4}\right) - \\ - \frac{k_1 \bar{r}}{2F_1 n^3} p^2 + \dots$$

where τ_h is the travel time of the head wave and $\bar{r} = \ell + \tilde{r}$. The quantity \tilde{r} was defined in equation (2.22) and in the present situation is evaluated at $q = n$. The distance the ray travels along the s -th interface is defined by ℓ . It should be noted that $\ell = r - r^*$ where r is the source-receiver offset and r^* , the critical distance, is the horizontal distance from the source at which the head wave from the s -th interface first appears. The above quantities are defined in Figure 2.5.

As before $R_s^m(q)$ can be expanded near $q = n$ as

$$(2.44) \quad R_s^m(q) \approx C_1^m(q) - m C_1^{m-1}(q) C_2(q) w_s.$$

The two terms in the expansion of $R_s^m(q)$ result in the expression for the head wave displacement being the sum of two integrals around the branch cut. As all

quantities in the first integral are the same on both sides of the cut, the contribution from this integral is zero. The argument of w_s changes by π from the left to the right hand side of the cut and consequently the integral involving this term is non-zero. The integration for the contributing term is then twice the integral over p from zero to infinity.

The head wave displacement has the form

$$(2.45) \quad u_* = \frac{-2}{F_1^{1/2}} e^{-i\omega(t-\tau_h)} - \frac{i\pi}{4} \left(\frac{k_1}{2\pi r} \right)^{1/2} \int_0^\infty mZ(p) C_1^{m-1}(p) C_2(p) \frac{p^{1/2}}{n} \times \left[p + 2(1-F_1 n^2)^{1/2} \exp\left(\frac{i\pi}{4}\right) \right]^{1/2} \exp \left[-\frac{k_1 \ell}{F_1} (1-F_1 n^2)^{1/2} p \exp\left(\frac{i\pi}{4}\right) - H_*(n) p^2 \right] \frac{dp}{q^{1/2}},$$

$$\text{where } H_*(n) = \frac{k_1 r}{2F_1^2 n^3}.$$

As in the case of the reflected wave it will be assumed that the major contribution of the integral occurs near $p = 0$ ($q=n$) so the following approximations will be made

$$(2.46) \quad \left[p + 2(1-F_1 n^2)^{1/2} \exp\left(\frac{i\pi}{4}\right) \right]^{1/2} \approx 2^{1/2} (1-F_1 n^2)^{1/4} \exp\left(\frac{i\pi}{8}\right)$$

$$\frac{Z(p) C_1^{m-1}(p) C_2(p)}{q^{1/2}} \approx \frac{Z(n) C_1^{m-1}(n) C_2(n)}{n^{1/2}} = \frac{Z(n) \tilde{\Gamma}}{n^{1/2}}$$

so that

$$(2.47) \quad u_* = 2e^{-i\omega(t-\tau_h) - \frac{i\pi}{8} \left(\frac{k_1}{\pi r n}\right)^{\frac{1}{2}} \frac{mZ(n) \tilde{\Gamma}(1-F_1 n^2)^{\frac{1}{4}}}{nF_1^{\frac{1}{2}}}} \\ \times \int_0^\infty \left[p^{\frac{1}{2}} \exp - \frac{k_1 \ell}{F_1} (1-F_1 n^2)^{\frac{1}{2}} p \exp\left(\frac{i\pi}{4}\right) - H_*(n) p^2 \right] dp.$$

With the change of variable $p \rightarrow (H_*(n))^{\frac{1}{2}} p$ equation (2.47) has the form

$$(2.48) \quad u_* = e^{-i\omega(t-\tau_h)} mZ(n) \tilde{\Gamma} F_1 \left[\frac{n^3 (1-F_1 n^2)}{2^3 k_1 r^2 \bar{r}^3} \right]^{\frac{1}{4}} g_2(p_*)$$

where

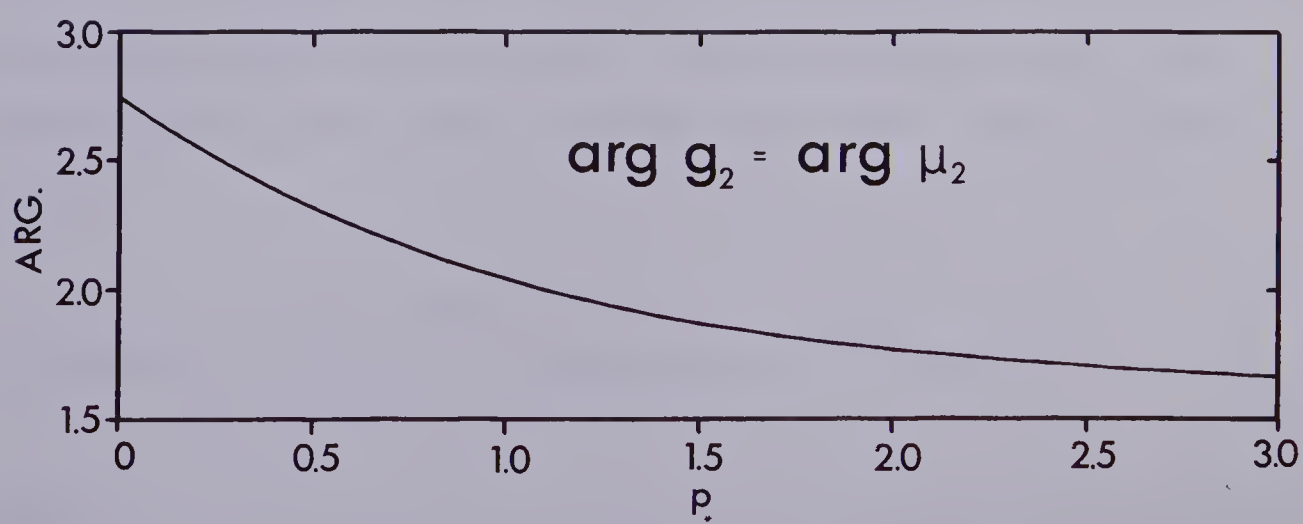
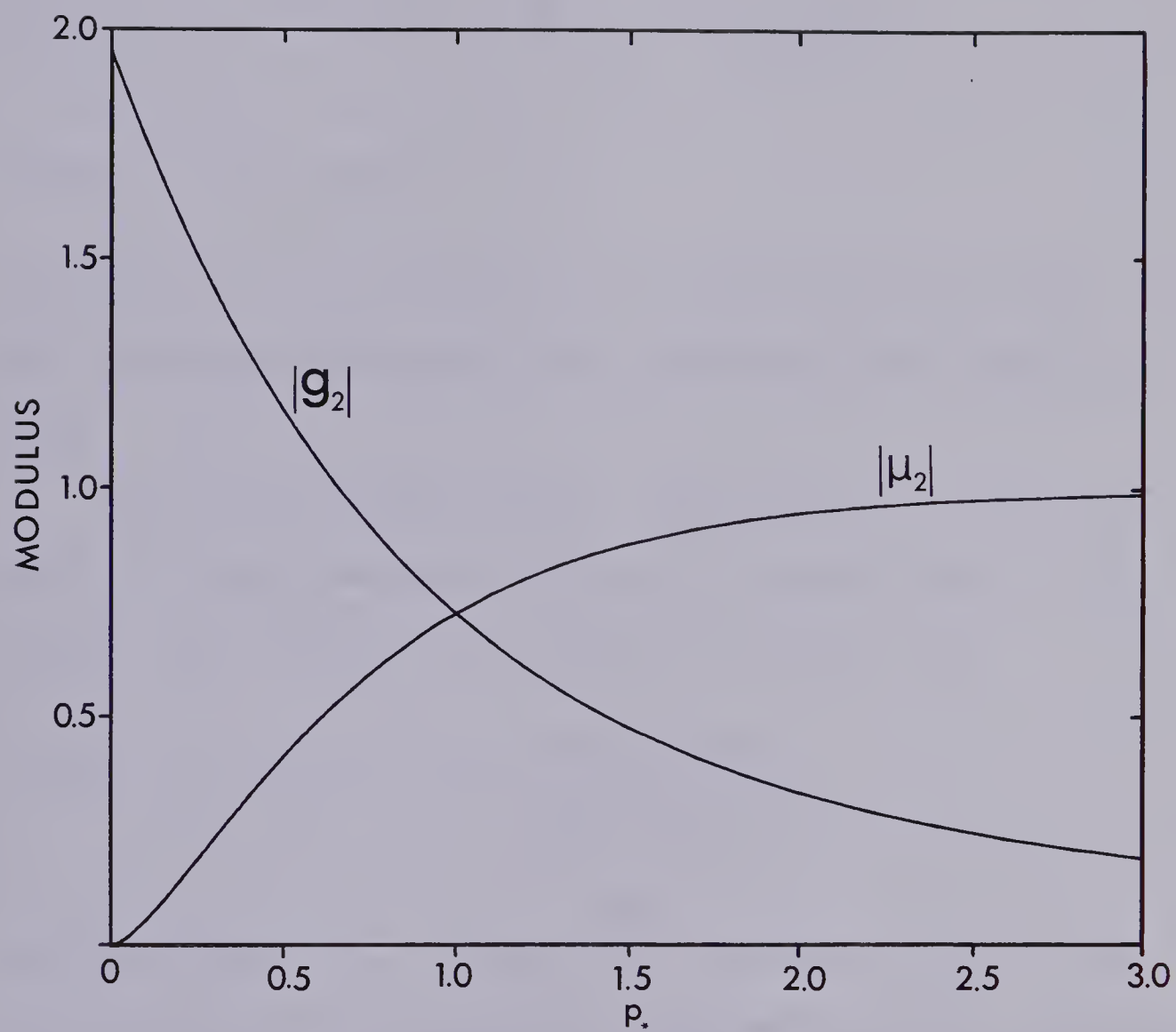
$$(2.49) \quad g_2(p_*) = 2^{5/2} \pi^{-\frac{1}{2}} \exp\left(\frac{7i\pi}{8}\right) \int_0^\infty p^{\frac{1}{2}} \exp\left[-p^2 - 2^{\frac{1}{2}}(1+i)p_* p\right] dp \\ p_* = \ell \left[\frac{k_1 n (1-F_1 n^2)}{2 \bar{r}} \right]^{\frac{1}{2}}.$$

The value p_* is proportional to ℓ and as such is equal to zero at the critical point and increases with distance from the critical point. As a result p_* is always real and positive. For large p_* the following approximation is valid (see Figure 5).

$$(2.50) \quad g_2(p_*) \approx \frac{e^{i\pi/2}}{p_*^{3/2}} \quad \text{for large } p_*.$$

Utilizing this asymptotic form for $g_2(p_*)$ and

Figure 2.5 The modulus and argument (in radians) of μ_2 and g_2 vs. p_* .



after some algebraic manipulation equation (2.48) can be written as

$$(2.51) \quad u_* = e^{-i\omega(t-\tau_h) + \frac{i\pi}{2} F_s^{\frac{1}{2}} \frac{mZ(n)\Gamma \tan \alpha_1}{r^{\frac{1}{2}} \ell^{3/2}}}$$

where $\Gamma = az_s \tilde{\Gamma}$.

Equation (2.51) is similar to the expression obtained for the head wave expression when geometrical ray theory is used.

Near the critical point ℓ and hence p_* is small so that the approximation (2.51) is no longer valid. Let $\mu_2(p_*) = p_*^{3/2} g_2(p_*)$ from which it follows that

$$(2.52) \quad u_* = F_1 e^{-i\omega(t-\tau_h) - \frac{mZ(n)\tilde{\Gamma}\mu_2(p_*)}{k_1 r^{\frac{1}{2}} (1-F_1 n^2)^{\frac{1}{2}}}}$$

where for large p_* , $\mu_2(p_*) \approx e^{\frac{i\pi}{2}}$. Because $\mu_2(p_*) \rightarrow 0$ as $\ell \rightarrow 0$ equation (2.52) is in an inconvenient form. Multiplying and dividing (2.52) by $L p_*^{3/2}$ (L being the geometrical spreading evaluated at $q=n$) the following final form is obtained for head wave displacement near the critical point

$$(2.53) \quad u_* = \frac{e^{-i\omega(t-\tau_h)}}{L} Z(n) g_*(n) 2^{-3/4} g_2(p_*)$$

where

$$(2.54) \quad g^*(n) = \frac{m\tilde{\Gamma} \left(1 - \frac{A_1}{B_1} n^2 \right)^{\frac{1}{4}}}{(k_1 n \tilde{r})^{\frac{1}{4}}} .$$

The term $\tilde{r}^{\frac{1}{4}}$ in the denominator of equation (2.54) should actually be \bar{r} , but since $\bar{r} = \tilde{r} + \ell$ and ℓ is small near the critical point \bar{r} has been replaced by \tilde{r} .

At this point it should be mentioned that (2.40) and (2.53) are approximations for the reflected wave and head wave near the critical point, and their accuracy diminishes with increasing distance from that point. However, at large distances from the critical point the asymptotic expressions (2.24) and (2.51) are generally good approximations.

2.6 Interference Reflected Head Wave

For the range of q_0 ($0 \leq q_0 < n$), only the reflected wave from the s -th interface exists. The point $q_0 = n$ corresponds to the onset of the head wave. In Sections 3 and 4 expressions were obtained for the reflected wave and head wave, equations (2.40) and (2.53) which are valid in the range ($n \leq q_0 \leq n + \epsilon$), where ϵ is small and its magnitude dependent on frequency. For values of q_0 greater than $n + \epsilon$ the asymptotic forms for the reflected and head waves can be used. The sum of the reflected and head wave displacement components in the range ($n \leq q_0 \leq n + \epsilon$) will be called the interference wave.

From equations (2.40) and (2.53) the interference

displacement component has the form

$$(2.55) \quad u = u_0 + u_* = \frac{e^{-i\omega(t-\tau_r)}}{L} Z(q_0) \left\{ R_s^m(q_0) - g^*(n) \right. \\ \left. [i2^{3/4}g_1(p_0) - i2^{3/4}p_0^{1/2}] + g^*(n)2^{-3/4}\exp(-i\bar{p})g_2(p_*) \right\}$$

where $\bar{p} = \omega^{1/2}(\tau_r - \tau_h)^{1/2}$ and it has been assumed that $Z(q_0) \approx Z(n)$. After some rearrangement (2.55) becomes

$$(2.56) \quad u = \frac{e^{-i\omega(t-\tau_r)}}{L} Z(q_0) \left\{ R_s^m(q_0) - g^*(n) [i2^{3/4}g_1(p_0) - \right. \\ \left. - i2^{3/4}p_0^{1/2} - 2^{-3/4}g_2(p_*)\exp(-i\bar{p}^2)] \right\}.$$

As the quantities p_0 , p_* and \bar{p} are all measures of the distance from the critical point, and in the vicinity of the critical point are all approximately equal, they can all be replaced by one value. The quantity \bar{p} is chosen because of its obvious physical significance.

Let

$$(2.57) \quad G(\bar{p}) = 2^{3/4}ig_1(\bar{p}) - 2^{3/4}i\bar{p}^{1/2} - 2^{-3/4}g_2(\bar{p})\exp(-i\bar{p}^2)$$

so that

$$(2.58) \quad u = \frac{e^{-i\omega(t-\tau_r)}}{L} Z(q_0) \left\{ R_s^m(q_0) - g^*(n)G(\bar{p}) \right\}.$$

With the aid of equations (2.33) and (2.49) the

expression for $G(\bar{p})$ can be written

$$(2.59) \quad G(\bar{p}) = -2^{3/4} \pi^{-1/2} \exp\left[\frac{7i\pi}{8} - i\bar{p}^2\right] \int_{-\infty}^{\infty} p_1^{1/2} \exp\left[-p_1^2 - 2\bar{p}p_1 \exp\left(\frac{i\pi}{4}\right)\right] dp_1 \\ - 2^{7/4} \pi^{-1/2} \exp\left\{\frac{7i\pi}{8} - i\bar{p}^2\right\} \int_0^{\infty} p^{1/2} \exp\left[-p^2 - 2\bar{p}p \exp\left(\frac{i\pi}{4}\right)\right] dp \\ - 2^{3/4} i\bar{p}^{-1/2}$$

where $\arg p_1^{1/2} = \pi$ for $p_1 > 0$. Extending the limits of integration of the second term in $G(\bar{p})$ results in the following

$$(2.60) \quad G(\bar{p}) = -2^{3/4} \pi^{1/2} \exp\left[\frac{7i\pi}{8} - i\bar{p}^2\right] \\ \times \int_{-\infty}^{\infty} p^{1/2} \exp\left[-p^2 - 2\bar{p}p \exp\left(\frac{i\pi}{4}\right)\right] dp - 2^{3/4} i\bar{p}^{-1/2}$$

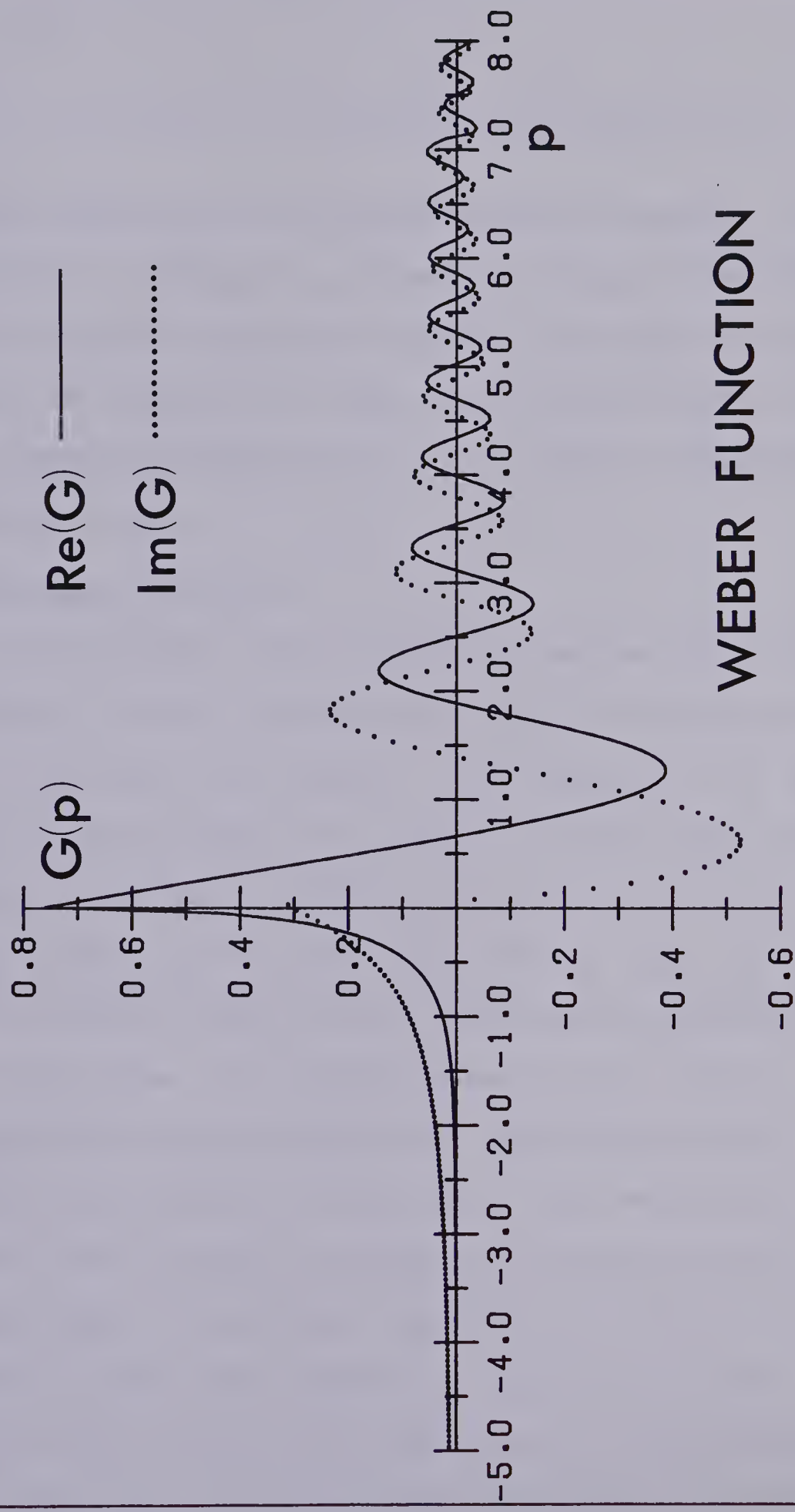
where $\arg p^{1/2} = 0$ for $p > 0$. (Cervený and Ravindra (1970)).

The form of $G(\bar{p})$ in equation (2.60) is such that it can be expressed in terms of the Weber-Hermite function (parabolic cylinder function) $D_{1/2}(\bar{p}(i-1))$ as

$$(2.61) \quad G(\bar{p}) = 2^{1/2} \exp\left[\frac{i\pi}{8} - i\bar{p}^2\right] D_{1/2}(\bar{p}(i-1)) - 2^{3/4} i\bar{p}^{-1/2}$$

with $D_{1/2}(\bar{p}(i-1))$ being defined by the identity

Figure 2.6 Real and imaginary parts of the Weber function for negative and positive arguments.



WEBER FUNCTION

$$\begin{aligned}
 (2.62) \quad & \int_{-\infty}^{\infty} s^{\frac{1}{2}} \exp \left[-s^2 - 2\bar{p}s \exp\left(\frac{i\pi}{4}\right) \right] ds \\
 & = (2\pi)^{\frac{1}{2}} 2^{-3/4} \exp \left[\frac{i\bar{p}^2}{2} + \frac{i\pi}{4} \right] D_{\frac{1}{2}}(\bar{p}(i-1)).
 \end{aligned}$$

The behaviour of the Weber-Hermite function is shown graphically in Figure 2.6. Other properties of the Weber-Hermite function and techniques for its numerical evaluation can be found in the paper by Marks and Hron (1977) and a numerical tabulation of it is given in Kireyeva and Karpov (1961).

2.7 Numerical Results

In this section the previously derived equations are applied to a simple hypothetical model of two plane layers overlying a halfspace. The description of the media is given in Table 1. Modulus of the amplitude vs. distance curves are plotted in the vicinity of the critical point for the two rays shown in the inserts of Figures 2.7 and 2.8; that is for rays having multiplicities of one and three. The significance of the factor m in the expression for the head wave amplitude is that for a ray with multiplicity m there are m rays arriving at the receiver with the same kinematic and dynamic properties.

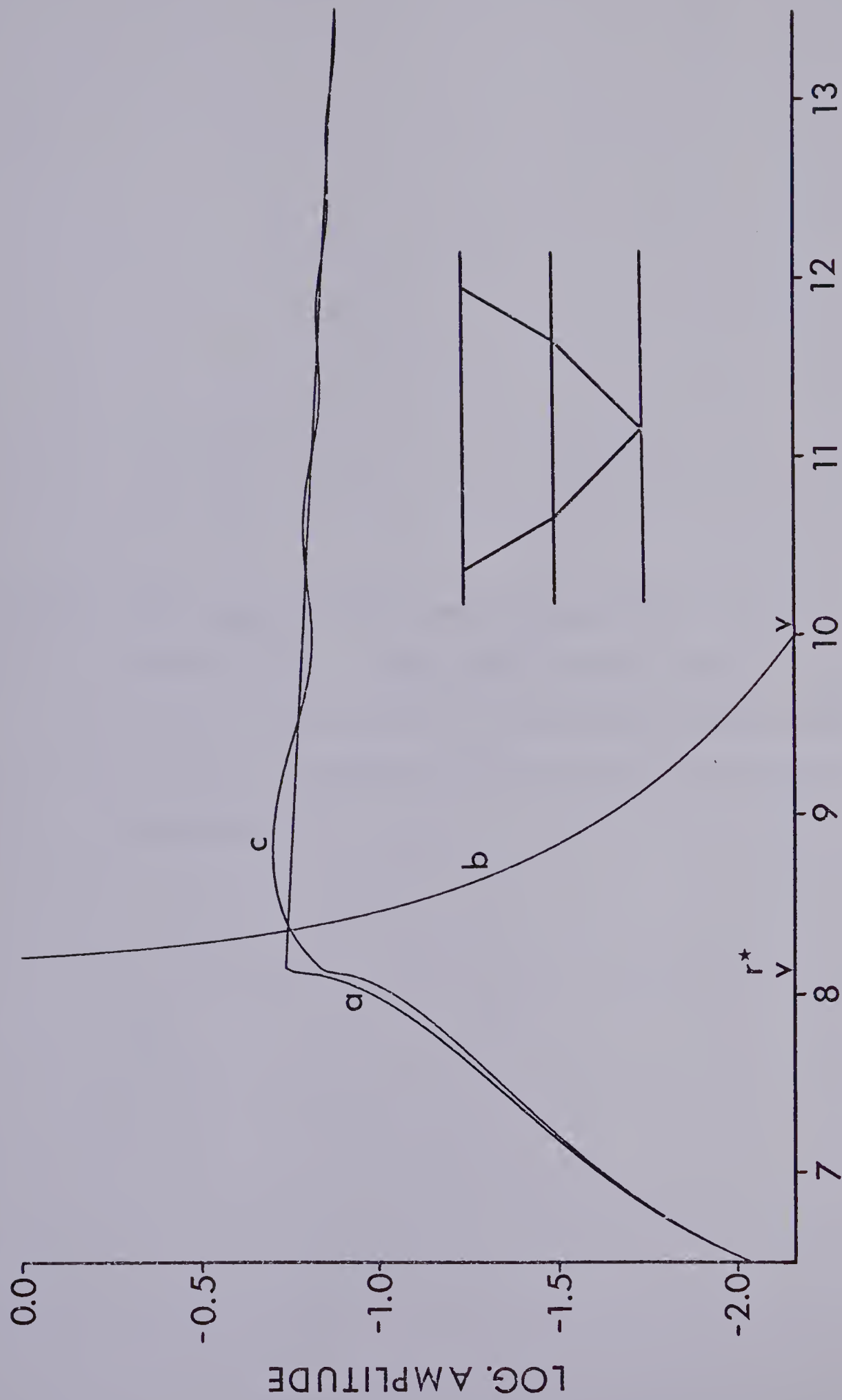
As noted in the figure captions the three curves presented are for the asymptotic solutions of the reflected wave (a) and the head wave (b) using equations (2.24) and (2.51) and the interference wave (c) from

TABLE 2.1

Specifications of the media used in Figures 2.7 and 2.8

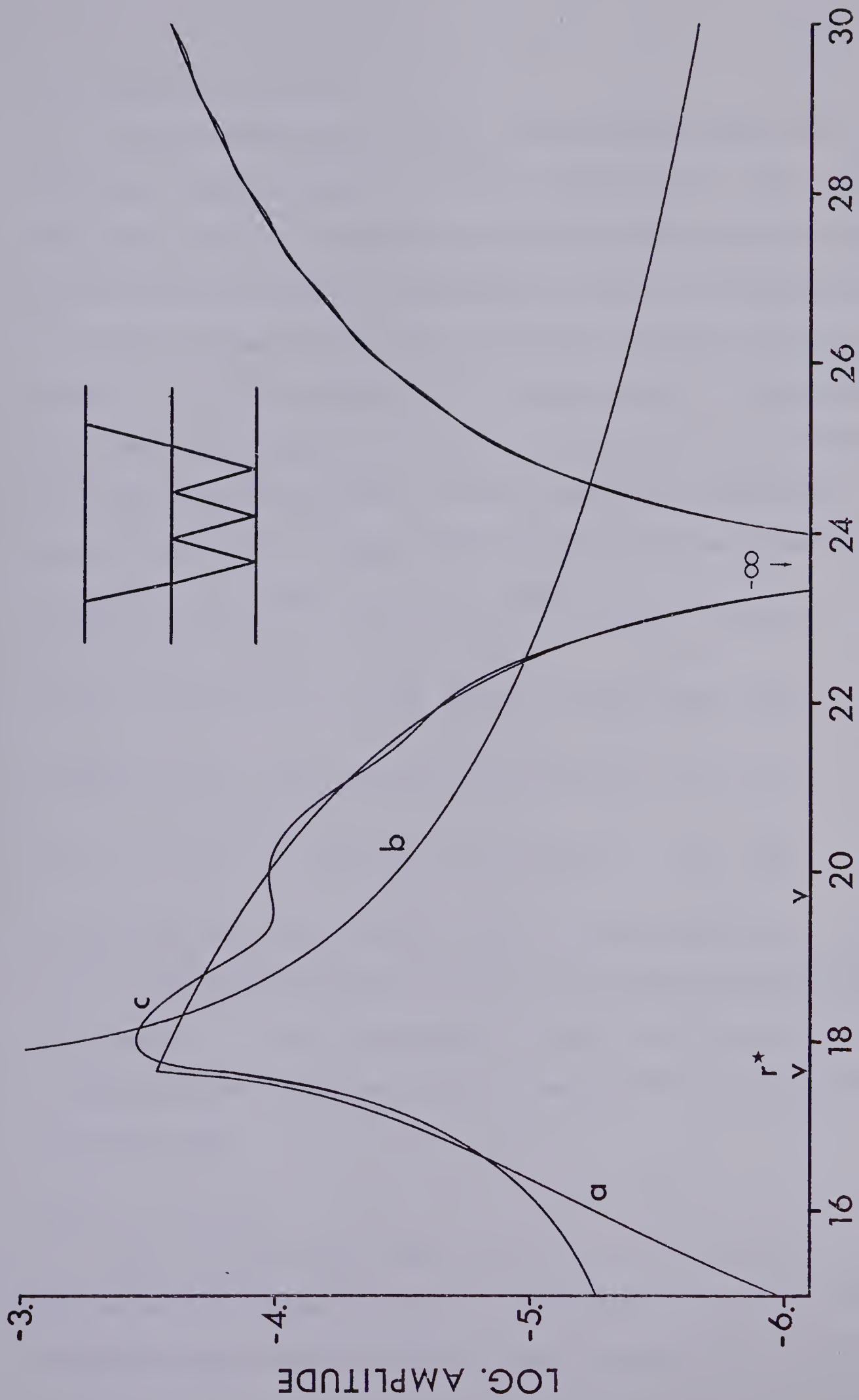
Layer	ax km./sec.	az km./sec.	ρ gm./cc	thickness km.
1	2.25	2.00	2.00	2.00
2	2.75	2.50	2.10	2.00
HSPACE	3.75	3.50	2.20	--

Figure 2.7 Log. amplitude-distance curves of the ray shown in the insert for (a) the reflected wave (b) the head wave (asymptotic form) and (c) the interference reflected-head wave. The critical distance is denoted by r^* and the interference zone for the source pulse given in the text lies between the v 's. It should be remembered that curve (c) is only valid in the interference zone.



DISTANCE - KM.

Figure 2.8 Log. amplitude-distance curves for a ray of multiplicity 3. The logarithmic singularity is due to a zero in the reflection coefficient of the ray incident from below at the second interface.



DISTANCE - KM.

from equation (2.58).

In the asymptotic limit, the head wave amplitude is inversely proportional to $(r-r^*)$, so that at $r=r^*$ this amplitude becomes infinite and is obviously non-physical. Also as was previously mentioned, since the difference in travel times between the reflected and head waves is small (i.e. the difference in travel times is less than the length of the source pulse) in the vicinity of the critical point, the two arrivals interfere with one another so that a simple summation of the two asymptotic

forms
$$u_t = e^{-i\omega(t-\tau_r)} \left[A_r + e^{-i\omega(t_r-t_h)} A_h \right]$$
 in this

region introduces further error. In the case under

consideration, for a source pulse $L(t) = \sin(2\pi f_o)$

$$\exp\left(-\left(\frac{2\pi f_o}{\gamma}\right)^2\right)$$
, with $f_o = 20$ Hz and $\gamma = 4.0$ the

length of the interference zone is approximately 1.9 km and is denoted in Figures 2.7 and 2.8 as the distance between the two v's. The development of the interference formula is an attempt to reduce the aforementioned inaccuracies in this zone.

2.8 Conclusion

The mathematical development of wave propagation for SH waves in a plane layered transversely isotropic homogeneous media using integral transform methods has been

presented. Asymptotic forms of the reflected and head wave displacement vectors have been derived along with special treatment of the interference of these two waves in the vicinity of the critical point, something which is not attainable if asymptotic ray theory is employed.

CHAPTER 3

RAY-REFLECTIVITY METHOD FOR SH WAVES IN
STACKS OF THIN AND THICK LAYERS

3.1 Introduction

Several methods including plane wave, reflectivity, integral transform and ray approaches have been employed in reflection studies of plane layered media to produce synthetic sections to aid in the interpretation of observed seismograms. As would be expected each of these methods has its own peculiar list of advantages and disadvantages.

The plane wave solution (for example, Wuenschel (1960), Sherwood and Trorey (1965), Treitel and Robinson (1966), Frasier (1969)) which is a direct consequence of the work of Thomson (1950) and Haskell (1953) has been used extensively and gives a good indication of the reflection response of a layered medium. However, a plane wave solution is a highly idealized approximation to an explosive point source generating spherical waves as it does not include the geometrical spreading of the wavefront as it propagates through a medium. It is also instructive to be able to identify individual arrivals on a seismic trace, an operation which is difficult to do using this method.

The papers of Fuchs and Müller (1971), Fuchs (1971) (1968) present the theory for computing synthetic

seismograms by the reflectivity method which is extremely useful in refraction studies when investigating the effects of a single transition zone. However for sub-critical (reflection) work the numerical integration used for refraction studies is not necessary and a stationary phase approximation suffices; whereupon inaccuracies in amplitudes are introduced if some layers in the transition zones are thick or if multiple transition zones separated by thick layers are to be considered.

Ray methods (Helmberger and Morris (1969), (1970), Müller (1971), Hron and Kanasewich (1970)) are useful in that they incorporate geometrical spreading and enable individual arrivals to be identified. If a partial ray expansion to the total wave field is desired (Hron (1971)) many rays must be considered to include all multiples and this places a severe restriction on the number of layers which can reasonably be considered. Albeit some success has been seen by including only the contributions from primaries and surface multiples, the seismograms produced may be misleading for some velocity depth structures. Another drawback of ray theory is that it breaks down if the dimensions of the layers are of the order of the wavelength (Cerveny (1977)).

The object of this paper is to present a compromise among the methods mentioned above that will provide greater flexibility in dealing with velocity depth

structures than any one method alone and at the same time maintain or increase the accuracy of the results.

The techniques employed here examine the velocity depth structure and separate it into thick layers separated by thin layered transition zones. The total wave field will be approximated by a partial ray expansion in the thick layers only while the thin layered (transition) zones that have been introduced will be treated as quasi-interfaces and analogues of reflection and transmission coefficients are calculated. The reflection and transmission effects of these thin layered zones are referred to in the literature as reflectivities and transmittivities. Their computation follows from the Thomson-Haskell technique and contain the same inherent numerical problems (Knopoff (1964), Dunkin (1965), Cervený (1974)).

In the text the simple case of SH waves propagating in the previously described medium will be discussed. This simple case was chosen because it presents the basic idea of the method without involving excessive mathematics which would be necessary if the coupled P-SV case were considered. However, the method is readily applicable to the P-SV problem and has been treated in a relatively inaccessible book in Russian by Ratnikova (1973).

3.2 Theoretical Preliminaries

Consider a system composed of m plane isotropic, homogeneous thick elastic layers between two halfspaces, the upper of which is a vacuum and the lower one isotropic and homogeneous (Figure 1). A point source $F(t)$ which radiates spherical SH waves is located (in cylindrical coordinate notation) at $r = 0$, $z = 0$, $\phi = 0$, and a receiver is situated at G , a distance r away. The coordinate location $z = 0$ corresponds to the free interface between the vacuum and layer 1 and z is assumed positive downwards.

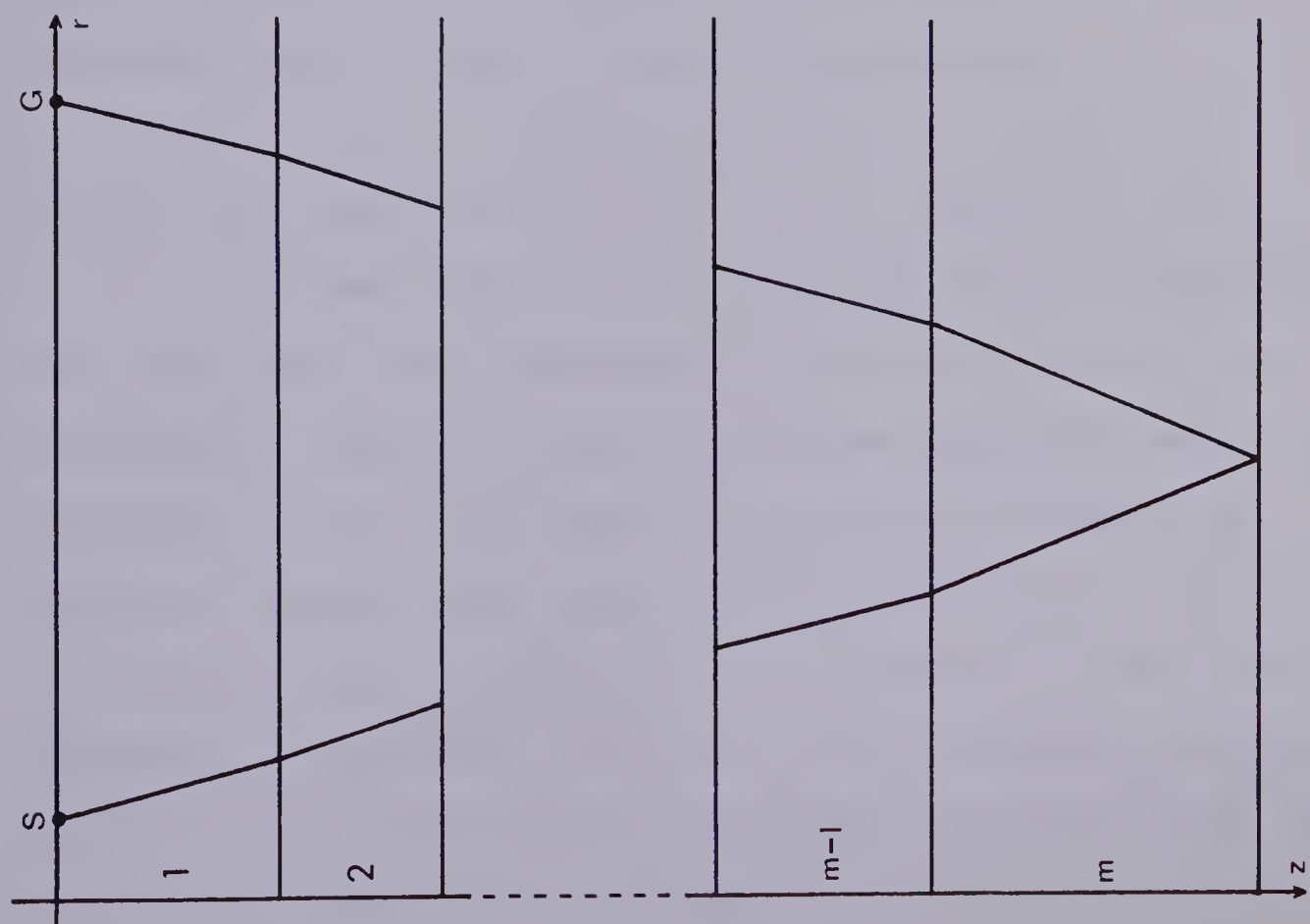
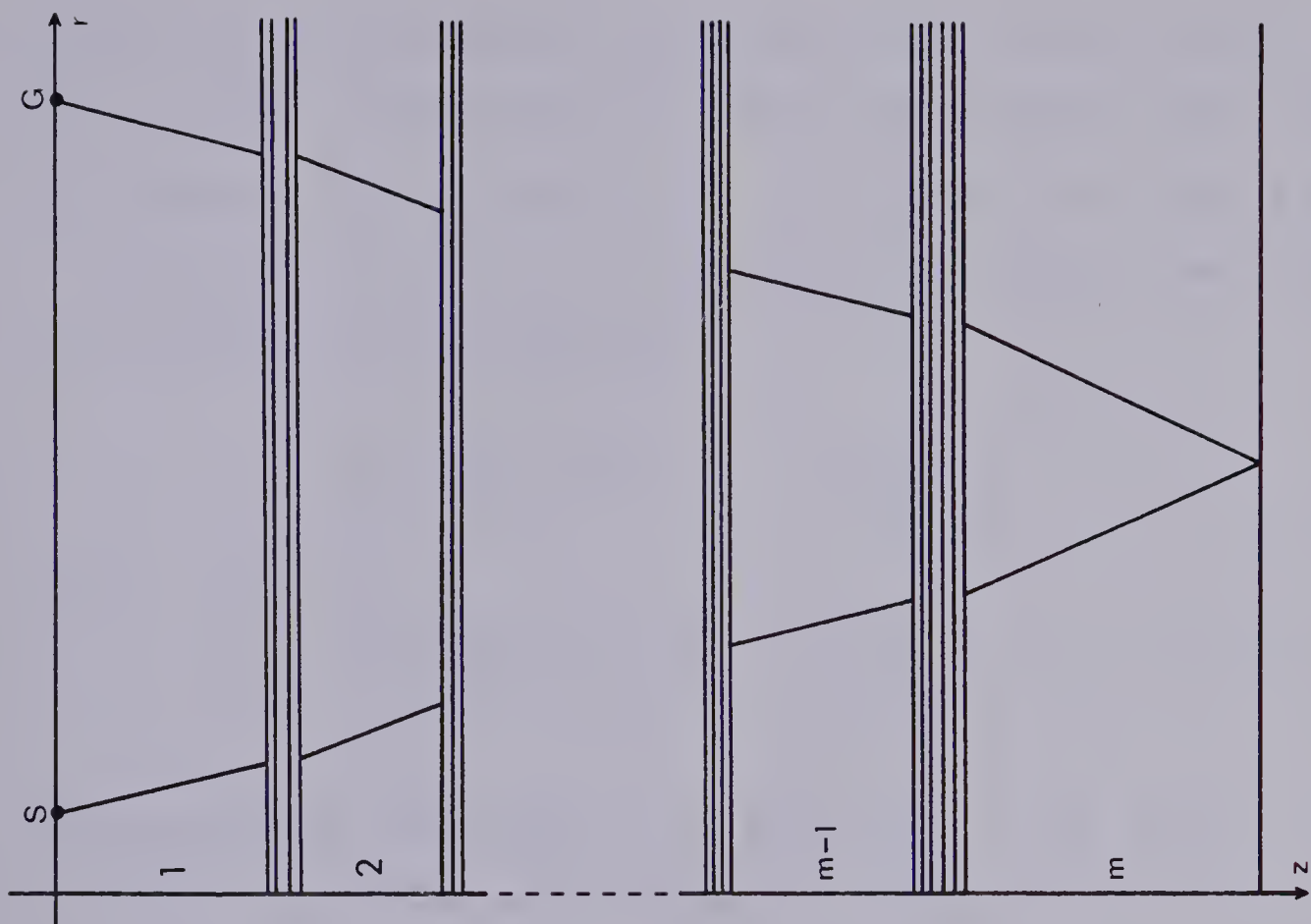
The displacement vector of an SH wave propagating in an isotropic homogeneous medium is perpendicular to the plane of incidence of the wave and is decoupled from the P-SV wave propagation. If the plane of incidence is chosen as the $\phi = 0$ plane, the displacement vector can be written without loss of generality as

$$(3.1) \quad \vec{u}(r, z, t) = u(r, z, t) \vec{n}_\phi$$

where \vec{n}_ϕ is a unit vector in the ϕ direction, and the Fourier time transformed disturbance due to an arbitrary ray propagating in some or all of the m layers at the point G can be written as (Daley and Hron (1979))

$$(3.2) \quad \tilde{u}(r, 0, \omega) = L(\omega) \int_0^\infty R(k) \exp \left[-i \sum_{n=1}^m N_n h_n v_n \right] J_0(kr) \frac{k dk}{i v_1}$$

Figure 3.1 Geometry of the media for (a) plane interfaces between thick layers and (b) quasi-interfaces between the thick layers composed of thin layered transition zones.



where $L(\omega)$ is the Fourier transform of the source pulse $F(t)$, $J_0(kr)$ is the Bessel function of the first kind and zero order, $R(k)$ is the product of all the reflection and transmission coefficients encountered by the ray, and the quantities v_n are defined by

$$(3.3) \quad v_n = \begin{cases} (k_n^2 - k^2)^{\frac{1}{2}} & c \geq \beta_n \\ -i(|k_n^2 - k^2|)^{\frac{1}{2}} & c < \beta_n. \end{cases}$$

The horizontal wavenumber k is given as $k = \frac{\omega}{c}$ and $k_n = \frac{\omega}{\beta_n}$, β_n is the shear velocity in the n -th layer, ω is circular frequency and the quantities N_n and h_n are the number of ray segments in the n -th layer and the thickness of the n -th layer respectively.

It will now be assumed that some or all of the interfaces encountered by the ray are replaced by thin transition zones; thin in the fact that their thicknesses are negligible when compared to the thicknesses of the other thick layers. These transition zones may take the form of a single thin high or low velocity channel or stack of several thin layers of varying velocity (Figure 1b).

In this case equation (3.2) is changed in that the frequency independent term $R(k)$ must be replaced by the product of the now frequency dependent reflectivities and transmittivities $P(\omega, k)$ so that

$$(3.4) \quad \tilde{u}(r, 0, \omega) = L(\omega) \int_0^{\infty} P(\omega, k) \exp \left[-i \sum_{n=1}^m N_n h_n v_n \right] J_0(kr) \frac{k dk}{i v_1}.$$

One of the most common methods of evaluating integrals of the type in equation (3.4) is by the stationary phase approximation. By comparison with direct numerical integration, this method will be shown to be a quite acceptable approximation for small source-receiver offsets. The condition which must be satisfied for the successful implementation of the stationary phase approximation is that the non-exponential terms in equation (3.4) are slowly varying implying that the region of applicability must be removed from all singular points (branch points and poles).

3.3 Reflectivity and Transmittivity

For completeness, the reflectivity and transmittivity of a thin layered or transition zone will be briefly discussed in this section. Similar treatments of this problem may be found in the literature, especially Cervený (1974) and Molotkov et al (1972).

A thin layered zone composed of s isotropic, homogeneous elastic layers will be assumed to lie in welded contact between the thick layers (layers 0 and $s+1$) which are also isotropic homogeneous and elastic. The vertical coordinate designating the bottom of the n -th layer will be denoted as z_n and the thickness of the n -th layer as

h_n . Without loss of generality, let $z_0 = 0$. Each layer can be fully defined for SH propagation by the density ρ_n and the shear wave velocity $\beta_n = (\mu_n/\rho_n)^{1/2}$ when μ_n is the shear modulus.

A slight deviation in notation will be used in this section as it is convenient to assume that a plane wave impinges on the thin layered zone when deriving the expressions for the reflectivity and transmittivity. This will require the introduction of a Cartesian coordinate system, with the plane of incidence being defined as the (x,z) plane (Figure 2). This assumption does not affect the results as it has been shown by Fuchs (1968), (1971) that the kernel $P(\omega,k)$ of the integral in equation (3.4) is the same whether a spherical or plane wave approach is used.

The solution of the wave equation $\nabla^2 u_n = \frac{1}{\beta_n^2} \frac{\partial^2 u_n}{\partial t^2}$ in each of the layers has the form

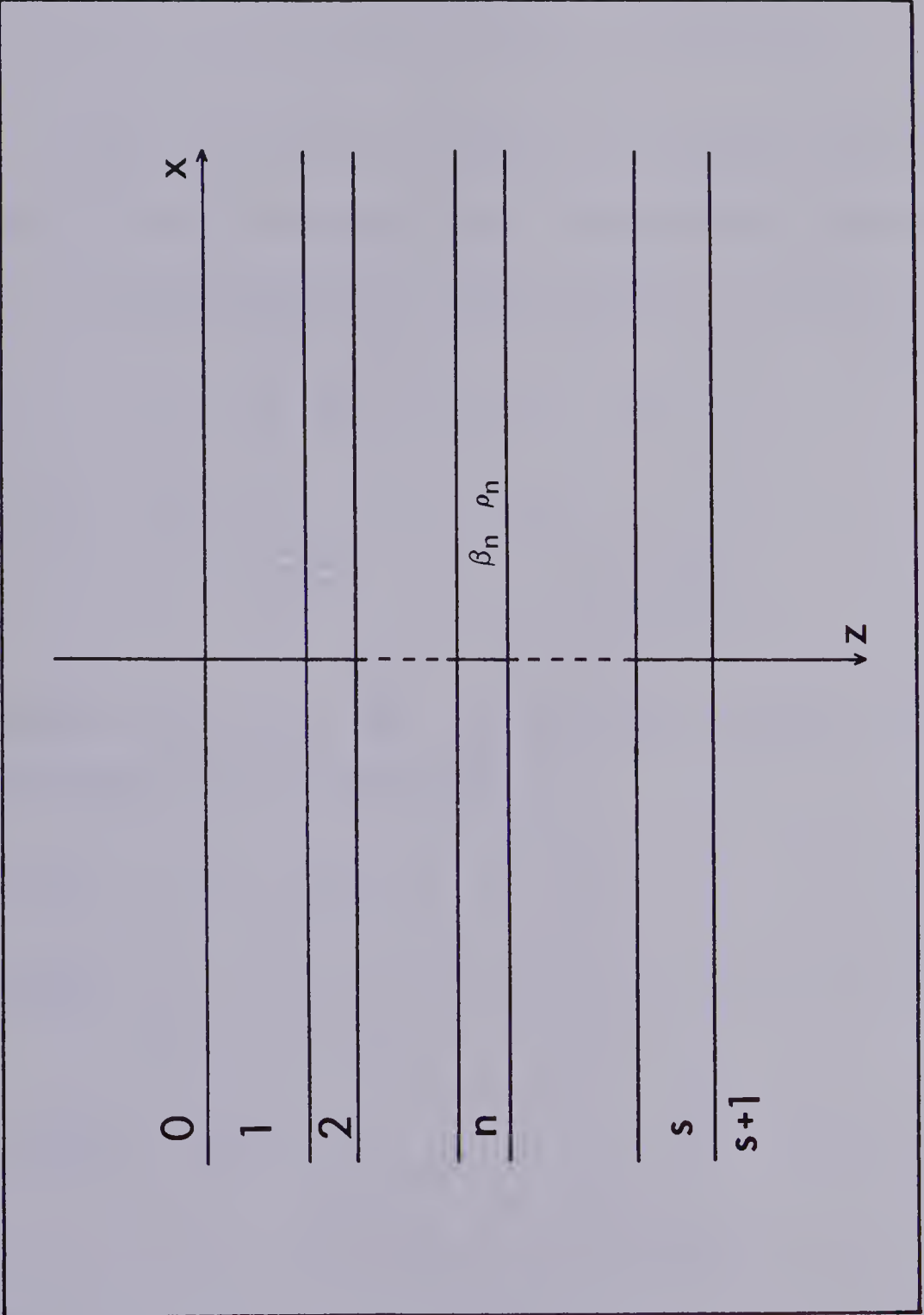
$$(3.5) \quad u_n = \phi_n^- + \phi_n^+$$

where the "+" and "-" signs indicate downward and upward propagating plane waves and have the form

$$(3.6) \quad \phi_n^\pm = A_n^\pm \exp[\mp i(z-z_{n-1})v_n] \exp[i(\omega t - kx)]$$

where as before

Figure 3.2 Description of layers and layer parameters for computing the reflectivities and transmittivities of a thin layered zone. β_n and ρ_n denote the shear wave velocity and density respectively of the n-th layer.



$$(3.7) \quad v_n = \begin{cases} (k_n^2 - k^2)^{\frac{1}{2}} & \text{for } c \geq \beta_n \\ -i(|k_n^2 - k^2|)^{\frac{1}{2}} & \text{for } c < \beta_n. \end{cases}$$

The quantities A_n^+ and A_n^- are complex functions of ω and k to be determined from the boundary conditions.

Introducing the column vectors Φ_n and S_n

$$(3.8) \quad \Phi_n = \begin{bmatrix} \phi_n^- \\ \phi_n^+ \end{bmatrix} \quad S_n = \begin{bmatrix} u_n \\ (\sigma_{yz})_n \end{bmatrix}$$

where $(\sigma_{yz})_n = \mu_n \frac{\partial u_n}{\partial z}$ is the shear stress, the following expression can be derived

$$(3.9) \quad S_n = T_n \Phi_n$$

where

$$(3.10) \quad T_n = \begin{bmatrix} 1 & 1 \\ i\mu_n v_n & -i\mu_n v_n \end{bmatrix}$$

and

$$(3.11) \quad T_n^{-1} = \frac{1}{2i\mu_n v_n} \begin{bmatrix} i\mu_n v_n & 1 \\ i\mu_n v_n & -1 \end{bmatrix}.$$

It also follows from equation (3.9) that

$$(3.12) \quad \phi_n = T_n^{-1} S_n.$$

The vector ϕ_n at the lower boundary of the n -th layer can be related to ϕ_n at the upper boundary of the n -th layer as

$$(3.13) \quad \phi_n(z_n) = E_n \phi_n(z_{n-1})$$

where it can be deduced that

$$(3.14) \quad L_n = \begin{bmatrix} \exp iQ_n & 0 \\ 0 & \exp -iQ_n \end{bmatrix}$$

with $Q_n = (z_n - z_{n-1})v_n = h_n v_n$.

Utilizing equations (3.9), (3.12) and (3.13) the following relation between the vector S_n at the bottom of the n -th layer (z_n) and the top of the n -th layer (z_{n-1}) can be obtained

$$(3.15) \quad S_n(z_n) = T_n \phi_n(z_n) = T_n E_n \phi_n(z_{n-1}) = T_n L_n T_n^{-1} S_n(z_{n-1}).$$

As the boundaries between the layers are in welded contact there must be continuity of displacement (u) and shear stress (σ_{yz}) at each interface, so that at the n -th interface

$$(3.16) \quad S_{n+1}(z_n) = S_n(z_n).$$

Continuing this analysis allows for the expression of the vector Φ_{s+1} , at the boundary of the lower halfspace ($z=z_s$) in terms of Φ_o at the boundary of the upper halfspace in the form

$$(3.17) \quad \Phi_{s+1}(z_s) = D \Phi_o(z_o)$$

where the matrix D is given by

$$(3.18) \quad D = T_{s+1}^{-1} \cdot (T_s E_s T_s^{-1}) \cdot (T_{s-1} E_{s-1} T_{s-1}^{-1}) \dots (T_1 E_1 T_1^{-1}) \cdot T_o$$

$$= T_{s+1}^{-1} \cdot C_s \cdot C_{s-1} \dots C_1 \cdot T_o$$

and it can be shown that the matrix C_n has the form

$$(3.19) \quad C_n = T_n E_n T_n^{-1} = \begin{bmatrix} \cos Q_n & \frac{\sin Q_n}{\mu_n v_n} \\ -\mu_n v_n \sin Q_n & \cos Q_n \end{bmatrix}.$$

The system of equations from equation (3.17) can be written

$$(3.20) \quad \begin{bmatrix} A_{s+1}^- \\ A_{s+1}^+ \end{bmatrix} = \begin{bmatrix} D_{11} & D_{12} \\ D_{21} & D_{22} \end{bmatrix} \begin{bmatrix} A_o^- \\ A_o^+ \end{bmatrix}$$

from which are obtained the relations

$$\begin{aligned}
 A_O^- &= \frac{1}{D_{11}} A_{s+1}^- - \frac{D_{12}}{D_{11}} A_O^+ \\
 (3.21) \quad A_{s+1}^+ &= \frac{D_{21}}{D_{11}} A_{s+1}^- + \frac{\det D}{D_{11}} A_O^+.
 \end{aligned}$$

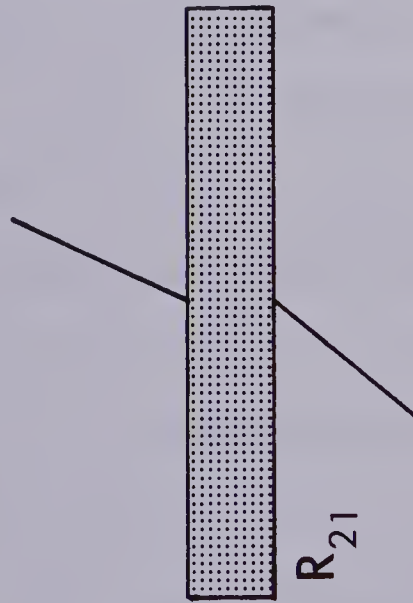
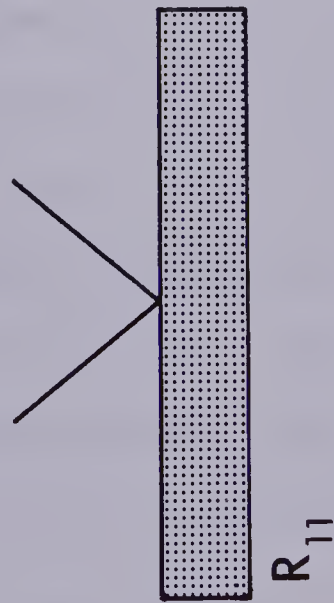
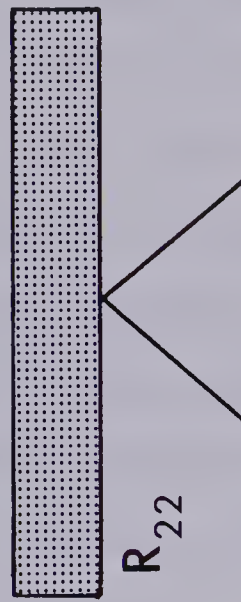
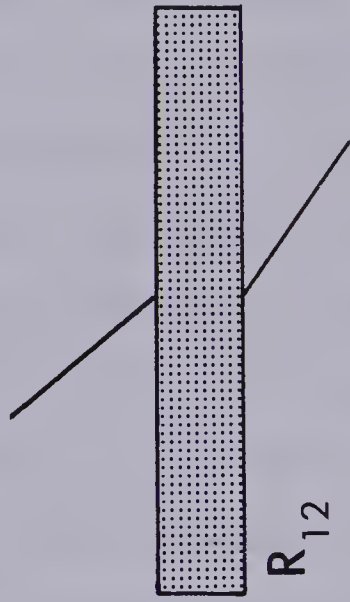
Introducing the notation R_{11} , R_{12} , R_{22} and R_{21} as in Figure 3 and using the relations given in equation (3.21), the reflectivity and transmittivity of a thin layered zone can be obtained. For incidence from the upper thick layer $A_{s+1}^- = 0$ and for incidence from the lower thick layer $A_O^+ = 0$ so that

$$\begin{aligned}
 R_{11} &= - \frac{D_{12}}{D_{11}} \\
 R_{12} &= \frac{\det D}{D_{11}} \\
 (3.22) \quad R_{22} &= \frac{D_{21}}{D_{11}} \\
 R_{21} &= \frac{1}{D_{11}}.
 \end{aligned}$$

The term $\Gamma(\omega, k)$ in equation (3.4) is the appropriate product of these reflectivities and transmittivities evaluated at the transition zones encountered by the ray. It is easily shown that for a single interface between two layers equation (3.22) produces ordinary reflection and transmission coefficients for the case of plane waves incident on a plane boundary.



Figure 3.3 Definition of the notation used in describing the reflectivity and transmittivity of a thin layered zone.



3.4 Stationary Phase Approximation

Equation (3.4) gives the exact displacement due to an arbitrary ray arriving at G. However, preserving this exactness requires that numerical integration be used to evaluate the integral. This method is unsuitable especially if the formula is used to construct synthetic seismograms where a great number of rays are to be considered, and hence a great many numerical integrations must be performed. Consequently, the integral in equation (3.4) will be approximated by the method of stationary phase which as previously mentioned corresponds quite reasonably to the exact solution for small source-receiver offsets.

For values of the integration variable k greater than some value k_{β_ℓ} where k_{β_ℓ} is the minimum in the series of values $(k_{\beta_1}, k_{\beta_2} \dots k_{\beta_j})$, j being the deepest thick layer the ray traverses ($1 \leq j \leq m$), ($1 \leq \ell \leq j$), the exponent in equation (3.4) will have a real negative term implying an exponentially decaying integrand. If the thickness of this layer ℓ is large, the integrand will decay fairly rapidly for values of $k > k_{\beta_\ell}$ and for this reason values of $k > k_{\beta_\ell}$ will not be considered. Thus after replacing the upper limit of integration by k_{β_ℓ} equation (3.4) becomes

$$(3.23) \quad \tilde{u}(r, 0, \omega) = L(\omega) \int_0^{k_{\beta_\ell}} P(\omega, k) \exp \left[-i \sum_{n=1}^j N_n h_n v_n \right] J_0(kr) \frac{k dk}{i v_1}.$$

Introducing the change of variable

$$(3.24) \quad k = k_1 q, \text{ the radicals become}$$

$$(3.25) \quad v_n = k_n \left[1 - (\beta_n / \beta_1 q)^2 \right]^{\frac{1}{2}} \text{ with } v_1 = k_1 (1 - q^2)^{\frac{1}{2}}$$

and the limits of integration are given by $(0, \beta_1 / \beta_\ell)$.

Equation (3.23) can be rewritten as

$$(3.26) \quad \tilde{u}(r, 0, \omega) = k_1 L(\omega) \int_0^{\beta_1 / \beta_\ell} P(\omega, q) \exp \left[-i \sum_{n=1}^j N_n h_n v_n(q) \right] \times J_0(k_1 q r) \frac{q dq}{i (1 - q^2)^{\frac{1}{2}}}.$$

If it is assumed that the argument of the Bessel function, $k_1 q r$, is large, $J_0(k_1 q r)$ can be used in its asymptotic form, viz.

$$(3.27) \quad J_0(k_1 q r) \approx \frac{1}{\sqrt{2\pi k_1 q r}} \left\{ \exp \left[i \left(k_1 q r + \frac{\pi}{4} \right) \right] + \exp \left[-i \left(k_1 q r + \frac{\pi}{4} \right) \right] \right\}.$$

Substituting equation (3.27) into equation (3.26) has

$$(3.28) \quad \tilde{u}(r, 0, \omega) = \left(\frac{k_1}{2\pi r} \right)^{\frac{1}{2}} L(\omega) e^{-i\pi/4} \int_0^{\beta_1 / \beta_\ell} P(\omega, q)$$

$$\begin{aligned}
& \times \exp \left\{ -i \left[\sum_{n=1}^j N_n h_n v_n(q) - k_1 q r \right] \frac{q^{\frac{1}{2}} dq}{(1-q^2)^{\frac{1}{2}}} \right. \\
& \quad \left. + \left(\frac{k_1}{2\pi r} \right)^{\frac{1}{2}} L(\omega) e^{-i3\pi/4} \int_0^{\beta_1/\beta_l} P(\omega, q) \right. \\
& \quad \left. \times \exp \left\{ -i \left[\sum_{n=1}^j N_n h_n v_n(q) + k_1 q r \right] \right\} \frac{q^{\frac{1}{2}} dq}{(1-q^2)^{\frac{1}{2}}} \right.
\end{aligned}$$

It will be assumed that the integrals in equation (3.28) can be approximated by the method of stationary phase and further that the phase of the product of the reflectivities and transmittivities need not be included in computing the stationary point. This second assumption is valid only for epicentral distances less than the critical distance, as after the critical distance the phase of $P(\omega, q)$ varies greatly, while before the critical distance its phase is approximately constant for changing values of q . Defining

$$(3.29) \quad f^{\pm}(q) = \pm k_1 q r + \sum_{n=1}^j N_n h_n v_n(q)$$

it follows that

$$(3.30) \quad \frac{df^{\pm}(q)}{dq} = \pm k_1 r - k_1 q \sum_{n=1}^j N_n h_n \left(1 - \frac{\beta_n}{\beta_1} q^2 \right)^{\frac{1}{2}} \frac{\beta_n}{\beta_1}.$$

$$\text{In the "+" case, } \left(\frac{df}{dq} \right)_{q=q_0} = 0 \quad \text{if } q_0 \frac{\beta_n}{\beta_1} \left(1 - \frac{\beta_n}{\beta_1} q_0^2 \right)^{-\frac{1}{2}}$$

$= \tan \theta_n$ where θ_n is the acute angle a ray segment in the n -th layer makes with the vertical axis. Thus it is required that

$$(3.31) \quad q_0 = \sin \theta_1.$$

The "-" case has no stationary point in the range of definition of $0 \leq q \leq \frac{\beta_1}{\beta_\ell}$ so that the first integral in equation (2.28) may be neglected.

Using the standard formula for the stationary phase approximation to an integral, the displacement can be written as

$$(3.32) \quad \tilde{u}(r, 0, \omega) = P(\omega, k) \frac{L(\omega)}{\cos \theta_1} \left[\frac{k_1 \sin \theta_1}{r f''(q_0)} \right]^{\frac{1}{2}} \exp[-i f(q_0)]$$

with

$$f(q_0) = k_1 \left[\sin \theta_1 r + \sum_{n=1}^m N_n h_n \frac{\beta_1}{\beta_n} \cos \theta_n \right]$$

and

$$f''(q_0) = k_1 \sum_{n=1}^m \frac{N_n h_n}{\cos^3 \theta_n} \frac{\beta_n}{\beta_1}.$$

As was previously mentioned the formula (3.32) is valid only for small source receiver offsets, so that none of the angles the ray segments make with the vertical axis

approach critical angle values. Also, it is assumed that the thickness of a transition zone is small when compared with the so-called thick layers, as spherical divergence or geometrical spreading is only incorporated in equation (3.32) for these thick layers. This geometrical spreading is given by the $k_1/\sqrt{rf''(q_0)}$ term.

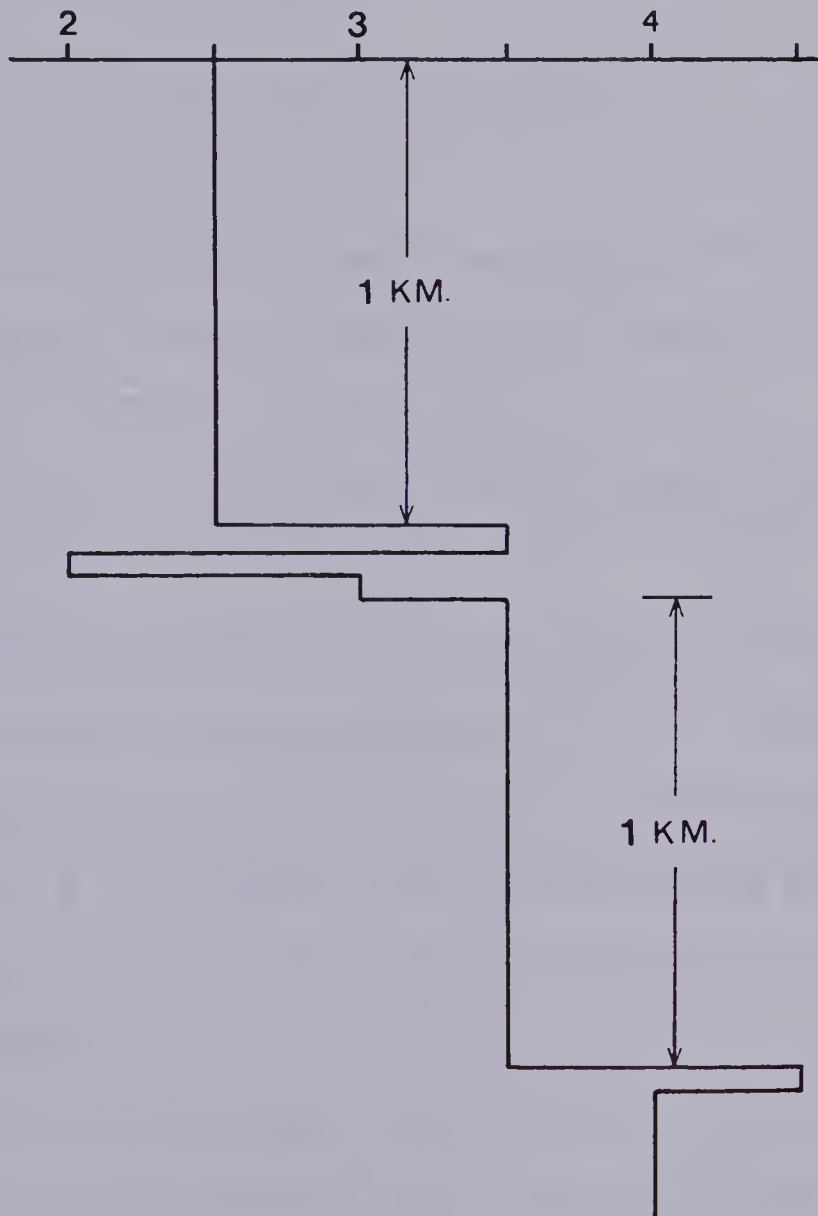
3.5 Numerical Results

A simple hypothetical model with two transition zones and two thick layers (Figure , Table 1) is used to compare three methods of computing synthetic seismograms; (a) ray theory, (b) numerical integration employing the reflectivity method, and (c) the stationary phase approximation discussed in this paper. The object of this comparison is to demonstrate the efficiency and reasonable accuracy of the ray-reflectivity method.

The number of total layers was kept small at six to enable a partial ray expansion (Hron (1971)) to approximate the total wave field by the ray method. In this method all possible rays up to those with a maximum of eighteen segments were generated in the six layers and included in the seismogram provided their arrivals were within the time window specified. In the ray-reflectivity method, rays needed only be generated in the two thick layers.

Figure 3.4 Velocity-depth structure of the model.

VELOCITY KM. per SEC.



Three separate programs were used for each of the traces shown in Figure 3.5. The ray method involved convolution in the time domain while the other two, numerical integration and ray-reflectivity, employed an FFT algorithm (Cooley and Tukey (1965)) when converting from the frequency to time domain.

The source pulse used was

$$(3.33) \quad F(t) = \sin 2\pi f_0 t \exp\left(-\frac{(2\pi f_0 t)^2}{\gamma}\right) \quad -\infty < t < \infty$$

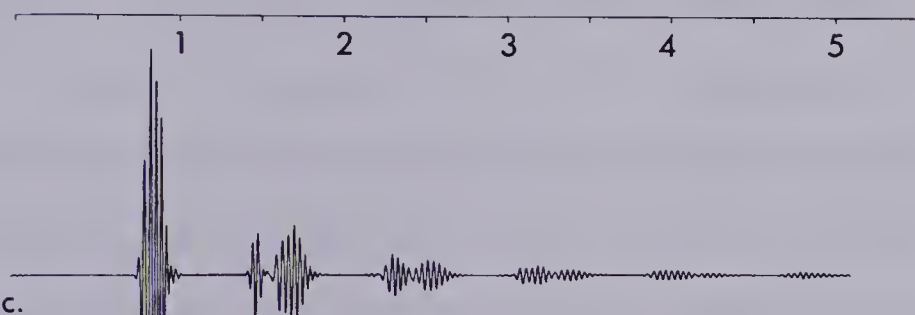
where f_0 is the predominant frequency of the pulse and γ is a damping factor. The Fourier transform of (3.33) is

$$(3.34) \quad \mathcal{O} \quad L(\omega) = -\frac{i\pi^{\frac{1}{2}}\gamma}{2\pi f_0} \exp\left[-\frac{\gamma^2}{4}\left(1+\left(\frac{\omega}{2\pi f_0}\right)^2\right)\right] \sinh\left(\frac{\gamma^2\omega}{4\pi f_0}\right).$$

This particular source pulse was chosen because of the ease with which it may be handled in the frequency domain as its spectrum is a Gaussian curve whose maximum is centered at f_0 . However, all three of the programs used can incorporate any source pulse whether in analytic or digital form.

Figure 3.5 indicates that the ray-reflectivity method gives a good approximation to the exact (numerical integration) solution even though in terms of CPU time it was about forty times faster. The times for the ray approach and the ray-reflectivity method were about equal, but it must be remembered that the model chosen was to

Figure 3.5 A comparison of three methods of computing synthetic seismograms for the model shown in Fig. 4. The three methods are (a) asymptotic ray theory (b) numerical integration and (c) ray-reflectivity method. The notation on the time axis in cases (a) and (c) identify the ray code of the arrival and its amplitude. The source-receiver offset in all cases is 1.0 Kft.



facilitate the ray approach and that the ray-reflectivity may handle much more complicated structures.

As the ratio of the dimension of the stack of thin layers to the dimension of the thick layers used here is quite large some error is introduced as can be seen when the ray-reflectivity trace is compared to the trace obtained by numerical integration. This error is reduced as the aforementioned ratio is decreased.

3.6 Conclusion

The technique presented is well suited for the computation of synthetic seismograms in oil exploration for comparison and interpretation of real data, as it correctly produces the extensive interference phenomena due to the fine layering. This is done without any effort to decompose them into individual ray paths in the thin layers. Physically justifiable amplitudes are produced as the method accounts for the divergence (in the thick layers) of wavefronts radiated from a point source and seismic energy partitioning due to reflections and transmission through the thin layer stacks.

The main advantage of this method is that a small number of rays may be used to generate synthetic seismograms in a many layered structure and their arrivals can be identified in the seismograms.

CHAPTER 4

A COMPARISON OF SYNTHETIC SEISMOGRAMS FOR A THINLY
STRATIFIED MEDIUM AND A TRANSVERSELY ISOTROPIC MEDIUM

4.1 Introduction

That a periodic isotropic two layered (PITL) medium behaves as a homogeneous transversely isotropic (HTI) medium in its kinematic and dynamic properties has been shown to be a valid assumption as far as the propagation of elastic waves is concerned provided that the seismic wavelengths used are large when compared to the thicknesses of the individual isotropic layers.

A review of the literature involving this problem to 1962 is contained in the paper of Backus (1962). Notable among the references are the works of Postma (1955), Uhrig and Van Melle (1955), White and Agona (1955), Rytov (1956), Ryznickenko (1949) and Anderson (1961). Subsequent to these are the publications of Gassmann (1966) in which is presented a comprehensive tutorial on the many aspects of elastic wave propagation in (HTI) media and Levin (1979) where instructional figures of wavefront profiles of (HTI) equivalents of actual (PITL) media may be found.

However, to the author's knowledge, no graphic comparison of methods can be found in the literature that these two formulations are equivalent. The intent of this paper is to consider a very simple example of a

(PITL) medium composed of $2N$ layers sandwiched between an isotropic layer and an isotropic halfspace and to compare kinematic and dynamic properties via synthetic seismograms to a similar geometry in which the (PITL) layer has been replaced by its equivalent (HTI) medium (Figure 4.1). This comparison will be done only for SH waves.

The two methods which will be employed to compute synthetic seismograms are (a) asymptotic ray theory for which the required theory and formulae were developed for SH waves in an (HTI) medium in Daley and Hron (1979) and (b) the numerical integration reflectivity method in which each of the $2N$ layers of the (PITL) medium are individually considered.

4.2 Notation and the Two Methods

Aside from the density ρ , two elastic parameters are required to fully describe SH wave propagation in an (HTI) medium, in which the wavefront is an ellipsoid of revolution. The parameters are C_{44} and C_{66} , are such that $A_{44} = \frac{C_{44}}{\rho}$ and $A_{66} = \frac{C_{66}}{\rho}$ have the dimensions of velocity squared. The square root of A_{44} and A_{66} are respectively, the velocity along the horizontal (r) and vertical (z) axis of the ellipsoid describing the wave surface.

The quantities C_{44} and C_{66} and density ρ are obtained from the shear moduli μ_I and μ_{II} and densities ρ_I and ρ_{II} of the two isotropic layers comprising the

(PITL) medium by the following averaging techniques

$$(4.1) \quad C_{44} = \frac{(d_I + d_{II})\mu_I\mu_{II}}{d_I\mu_{II} + d_{II}\mu_I}$$

$$(4.2) \quad C_{66} = \frac{\mu_I d_I + \mu_{II} d_{II}}{d_I + d_{II}}$$

$$(4.3) \quad \rho = \frac{d_I \rho_I + d_{II} \rho_{II}}{d_I + d_{II}}$$

where d_I and d_{II} are the thicknesses of isotropic layers I and II and $N(d_I + d_{II})$ is the thickness of the (PITL) medium.

In what follows the subscripts 1, 2 and 3 will refer respectively to quantities in layers 1 and 2 and the halfspace. In particular β_i is the shear wave velocity and ρ_i is the density in the i -th layer. In the (HTI) equivalent of the (PITL) medium (layer 2) the shear wave velocity β_2 (the velocity of energy propagation) is defined by

$$(4.4) \quad \frac{1}{\beta_2^2} = \frac{\sin^2 \phi}{A_{44}} + \frac{\cos^2 \phi}{A_{66}},$$

ϕ being the acute angle between the ray and the vertical (z) axis (Daley and Hron (1979)).

As was previously mentioned, the asymptotic ray theory solution to the propagation of SH waves in a (HTI)

Figure 4.1 Geometry of the media and definition of parameters.



β_1 ρ_1



μ_1 μ_{11} ρ_1 ρ_{11}



A_{44} A_{66} ρ



β_3 ρ_3



medium has been presented by Daley and Hron (1979) and all relevant formulae for the computation of synthetic seismograms may be found there. In that work the first order approximation of asymptotic ray theory is employed to determine the solution for the disturbance at a given source-receiver offset and is assumed to be the sum of the disturbances of a finite number of rays which is taken to approximate the total wave field. As the numerical integration method will yield head wave arrivals as well as reflected arrivals the high frequency ray approximation for head wave arrivals is also included in the seismograms.

The time transformed expression for the SH displacement (\vec{u}) at a point (r, z) in cylindrical polar notation within an isotropic layer due to the reflection from a stack of layers is

$$(4.5) \quad \vec{u}(r, z, \omega) = \frac{L(\omega)}{i} \int_0^{\infty} R(k, \omega) J_0(kr) \exp[i v_1(z-2h)] \frac{k dk}{v_1} \vec{j}$$

where

ω - circular frequency

k - horizontal wave number

r - source receiver offset

h - thickness of overlaying isotropic layer

J_0 - zero order Bessel function of the first kind

$L(\omega)$ - time transform of the source function $f(t)$

$R(k, \omega)$ - reflectivity of the thin layered zone

$$v_1 = \begin{cases} (k_1^2 - k^2)^{\frac{1}{2}} & \text{for } c \geq \beta_1 \\ -i(|k_1^2 - k^2|)^{\frac{1}{2}} & \text{for } c < \beta_1 \end{cases}$$

$$c = \frac{\omega}{k}$$

\vec{j} - unit vector perpendicular to the plane of incidence ((r,z) plane) and the orientation of axes and geometry is shown in Figure (4.1). If the receiver is located on the surface, $z=0$.

The term $R(\omega, k)$ is the reflectivity of the PITL layer and is defined as

$$(4.6) \quad R(\omega, k) = - \frac{D(1, 2)}{D(1, 1)}$$

where

$$(4.7) \quad D = T_3^{-1} (C_I C_{II})^n T_1$$

and

$$(4.8) \quad T_1 = \begin{bmatrix} 1 & 1 \\ i\mu_1 v_1 & -i\mu_1 v_1 \end{bmatrix}$$

$$(4.9) \quad T_3^{-1} = \frac{1}{2i\mu_3 v_3} \begin{bmatrix} i\mu_3 v_3 & 1 \\ i\mu_3 v_3 & -1 \end{bmatrix}$$

$$(4.10) \quad C_j = \begin{bmatrix} \cos Q_j & \frac{\sin Q_u}{\mu_j v_j} \\ -\mu_j v_j \sin Q_j & \cos Q_j \end{bmatrix} \quad j = I, II$$

$$(4.11) \text{ with } v_\kappa = \begin{cases} (k^2 - k_\kappa^2)^{\frac{1}{2}} & \text{for } c \geq \beta_\kappa \\ -i(|k_\kappa^2 - k^2|)^{\frac{1}{2}} & \text{for } c < \beta_\kappa \end{cases}$$

$$\kappa = 1, 3, I, II.$$

and $Q_j = h_j v_j$, k_j being the thickness of the j -th isotropic layer making up the PITL medium.

To simplify computation and to greatly reduce computer time, the matrix $A = C_I C_{II}$ can be diagonalized which minimizes the number of operations to compute A^n .

Thus A takes the form

$$(4.12) \quad A = P^{-1} \Lambda P$$

where Λ is a two by two diagonal matrix whose elements are the eigenvalues (λ_1 and λ_2) of A . These eigenvalues are obtained from the solution of

$$\begin{aligned}
 (4.13) \quad & \lambda^2 - \left\{ 2\cos Q_I \cos Q_{II} + \delta \sin Q_I \sin Q_{II} \right\} \lambda \\
 & + \left\{ \cos^2 Q_I \cos^2 Q_{II} + \sin^2 Q_I \sin^2 Q_{II} \right. \\
 & \left. - \delta \sin Q_I \sin Q_{II} \cos Q_I \cos Q_{II} \right\} = 0
 \end{aligned}$$

with

$$\delta = \frac{\mu_I v_I}{\mu_{II} v_{II}} + \frac{\mu_{II} v_{II}}{\mu_I v_I} .$$

P is the matrix whose columns are the eigenvectors corresponding to the two eigenvalues and P^{-1} is its inverse. As a consequence

$$(4.14) \quad A^n = P^{-1} \Lambda^n P.$$

The determination of the eigenvalues and ultimately Λ and P is done numerically utilizing the IMSL routing EIGCC.

4.3 Numerical Discussion

As was indicated earlier the model to be used in comparing the two techniques in computing synthetic seismograms is an isotropic layer over a (PITL) or (HTI) layer over a half space. The (PITL) medium was chosen to be composed of 500 combinations of alternating layers of shale and limestone each of one meter thickness for a total layer thickness of one kilometer. The velocities and densities used are given in Table (4.1).

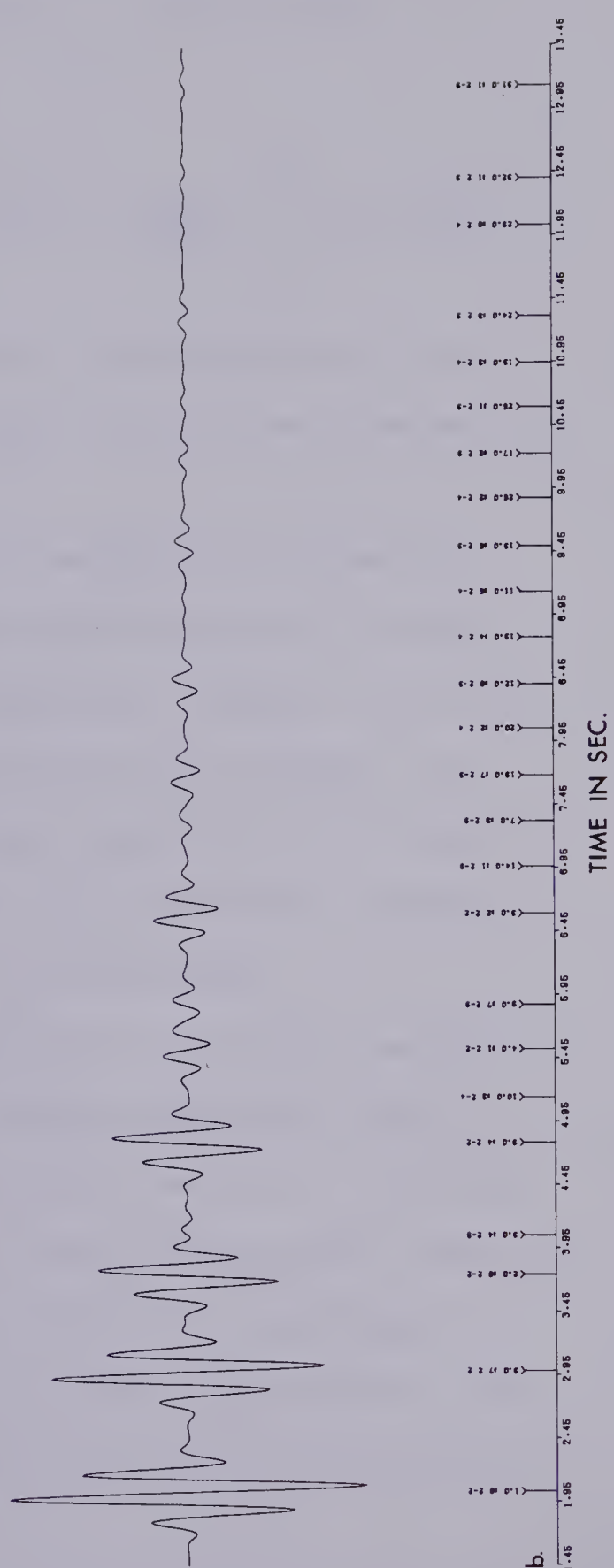
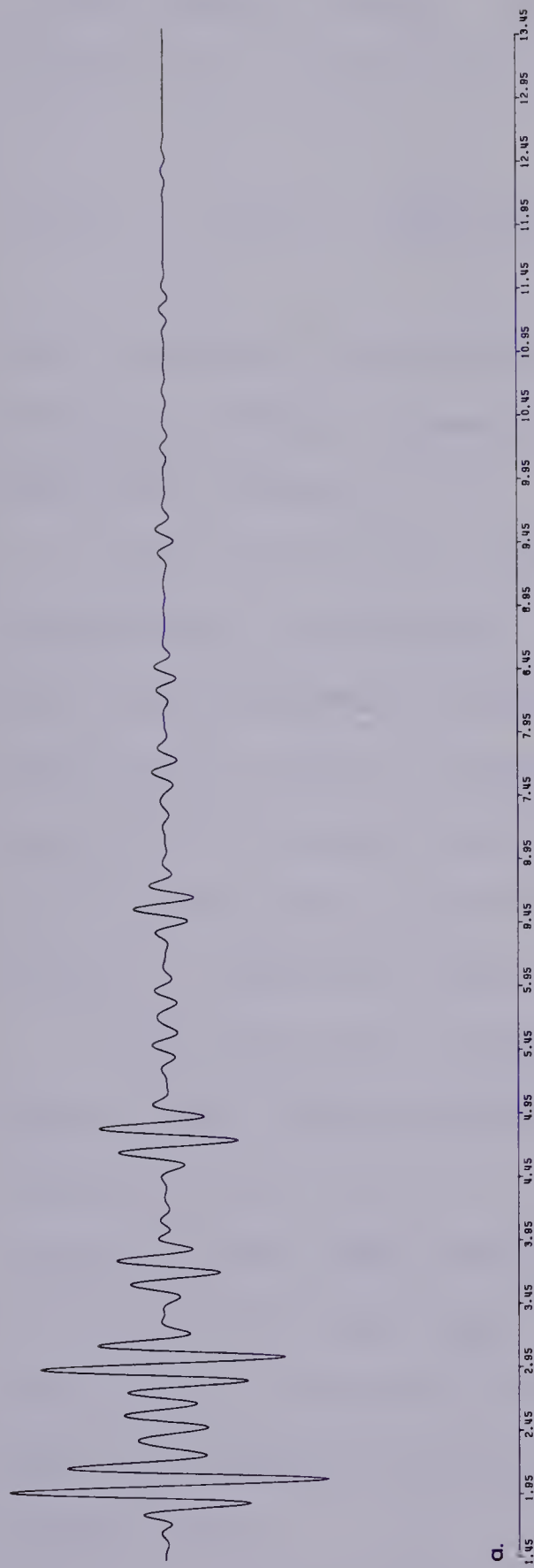
In the numerical integration approach a transformation was made so that the integration variable was the angle of incidence in the overlaying isotropic layer (Fuchs 1971). Angular increments of 0.1 degree were chosen and a trapezoidal numerical integration scheme was employed. As the source receiver offset chosen for the comparison of the methods was 4 kilometers the asymptotic approximation to the Bessel function was used. As the reflectivity of the (PITL) medium is frequency dependent the numerical integration was carried out at 543 equally spaced points in the frequency domain spanning the range of frequencies where the amplitude spectrum of the source pulse was non zero. The Cooley-Tukey (1965) FFT algorithm was used to invert to the time domain. The resultant seismic trace is shown in Figure 2.

The second trace in Figure 2 is the seismogram computed via the ray method. All possible rays up to those with a maximum of 18 ray segments are generated and if they arrive within the specified time window they are included in the seismogram. The major arrivals and their amplitudes are identified along the time axis.

The time dependence of the source pulse used is

$$(4.15) \quad f(t) = \sin(2\pi f_o t) \exp \left[- \left(\frac{2\pi f_o t}{\gamma} \right)^2 \right] \quad -\infty < t < \infty$$

Figure 4.2 Comparison of the two methods of computing synthetic seismograms; (a) numerical integration (b) asymptotic ray theory.



where f_0 is the predominant frequency of the pulse and γ is the damping factor. In case, $f_0 = 30$ Hz and $\gamma = 6$. The Fourier transform of (4.) is

$$(4.16) \quad L(\omega) = -\frac{i\pi^{\frac{1}{2}}\gamma}{2\pi f_0} \exp\left[-\frac{\gamma^2}{4}\left(1+\left(\frac{\omega}{2\pi f_0}\right)^2\right)\right] \sinh\left(\frac{\gamma^2\omega}{4\pi f_0}\right).$$

This pulse was chosen because of its simplicity in the frequency domain; however, any pulse may be incorporated into the programs.

It is evident that the two methods discussed are equivalent in this highly idealized situation in which only two alternating layers are used. Backus (1962) has shown that a medium composed of many thin layers, not necessarily periodic, may be approximated in the long wave length limit by an (HTI) layer provided a certain number of stability criteria are satisfied.

The comparison of seismograms of the above mentioned type of thin layered medium and its equivalent (HTI) medium is precluded at the present time due to the large amounts of CPU time required. As an example for the case considered here the numerical integration procedure required 250 times the CPU time as the ray method, even with the diagonalization simplification in computing the reflectivity.

Table 4.1 Specification of the Media

Layer	β (km/sec)	ρ (gm/cc)	Thickness (km)
1	1.100	1.95	1.00
(PITL) 2	Limestone	2.50	1.00
	Shale	2.38	
3	2.950	2.70	--

(HTI) 2	$\sqrt{A_{44}} = 2.086$ km/sec	$\sqrt{A_{66}} = 1.819$ km/sec	$\rho = 2.44$ gm/cc

APPENDIX A

If the volume of a ray tube which is truncated at both ends by the wavefronts at t_0 and t is denoted by γ , Gauss' integral theorem has

$$\begin{aligned}
 (A1) \quad \int \int \int_{\gamma} \nabla \cdot \rho \vec{a} d\gamma &= \int \int_{\Sigma(t)} \rho(t) \vec{a} \cdot d\vec{\sigma}_t + \int \int_{\Sigma(t_0)} \rho(t_0) \vec{a} \cdot d\vec{\sigma}_{t_0} \\
 &= \int \int_{\Sigma(t)} \rho(t) V(t) d\sigma_t - \int \int_{\Sigma(t_0)} \rho(t_0) V(t_0) d\sigma_{t_0}
 \end{aligned}$$

where

- $d\sigma$ - incremental surface area of the wavefront at τ
- $V(\tau)$ - normal velocity of the wavefront at τ
- $\rho(\tau)$ - density of the medium at τ
- \vec{a} - ray velocity.

The surface integration need not be carried out over the sides of the ray tube, as \vec{a} , the ray velocity is always tangent to them. The normal direction to the surface of γ is chosen positive outwards so that at $\tau=t_0$, $\vec{V}(t_0)$ and $d\vec{\sigma}_{t_0}$ point in opposite directions accounting for the minus sign in the second integral in A1.

The incremental area $d\sigma_{\tau}$ can be expressed in terms of the ray coordinates (α, β, τ) , (Babich and Buldirev (1972)) as

$$(A2) \quad d\sigma_{\tau} = J(\tau) d\alpha d\beta$$

where the non-negative function J is linked to the

Jacobian of the transformation of Cartesian coordinates to ray coordinates by the relation

$$(A3) \quad J = \frac{1}{a} \left| \frac{D(x_1, x_2, x_3)}{D(\alpha, \beta, \tau)} \right|$$

where a is the magnitude of the ray velocity \vec{a} . The function $J(\tau)$ for a particular wavefront at time τ is equal.

$$(A4) \quad J(\tau) = \left| \vec{x}_\alpha \times \vec{x}_\beta \right|$$

where $\vec{x}_\alpha = \left(\frac{\partial x_1}{\partial \alpha}, \frac{\partial x_2}{\partial \alpha}, \frac{\partial x_3}{\partial \alpha} \right)$ and \vec{x}_β are similar. From this it follows that

$$(A5) \quad J = (EH - G^2)^{\frac{1}{2}}$$

$$E = \vec{x}_\alpha \cdot \vec{x}_\alpha, \quad H = \vec{x}_\beta \cdot \vec{x}_\beta, \quad G = \vec{x}_\alpha \cdot \vec{x}_\beta.$$

Thus it follows that since $d\sigma_t = \frac{J(t)}{J(t_0)} d\sigma_{t_0}$

$$(A6) \quad \int \int \int_Y \nabla \cdot \rho \vec{a} d\gamma = \int \int_{\Sigma(t_0)} \{ \rho(t) V(t) J(t) - (t_0) V(t_0) J(t_0) \} d\alpha d\beta$$

$$= \int \int_{\Sigma(t_0)} \int_{t_0}^t \frac{d}{d\tau} \left(\rho(\tau) V(\tau) J(\tau) \right) d\tau d\alpha d\beta$$

$$\begin{aligned}
&= \int \int_{\gamma} \int \frac{1}{V(\tau)J(\tau)} \frac{d}{d\tau} (\rho(\tau)V(\tau)J(\tau)) V(\tau) d\tau J(\tau) d\alpha d\beta \\
&= \int \int_{\gamma} \int \left\{ \frac{1}{V(\tau)J(\tau)} \frac{d}{d\tau} (\rho(\tau)V(\tau)J(\tau)) \right\} d\gamma
\end{aligned}$$

and hence

$$(A7) \quad \nabla \cdot \rho \vec{a} = \frac{1}{V(\tau)J(\tau)} \frac{d}{d\tau} (\rho(\tau)V(\tau)J(\tau)).$$

APPENDIX B

REFLECTION AND TRANSMISSION COEFFICIENTS

At an interface between two elastic media in welded contact certain boundary conditions must be satisfied when an SH ray is incident at the interface and produces a reflected and transmitted ray. These conditions are the continuity of displacement and shear stress at the interface.

Displacement:

$$(B1) \quad u_i + u_r = u_t$$

where the subscripted variables u_i , u_r and u_t refer to the displacement components of the incident, reflected and transmitted rays respectively.

Shear Stress:

$$(B2) \quad \sigma(u_i) + \sigma(u_r) = \sigma(u_t)$$

with
$$\sigma(u) = \rho \frac{B \partial u}{\partial z}$$

ρ - density

B - as defined previously in the text.

If the $z=0$ plane is denoted as the interface and the upper and lower media are labelled 1 and 2, employing equations (2.7), (2.8) and (2.9) from the text, yields the following set of two equations in two unknowns.

$$(B3) \quad \begin{bmatrix} 1 & -1 \\ \rho_1 B_1 \lambda_1 & \rho_2 B_2 \lambda_2 \end{bmatrix} \begin{bmatrix} R(k) \\ T(k) \end{bmatrix} = \begin{bmatrix} -1 \\ \rho_1 B_1 \lambda_1 \end{bmatrix} .$$

$R(k)$ and $T(k)$ are the reflection and transmission coefficients and

$$\lambda_j = \left(\frac{A_j k^2}{B_j} - \frac{\omega^2}{B_j} \right)^{\frac{1}{2}} .$$

With the change of variable $k = \frac{\omega}{\sqrt{B_1}} q$ the system of equations (A3) becomes

$$(B4) \quad \begin{bmatrix} 1 & -1 \\ M_1 w_1 & M_2 w_2 \end{bmatrix} \begin{bmatrix} R(q) \\ T(q) \end{bmatrix} = \begin{bmatrix} -1 \\ M_1 w_1 \end{bmatrix}$$

where $M_j = \rho_j B_j k_j$

$$k_j = \frac{\omega}{\sqrt{B_j}}$$

$$w_j = \left(1 - \frac{A_j}{B_1} q^2 \right)^{\frac{1}{2}} .$$

The solutions of (B4) are given by

$$(B5) \quad R(q) = \frac{M_1 w_1 - M_2 w_2}{M_1 w_1 + M_2 w_2}$$

$$(B6) \quad T(q) = \frac{2M_1 w_1}{M_1 w_1 + M_2 w_2} .$$

Multiplying both the numerator and denominator of (B5) by $M_1 w_1 - M_2 w_2$ results in the following alternate expression for the reflection coefficient

$$(B7) \quad R(q) = C_1(q) - C_2(q)w_2$$

with

$$C_1(q) = \frac{(M_1 w_1)^2 + (M_2 w_2)^2}{(M_1 w_1)^2 - (M_2 w_2)^2}$$

$$C_2(q) = \frac{2M_1 M_2 w_1}{(M_1 w_1)^2 - (M_2 w_2)^2} \cdot$$

BIBLIOGRAPHY

- Anderson, D.L. (1961). Elastic wave propagation in layered anisotropic media. J. Geophys. Res., 66, 2953-2964.
- Babich, V.M. and A.S. Alekseev (1958). A ray method of computing wave front intensities. Izv. Akad. Nauk, SSSR, Geophys. Ser. 1, 9-15 in English translation, 17-31 in Russian.
- Babich, V.M. and V.S. Buldirev (1972). Asymptotic method in the diffraction problems of short waves. NAUKA, Moscow (in Russian).
- Babich, V.M. and N.Ya. Kirpichnikova (1974). Boundary layered method in the diffraction problems. Leningrad University Press, Leningrad (in Russian).
- Backus, G.E. (1962). Long-wave elastic anisotropy produced by horizontal layering. J. Geophys. Res., 67, 4427-4440.
- Cervený, V. (1962). On reflected and head waves around the first and second critical point. Geofysikalni Sbornik, 165, 43-94.
- Cervený, V. (1965). The dynamic properties of reflected and head waves around the critical point. Geofysikalni Sbornik, 221, 135-245.
- Cervený, V. (1967). The theory of reflected and head waves in the case of layered overburden. Geofysikalni Sbornik, 269, 133-180.
- Cervený, V. (1972). Seismic rays and ray intensities in homogeneous anisotropic media. Geophys. J., 29, 1-13.
- Cervený, V. (1974). Reflection and transmission coefficients for transition layers. Studia. Geoph. et Geod., 13, 59-68.
- Cervený, V. and R. Ravindra (1971). Theory of seismic head waves. University of Toronto Press, Toronto, 312 pp.

- Cervený, V. and I. Psencik (1972). Rays and travel time curves in inhomogeneous anisotropic media. *Z. Geophysik*, 38, 565-577.
- Cervený, V., I.A. Molotkov and I. Psencik (1977). Ray method in seismology, Charles University Press, Prague.
- Choi, A.P. (1978). Rays and caustics in vertically inhomogeneous elastic media. M.Sc. Thesis, University of Alberta, Edmonton.
- Cooley, J.W. and J.W. Tukey (1965). An algorithm for the machine calculation of complex Fourier series. *Math. Computation*, 19, 297-301.
- Courant, R. and D. Hilbert (1962). Methods of mathematical physics, Vol. 2: Partial differential equations. Interscience, New York.
- Daley, P.F. and F. Hron (1978). Reflection and transmission coefficients for seismic waves in ellipsoidally anisotropic media. *Geophysics*, 44, 27-38.
- Daley, P.F. and F. Hron (1979). SH waves in transversely isotropic media - an asymptotic expansion approach. *Bull. Seism. Soc. Am.*, 69, 689-711.
- Daley, P.F. and F. Hron (1979). SH waves in transversely isotropic media - a wave approach. *Can. J. Earth Sci.*, 16, 1998-2008.
- Dunkin, J.W. (1965). Computation of model solutions in layered, elastic media at high frequencies. *Bull. Seism. Soc. Am.*, 55, 335-358.
- Frasier, C.W. (1970). Discrete time solution of plane P-SV waves in a plane layered medium. *Geophysics*, 35, 197-219.
- Fuchs, K. (1968). The reflection of spherical waves from transition zones with arbitrary depth-dependent elastic moduli and density. *J. Phys. Earth*, 16, 27-41.
- Fuchs, K. (1971). The method of stationary phase applied to the reflection of spherical waves from transition zones with arbitrary depth-dependent elastic moduli and density. *Z. Geophysik*, 37, 89-117.

- Fuchs, K. and G. Müller (1971). Computation of synthetic seismograms with the reflectivity method and comparison with observations. Geophys. J.R. astr. Soc., 23, 417-433.
- Gassmann, F. (1966). Introduction to seismic travel time methods in anisotropic media. Pure Appl. Geophys., 58, 53-112.
- Haskell, N.A. (1953). The dispersion of surface wave on multilayered media. Bull. Seism. Soc. Am., 43, 17-34.
- Helmberger, D.V. and G.B. Morris (1969). A travel time and amplitude interpretation of a marine refraction profile: primary waves. J. Geophys. Res., 74, 483-497.
- Helmberger, D.V. and G.B. Morris (1970). A travel time and amplitude interpretation of a marine refraction profile: transformed shear waves. Bull. Seism. Soc. Am., 60, 593-608.
- Hron, F. (1971). Criteria for selection of phases in synthetic seismograms for layered media. Bull. Seism. Soc. Am., 61, 765-779.
- Hron, F. (1972). Numerical methods of ray generation in multilayered media, in Methods in computational physics, Vol. 12, Theoretical seismology, ed. B.A. Bolt, Academic Press, New York and London.
- Hron, F. and E.R. Kanasewich (1971). Synthetic seismograms for deep seismic sounding studies using asymptotic ray theory. Bull. Seism. Soc. Am., 61, 1169-1200.
- Karal, F.C. Jr. and J.B. Keller (1959). Elastic wave propagation in homogeneous and inhomogeneous media. J. Acoust. Soc. Am., 31, 694-705.
- Kireyeva, I. and K. Karpov (1961). Tables of Weber functions. Pergamon Press, London, 340 pp.
- Kline, M. (1951). An asymptotic solution of Maxwell's equations. Comm. Pure Appl. Math., 4, 225-263.
- Knopoff, L. (1964). A matrix method for elastic wave problems. Bull. Seism. Soc. Am., 54, 431-438.

- Kraut, A.E. (1963). A review of anisotropic wave propagation. Rev. Geophys., 1, 401-448.
- Levin, F.K. (1979). Seismic velocities in transversely isotropic media. Geophysics, 20, 780-806.
- Luneberg, R.K. (1944). The mathematical theory of optics. Lecture Notes, Brown University, published as a monograph by University of California Press, Berkeley and Los Angeles (1964), 448 pp.
- Marks, L.W. and F. Hron (1977). Weber function computation in the interference reflected-head wave amplitude. Geophys. Res. Lett., 4, 255-258.
- Molotkov, L.A., V. Cervený and O. Novotny (1976). Low-frequency and high-frequency expressions for the reflection and transmission coefficients of seismic waves for transition layers. Studia Geoph. et Geod., 20, 219-235.
- Müller, G. (1971). Approximate treatment of elastic body waves in media with spherical symmetry. Geophys. J.R. astr. Soc., 23, 435-449.
- Musgrave, M.J.P. (1970). Crystal acoustics, Holden-Day, San Francisco.
- Potsma, G.W. (1955). Wave propagation in a stratified medium. Geophysics, 20, 780-806.
- Ratnikova, L.I. (1973). The method of seismic wave computation in thinly layered media. NAUKA, Moscow, 123 pp. (in Russian).
- Riznichenko, Y.V. (1949). On seismic anisotropy. Izv. Akad. Nauk. SSSR, Ser. Geograf. i Geofiz., 518-544.
- Rytov, S.M. (1956). The acoustical properties of a finely layered medium. Sov. Phys. Acoust. 2, 67.
- Sato, R. and E.R. Lapwood (1968). SH waves in a transversely isotropic medium - 1. Geophys. J.R. astr. Soc., 14, 463-470.
- Sherwood, J.W.C. and A.W. Trorey (1965). Minimum-phase and related properties of a horizontally stratified absorptive earth to plane acoustic wave. Geophysics, 20, 191-197.

- Stavroudis, O.N. (1972). The optics of rays, wavefronts and caustics, Academic Press, New York.
- Thomson, W.T. (1950). Transmission of elastic waves through a stratified solid medium. J. Appl. Phys., 21, 89-93.
- Treitel, S. and E.A. Robinson (1966). Seismic wave propagation in layered media in terms of communication theory. Geophysics. 31, 17-32.
- Uhrig, L.F. and F.A. Van Melle (1955). Velocity anisotropy in stratified media. Geophysics, 20, 774-779.
- Watson, G.N. (1944). A treatise on the theory of Bessel functions. Cambridge University Press, London.
- White, J.E. and F.A. Agona (1955). Elastic wave velocities in laminated media. J. Acous. Soc. Am., 27, 310-317.

B30306